GEOTECHNICAL ENGINEERING

MATERIALS STUDIES RELATED TO LUNAR SURFACE EXPLORATION

by

J. K. MITCHELL
I. S. E. CARMICHAEL
R. E. GOODMAN
J. FRISCH
P. A. WITHERSPOON
F. E. HEUZÉ

FINAL REPORT: VOLUME I OF IV

PREPARED FOR MARSHALL SPACE FLIGHT CENTER
HUNTSVILLE, ALABAMA UNDER NASA CONTRACT
NSR 05-003-189

MARCH, 1969

SPACE SCIENCES LABORATORY

UNIVERSITY OF CALIFORNIA · BERKELEY

G E O T E C H N I C A L E N G I N E E R I N G

MATERIAL STUDIES RELATED TO LUNAR SURFACE EXPLORATION

By

James K. Mitchell
Ian C. Carmichael
Joseph Frisch
Richard E. Goodman
Paul A. Witherspoon
Francois E. Heuzé

FINAL REPORT: VOLUME I OF IV

Prepared for Marshall Space Flight Center
Huntsville, Alabama, under NASA Contract
NSR 05-003-189

March 1969

Space Sciences Laboratory

University of California, Berkeley 94720

TABLE OF CONTENTS

LIST OF ILLUSTRATIONS

LIST OF TABLES

PREFACE

This report presents in its four volumes the results of studies conducted during the period March 6, 1967 — June 30, 1968, under NASA research contract NSR 05-003-189, "Materials Studies Related to Lunar Surface Exploration." This study was sponsored by the Advanced Lunar Missions Directorate, NASA Headquarters, and was under the technical cognizance of Dr. N. C. Costes, Space Sciences Laboratory, George C. Marshall Space Flight Center.

This report reflects the combined effort of five faculty investigators and a full time project manager/engineer assisted by six graduate research assistants, representing several engineering and scientific disciplines pertinent to study of lunar surface material properties. James K. Mitchell, Professor of Civil Engineering, served as Principal Investigator and was responsible for those phases of the work concerned with problems relating to lunar soil mechanics and the engineering properties of lunar soils. Co-investigators were Ian C. Carmichael, Professor of Geology, in charge of geological studies; Joseph Frisch, Professor of Mechanical Engineering, who was responsible for analysis of friction and adhesion problems and the testing of materials under high-vacuum conditions; Richard E. Goodman, Associate Professor of Geological Engineering, who was concerned with the engineering geology and rock mechanics aspects of the lunar surface; and Paul A. Witherspoon, Professor of Geological Engineering, who conducted studies related to thermal and permeability measurements on the lunar surface. Francois E. Heuzé, Assistant Specialist, served as project manager and contributed to studies in the areas of rock mechanics and engineering geology.

INTRODUCTION

I. OBJECTIVES

It is axiomatic that, among the myriad of technical and scientific factors that must be considered in the lunar exploration program, the nature of lunar soil and rock surface materials is of prime importance in the design of spacecraft landing systems, the design of surface mobility systems, the design of experiments to be conducted on the lunar surface, mission planning, and, ultimately, to mission success. Without specific knowledge of the mechanical properties of lunar soils, designers and mission planners have no choice but to adopt ultraconservative designs and procedures in an effort to insure astronaut safety. Thus it is of paramount importance that as much specific information as possible about lunar surface material properties be obtained prior to the first manned lunar mission, and that planning and design options for further missions remain open thereafter in order to accommodate changes as more and more specific data become available.

The study described in this report was initiated in an effort to better define both the surface material related engineering problems and the relevant properties of the materials themselves. Information developed as a result of this effort was then utilized in specific studies of problems considered to be of critical importance and for the development of analysis and testing methods that appear particularly promising for the study of lunar surface properties by both remote and tactile means.

Specific objectives that were set at the onset of the study were:

1. To define geological and engineering problems associated with on-site lunar exploartion dependent on knowledge of soil and rock properties for solution.

2. To critically evaluate current knowledge concerning lunar surface materials, their properties, and their relationships to problems associated with on-site lunar exploration, and to select reasonable models for lunar surface conditions.

3. To make preliminary formulations of desirable on-site soil and rock mechanics studies for extended lunar exploration and to make recommendations as to appropriate apparatus and required astronaut skills for performance of such investigations.

4. To undertake preliminary studies for development of rock testing devices for use in a borehole on the lunar surface for the determination of the stress-strain characteristics of rocks.

5. To review friction and adhesion problems and to make recommendations for improved design of existing apparatus for determination of frictional and adhesive characteristics of different metallic and nonmetallic materials under high vacuum and at high and low temperatures.

6. To make recommendations and cost estimates for the design of apparatus for measuring silicate mineral solubility and viscosity at high temperatures and pressures and for determining the distribution of silicates between gas and liquid phases.

7. To review critically theories for the origin of the moon and to consider logical sequences for investigations to be carried out on the lunar surface for most efficient determination of composition, structure and history of the moon.

The results of studies of this type are intended to aid in attainment of the following longer range goals:

1. Development of capability for predicting, at least in a semi-quantitative manner, soil conditions at any point on the moon on the basis of remote measurements.

2. Development of capability for detailed quantitative determination of soil and rock properties at any chosen site where scientific or engineering work is contemplated.

3. Development of methods of analysis suitable for solution of soil and rock mechanics problems on the moon.

4. Utilization of the information obtained, both as an aid in the interpretation of geologic processes on the moon and as a means for developing improved understanding of soil and rock behavior on the earth.

II. SCOPE OF WORK AND OUTLINE OF FINAL REPORT

As work proceeded on each of these objectives several specific topics emerged as particularly needing more detailed study, and, consequently, during the later phases of the study efforts were intensively directed at these topics. Thus the trend has been from studies of a braod and general nature within a particular area to the isolation of specific problems and more detailed studies of these problems. This is reflected in the general outline of the 4 volumes constituting this report, as shown below:

VOLUME I

LUNAR SOIL MECHANICS AND SOIL PROPERTIES

Chapter 1. Lunar Soil and Rock Problems and Considerations in Their Solution
(James K. Mitchell)

Chapter 2. Engineering Properties of Lunar Soils
(James K. Mitchell and Scott S. Smith)

Chapter 3. Materials Properties Evaluations from Boulder Tracks on the Lunar Surface
(James K. Mitchell and Scott S. Smith)

Chapter 4. Impact Records as a Source of Lunar Surface Material Property Data
(James K. Mitchell, Donald W. Quigley, and Scott S. Smith)

Chapter 5. Lunar Stratigraphy as Revealed by Crater Morphology
(Francois E. Heuzé and Richard E. Goodman)

Chapter 6. Geochemical Studies
(I. S. E. Carmichael and J. Nicholls)

Appendix. Library of Lunar Surface Exploration Materials
(Francois E. Heuzé)

VOLUME II

APPLICATION OF GEOPHYSICAL AND GEOTECHNICAL METHODS TO LUNAR SITES EXPLORATION

—

VOLUME III

PRELIMINARY STUDIES ON SOIL/ROCK ENGINEERING PROBLEMS RELATED TO LUNAR EXPLORATION

VOLUME III (Con't.)

—

VOLUME IV

PRELIMINARY STUDIES FOR THE DESIGN OF ENGINEERING PROBES

C H A P T E R 1

LUNAR SOIL AND ROCK PROBLEMS

AND CONSIDERATIONS IN THEIR SOLUTION

by

James K. Mitchell

CHAPTER 1

LUNAR SOIL AND ROCK PROBLEMS AND CONSIDERATIONS IN THEIR SOLUTION

(James K. Mitchell)

I. INTRODUCTION

A number of geotechnical engineering (soil mechanics, engineering geology, rock mechanics) problems related to lunar exploration have been identified. In this section these problems are listed, and an assessment of priorities for acquisition of the data needed for their solution is given, as well as a statement of the suitability of existing analysis methods. General considerations on the measurement of lunar soil and rock properties are listed, and possible test methods for their determination are suggested.

II. PROBLEMS

Geotechnical engineering problems that are related to lunar exploration can be divided conveniently into two groups: (1) those that must be solved for early lunar science missions and (2) those pertinent to extended lunar exploration and the development of lunar bases.

A. Early Mission Problems

1. Dynamic and static bearing capacity of the lunar surface. Spacecraft must be designed to land safely on the lunar surface without danger of excessive sinkage or tilting during the landing event. The surface static bearing capacity must be adequate to support the spacecraft after landing and to support astronauts during their extravehicular activities. Results from the Surveyor Program have indicated, however, that inadequate bearing capacity is not likely to be a major problem, at least in areas similar to the Surveyor landing sites.

2. Surface erosion by rocket exhaust. Spacecraft support must not be impaired during either landing or takeoff as a result of surface material erosion under the action of rocket engine exhaust. The results of the Surveyor V erosion experiment have indicated that the lunar surface material can be eroded by the rocket exhaust gases.

3. Contamination of systems by eroded surface material and exhaust gases. Characteristics of materials that are likely to be eroded by exhuast gases should be determined and the probability of spacecraft systems becoming contaminated by eroded material must be assessed. Aseptic sampling requires that the depth and radial distance beyond the exhaust gas impingement point to which contamination has extended be determined.

4. Trafficability of lunar soils and mobility of lunar surface vehicles. Mission safety demands that sufficient data be available for assessment of vehicle mobility on a "go — nc go" basis for any proposed roving vehicle (or walking astronaut). Proper vehicle design and mission planning will require much more specific information concerning vehicle-surface interaction.

5. Siting of ALSEP Packages. Apollo Lunar Surface Experiment Packages must be located on stable ground, and soil conditions must be adequate to insure continued stability for the life of the experiment. A high degree of stability will be particularly important in the case of emplacement of astronomical observation devices.

6. Sampling. The return of representative samples of lunar surface materials is of prime importance in the attainment of lunar science objectives. Sampling techniques and sampling devices cannot be designed without some knowledge of the properties of the materials to be sampled.

7. Drilling. The drilling of bore holes for sample recovery from depth or the emplacement of test devices requires knowledge of material properties for design of drills,

selection of coring and sample recovery procedures, determination of power requirements, and anticipation of special problems, such as the prevention of caving of the bore holes.

8. Identification of hazard areas. Safety requires that potentially hazardous areas be avoided. Such areas as unstable slopes and crater walls, hidden crevasses and cavities, and local soft spots must be identified during mission planning if possible.

B. Problems Related to Extended Lunar Exploration and Lunar Base Development

All of the problems listed above may be expected to continue to be important during advanced phases of lunar exploration and development. In addition, the following problems must be considered. Each will involve considerations of soil and/or rock mechanics and soil and/or rock properties if satisfactory solutions are to be developed. These problems include:

1. Excavation
2. Undergound construction
3. Underground storage
4. Waste disposal
5. Radiation shielding using soil materials
6. Thermal insulation
7. Location of construction materials
8. Mineral resource location

III. PRIORITIES

Methods of analysis to be used for solution of these problems, except possibly in the areas of soil trafficability and vehicle mobility, are reasonably well advanced and probably adequate, provided the appropriate soil data are available. The results of the Surveyor Program have been

invaluable in providing improved estimates of pertinent soil properties; however, the ranges of values must be narrowed and the variability for different sites determined. Unproven assumptions remain in most quantitative estimates of soil properties that have been made thus far.

Consequently first priority should be given to determination of the engineering parameters of lunar soils. All available data from the Surveyor Program should be carefully evaluated in an effort to select the best quantitative values possible. Orbiter photographs should be carefully studied and techniques perfected for the determination of physical properties from photographic and other remote sensing techniques. Considerable progress in this area has already been made and is discussed in more detail in Chapters 3, 4, and 5 of this volume.

Since planning for early Apollo missions is now well along, and it is known that the mission constraints will permit only the simplest testing and sampling programs by the astronauts, every effort should be made to extract significant soil property data from the various phases of lunar surface operations. Examples of the types of data that, while not specifically obtained to provide direct measures of soil properties, can be used for estimating properties, include strain gage records during spacecraft landing, photographic records of astronaut footprints, LM sinkage into the lunar surface, photographic records of soil disturbance during landing, verbal descriptions of materials by the astronauts, and determination of slope angles and surface characteristics from photographs. Development of techniques for analyzing these types of information should be made prior to missions and the mission plan adjusted when practicable to optimize the quality of the data obtained.

In later Apollo missions it may be possible to conduct direct tests on the lunar surface for determination of strength, compressibility, and permeability. Apparatus for such tests must be simple, lightweight, rugged, adaptable to the harsh lunar environment, and automated to the extent possible. The test methods should yield data which can be interpreted meaningfully in terms of the parameters needed for soil and rock mechanics analyses. Existing and proven theories and methods of analyses

should be used wherever possible. Specific test methods and apparatus design concepts are under study as a part of a continuation of our work under a new contract.

As test results become available they should be correlated with remote sensing data so that the reliability of analyses based on remote measurements can be improved. Remote sensing, provided reliable methods can be developed, may prove ultimately to be the most economical means for determination of general surface material properties.

Since in early missions opportunities for direct measurement of the mechanical properties of lunar soils will be limited, studies of returned lunar samples will play an important role. Thus attention must be directed to the design of samplers and sampling methods. The returned samples from early missions will be severely limited in both size and quantity and chances for complete preservation of the in-situ soil structure are probably small. Thus meaningful direct measurements of pertinent mechanical properties will have to be inferred from observations of other characteristics; e.g. grain size, shape, and textures.

IV. PROPERTY DATA NEEDED FOR SOLUTION OF DIFFERENT PROBLEMS

Table 1-1 has been prepared, based on the major problem areas listed above, to indicate specific properties of lunar materials that must be known if reasonable solutions to the problems are to be obtained. Also listed is an assessment of the suitability of existing analytical methods for handling the problems. Problems are listed in order of decreasing chronological importance, assuming that initial missions will involve primarily landing, sampling, and limited surface mobility; whereas, the development of semi-permanent or permanent lunar bases may become a reality in the future.

V. PROPERTY MEASUREMENT

Whereas Table 1-1 relates soil and rock properties to specific problems associated with the scientific and engineering aspects of lunar exploration, Table 1-2 is concerned with methods for determining the different properties.

TABLE 1-1

SOIL AND ROCK DATA NEEDED FOR SOLUTION OF ENGINEERING PROBLEMS RELATED TO LUNAR EXPLORATION

Problem	Needed Property Values	Suitability of Existing Analytical Methods
1. Dynamic and static bearing bearing capacity	strength parameters, compressibility, density, dynamic modulis	Adequate for static, probably adequate for dynamic
2. Rocket blast erosion	density, porosity, cohesion, adhesion of soil to other materials, particle size and shape, aerodynamic friction and drag coefficients	Probably adequate. Give reasonable results for Surveyor V
3. Contamination of systems by eroded material	density, particle size and shape, cohesion, adhesion properties	Analytical methods not needed
4. Location of hazard areas	compressibility, slope angles, susceptibility to densification under dynamic loads, relative density	May be inadequate in case of cohesionless materials
5. Sampling	density, hardness, grain size and size distribution, strength, adhesion properties, penetration resistance	Analytical methods not needed
6. Siting of ALSEP packages	density, strength parameters, subsoil profile, strength under transient and cyclic loading, slope angles, relative density	Adequate
7. Drilling	hardness, grain size and shape, fracture patterns, adhesion characteristics, density, thermal conductivity, heat capacity	Semi-emipirical correlations on drillability available

NOTE: Time-dependency of stress-strain and strength characteristics may be important.

TABLE 1-1 (Continued)

Problem	Needed Property Values	Suitability of Existing Analytical Methods
8. Trafficability	density, strength, compressibility, stress-strain characteristics, details of surface topography and roughness	Probably need improvement
9. Radiation shielding	density, porosity, absorption properties	Adequate (?)
10. Thermal insulation	thermal conductivity, density, specific heat	Adequate
11. Waste disposal (underground)	same as underground storage plus interaction characteristics of wastes and in-situ materials	Don't know
12. Construction materials (evaluation of)	density, durability, strength, composition, stress-strain characteristics, grain size and size distribution, grain shape, texture, fabric	Analytical methods not needed
13. Underground storage	thermal conductivity, heat capacity, permeability, plus those for underground construction	Probably adequate or appropriate solutions can be developed fairly easily
14. Excavation and blasting	density, porosity, strength, stress-strain characteristics (brittleness), particle sizes and size distribution, adhesion characteristics, knowledge of absolute stresses	Semi-empirical laws for blasting available, adequate for design of bracing and supports

TABLE 1-1 (Continued)

Problem	Needed Property Values	Suitability of Existing Analytical Methods
15. Underground construction	density, porosity, strength, stress-strain characteristics, dynamic moduli, in-situ stress, susceptibility to change in properties under changed environment	Probably adequate
16. Mineral resources (location of)		Analytical methods not needed (?) Geophysical methods for mineral location

TABLE 1-2

GENERAL CONSIDERATIONS ON THE MEASUREMENT OF LUNAR SOIL AND ROCK PROPERTIES

Property	Approach For Determination[1]	To Be Used For[2]
1. Visual classification and general description of material*[3]	RS TIS ERS LBS	C, PMP
2. Grain size, shape and size distribution*	RS ERS LBS	C, PMP C, FMP, DP C, FMP, DP
3. Penetration resistance	RS TIS	C, PMP C, DP
4. Density*	RS TIS ERS LBS	C, PMP C, DP PMP, FMP, DP DP
5. Strength, including friction and cohesion	RS TIS ERS LBS	C, PMP DP PMP, FMP, DP DP

---

[1]RS — remote sensing
TIS — tests in-situ
ERS — tests on earth returned sample
LBS — tests on sample at lunar base

[2]C — classification data
PMP — preliminary mission planning
FMP — final mission planning
DP — determination of design parameters

[3]* indicates a property of particular usefulness for scientific interpretation of the moon

All property data will be used for post mission analysis

TABLE 1-2 (Continued)

Property	Approach For Determination[1]	To Be Used For[2]
6. Stress-strain characteristics, including compressibility	TIS	DP
	ERS	PMP, FMP, DP
	LBS	DP
7. Adhesion properties*	RS	C, PMP
	TIS	DP
	LBS	C, DP
8. Dynamic Moduli	RS	PMP
	TIS	DP
	ERS	PMP, FMP, DP
	LBS	DP
9. Permeability	TIS	DP
	ERS	PMP, FMP, DP
	LBS	DP
10. Thermal properties* (conductivity and heat capacity)	RS	C
	TIS	C, DP
	ERS	C, PMP, FMP
	LBS	C, DP
11. Porosity*	RS	C, PMP
	TIS	DP
	ERS	C, PMP, FMP
	LBS	C, DP
12. Relative density	TIS	FMP, DP
	ERS(?)	C, DP
	LBS	C, DP

TABLE 1-2 (Continued)

Property	Approach For Determination[1]	To Be Used For[2]
13. Durability	RS	PMP
	LBS	FMP, DP
14. Composition*	RS	C, PMP
	TIS	C
	ERS	C, PMP, FMP
	LBS	C, FMP
15. Absolute stresses*	TIS	FMP, DP

Properties are listed in order of decreasing importance as relates to solution of the problems listed in Table 1. Note is made also of those properties of particular importance for scientific interpretation of the moon. An indication (which in many cases is an opinion) is given for each of the following factors wherever possible.

A. Whether the determination can be made by remote sensing (RS), tests-in-situ (TIS), tests on earth returned samples (ERS), or tests on samples at a lunar base (LBS).

B. A recommendation as to which of the four possible approaches listed in A should be used for

1. Gathering data for classification and science purposes (C).
2. Preliminary mission planning (PMP).
3. Final mission planning (FMP).
4. Determination of design parameters (DP).

The recommendations under B are idealizations and represent what might be considered the best engineering applications of the data obtained by the various approaches. Time, cost, and other factors will probably not allow (1) extensive testing in-situ, (2) the return of undistrubed samples suitable for detailed measurement of mechanical properties, or (3) tests at a lunar base. Thus in most instances it is probable that design and planning will have to be based on remote observations and extrapolations of in-situ data from one location to another.

VI. TEST METHODS

Table 1-3 presents a listing of some specific test methods which might be used for acquisition of the data necessary for property determination. An indication is given (again an opinion in most cases) concerning the suitability of existing test methods, that are widely used for studies of terrestrial soils and rocks, for use in determination of lunar material properties. Useful techniques already developed for study of lunar surface materials are noted where appropriate. Of particular importance in the development of testing methods and apparatus for in-situ lunar soil tests and tests performed at lunar bases are (1) the harsh environment,

TABLE 1-3

TEST METHODS FOR LUNAR SOIL AND ROCK ENGINEERING PROPERTY DETERMINATION

Property	Possible Test Methods (In Order of Decreasing Ease of Performance)	Suitability of Existing Methods
1. Visual classification and general description	Direct observation of samples and photographs	Adequate
2. Grain size, shape, and size distribution	Photographs	Limited by camera resolution and to surface material
	Direct observation	Adequate for coarse particles
	Sieving	ERS* only
	Light microscope	Adequate
	Electron microscope	ERS only
3. Penetration resistance	Remote sensing	
	(a) crater ejecta as penetrators	Under investigation
	(b) dropped penetrators	Potentially useful
	Direct	
	(a) cone penetrometers	Probably very useful
	(b) dynamic (hammers)	Standard penetration test used for terrestrial soils not practical on moon
4. Density	Remote sensing	
	(a) penetration records	(a)(b)(c) require assumption of other soil parameters
	(b) thermal properties	
	(c) slope analyses	
	(d) Surveyor scoop type experiments	Not known
	(e) nuclear density meters	Give variable results

*Earth-returned samples

TABLE 1-3 (Continued)

Property	Possible Tests Methods (In Order of Decreasing Ease of Performance)	Suitability of Existing Methods
4. Density (continued)	Sampling — various field density methods	Should be adequate
	Bore hole probes with nuclear units	Under development
5. Strength, including friction and cohesion	Remote sensing — lower bound values from stability of existing slopes	Requires assumption of other soil properties
	Landing dynamics records	Requires assumptions of other soil parameters
	Penetration tests	See 3
	Vane shear tests	Probably useful in fine-grained, weak materials
	Direct shear tests	Good for ERS, may be difficult on moon
	Triaxial shear tests	Good for ERS, may be difficult on moon
	Transient and cyclic loading	Good for ERS, difficult on moon
6. Stress-strain characteristics	Landing dynamics	Requires assumptions
	Instrumented penetrometers	Unknown
	Seismic response characteristics	
	Strength tests	Adequate
	Plate load tests	Adequate
7. Adhesion properties	Observation of material sticking to instruments, etc.	
	Shear along contact surface between unlike materials	Not known

TABLE 1-3 (Continued)

Property	Possible Tests Methods (In Order of Decreasing Ease of Performance)	Suitability of Existing Methods
8. Dynamic moduli	Records of landing dynamics	Requires assumption of other soil properties
	Data from strength tests	Adequate, but requires undisturbed sample
	Seismic surveys — wave propagation	Depends on complexity of soil and rock profile
	Plate load tests	May be difficult on moon
	Vibration and cyclic load tests	May be useful, at least on ERS
9. Permeability	Calculation from grain size and porosity	Fair for sand sizes, unsatisfactory for finer material
	In-situ bore hole test-gas	Should be developed
	Direct measurement on samples	Adequate for ERS
10. Thermal properties (conductivity and heat capacity)	Remote sensing (a) Infrared (b) Other	(a)(b) require assumptions
	Direct	
	(a) emplaced temperature sensors	Adequate
	(b) borehole probe	Under development
	(c) thermal conductivity tests	Adequate
11. Porosity	Remote sensing	
	(a) albedo	(a)(b)(c) require assumptions
	(b) thermal properties	
	(c) radar, radio wave, etc.	
	(d) photographs	
	Direct determination in-situ or on samples	Adequate

TABLE 1-3 (Continued)

Property	Possible Tests Methods (In Order of Decreasing Ease of Performance)	Suitability of Existing Methods
12. Relative density	Penetration tests	Large experience factor needed to develop classification
	Sampling	Unsatisfactory for cohesionless materials
13. Durability	Visual observation Response to changes in environmental conditions	
	Standard degration tests	Adequate for ERS
14. Composition	Remote (a) photographs (b) thermal, electrical, magnetic properties	(a)(b) require assumptions
	Direct (a) visual observation (b) borehole camera (c) microscope (d) x-ray diffraction (e) chemical analysis (f) electron microscope	
15. Absolute stresses	Empirical, based on (a) sonic velocity (b) resistivity	Questionable (unreliable)
	Bottom hole convergence	Still being worked on
	Overcoring	To be adapted (satisfactory on earth)
	Flat jack	Cannot use in bore hole

(2) the necessity to keep payloads to a minimum, (3) the limited dexterity of a space-suited astronaut, and (4) the desirability for techniques that are simple, reliable, and rapid.

The possible test methods in Table 3 are listed in order of decreasing ease of data acquisition within the framework of current information concerning the experiment plans for lunar missions. In general, the acquisition of the most reliable data for good quantitative determination of soil properties requires the use of the less easily performed test methods.

The data that are most urgently needed from analysis of Orbiter and Surveyor data and from early Apollo missions to the moon are those that will permit evaluation of bearing capacity, erodability, load-sinkage characteristics, and lunar soil trafficability characteristics.

Unfortunately the quantitative reliability of property values that can be deduced from Orbiter photographs is quite restricted. The Surveyor data are considerably better from a quantitative standpoint, however, the information covers only a limited number of locations on the moon. It is imperative therefore that maximum advantage be taken of early Apollo missions for acquisition of additional data. The problem in connection with these missions, however, is that astronaut time and payload are very severely restricted. Thus maximum use must be made of data that are automatically obtained or acquired with a minimum expenditure of time and effort. Studies should begin at once for the purpose of determining the extent to which such data as those provided by LM landing dynamics records, photographic coverage of landing pad sinkage and astronaut footrpints, and simple tests (e.g., penetration, trenching, sliding) using the Apollo hand tools can be used to determine quantitative values for the needed properties.

It is essential also that a method for lunar trafficability analysis be decided upon and that appropriate methods, preferably using simple tests and test apparatus, be developed as soon as possible.

VII. CONCLUSION

Table 1-3 represents a first attempt at classification of problems, soil and rock properties, and test methods in a form which has been helpful for formulation of subsequent research efforts. Further refinement of all aspects of the topics covered will ultimately be needed. Emphasis has been on determination of properties for use in solution of specific engineering problems. Data obtained from measurements of the type suggested, however, may be expected to be of scientific value as well. For example, particle size, shape, and size distribution are a direct consequence of the lunar processes which caused them. Relative density reflects the extent of past static and dynamic loadings and in-situ stresses and can be used to deduce past stress and deformation history. Consolidation data may reveal the extent of any lunar erosion processes from comparison of present overburden pressure and maximum past pressure. It goes without saying, of course, that compositional data are essential for scientific study of the moon.

C H A P T E R 2

ENGINEERING PROPERTIES OF LUNAR SOILS

by

James K. Mitchell and Scott S. Smith

CHAPTER 2

ENGINEERING PROPERTIES OF LUNAR SOILS

(James K. Mitchell and Scott S. Smith)

I. INTRODUCTION

Speculation concerning the composition and properties of lunar soils and rocks has been widespread for hundreds of years. Until July 28, 1964, when Ranger VII sent back the first close up photographs of the lunar surface, this speculation was based on the results of earth-based observations of various types, and there were several hypotheses, summarized by Mitchell (1964), for the nature of the materials. These hypotheses ranged from thick layers of loose, unconsolidated dust through a slag-like surface to vesicular rock froth.

The Ranger and Orbiter programs have provided the first close up photographic information about the lunar surface, and the Surveyor and Luna programs have yielded a wealth of both photographic and tactile data. Thus the earlier speculations are largely of historical scientific interest; whereas, the results of these later space programs have provided a reasonable basis in fact concerning the nature of lunar soils and rocks. A large number of papers and reports have appeared which detail the findings of the various missions in these programs, and many analyses have been made from which the compositional and mechanical properties of lunar surface materials have been deduced using a variety of data and analysis methods.

A critical review of this information has been made and the results are summarized in Table 2-1. Emphasis was concentrated on information derived from the Ranger, Orbiter, Surveyor, and Luna Programs, although some consideration was also given to earth based observations and tests on simulated materials. Each section of the table pertains to a different property or characteristic. Quantitative values are included wherever possible. The first column gives the reference. The second column

provides a brief indication of the basis used for determination of the property considered. The third column indicates whether the determination was made on the basis of remote or direct observation, or from the results of tests on simulated lunar soils. Photographic data obtained from the Ranger and Orbiter series have arbitrarily been classed as remote, whereas, Surveyor TV data are considered as direct observations. In the last column the value or nature of the characteristics under consideration is listed.

Since these tables are largely self-explanatory, only brief discussion is included here. Surveyor VI and VII reports were not available at the time of preparation of this report, thus no data from these missions are included in Table 2-1. Some findings from these missions have been obtained, via personal communication with Dr. R. F. Scott and others active in these missions, and are included in the discussion where appropriate. Following this a summary table (Table 2-1) is presented indicating our best estimate of the various properties. Future revision of the table will be made if appropriate, based on final analyses of the data from all Surveyor missions.

II. GENERAL LUNAR SOIL PROFILE

It now appears well established that the moon is covered with a fragmental layer of variable thickness. This layer appears to be granular and lightly cohesive, with particle sizes ranging from large blocks down to 1 micron. The thickness of this layer apparently may range from a few centimeters or less to tens of meters. Evidence from the Soil Mechanics Surface Sampler (SMSS) tests during the Surveyor III and VII missions suggests that the strength of the fragmental layer increases with depth.

Except in regions where rock outcrops can be seen, the precise depth to bedrock is somewhat uncertain, although estimates are possible through study of crater morphology. A critical review of the determination of lunar stratigraphy from study of crater morphology is presented in Chapter 5, this volume.

III. LUNAR SLOPE ANGLES

Choate (1966) determined lunar slope angles in the vicinity of the Ranger 7, 8, and 9 impact areas. He found that most craters have uniform slopes with a short, nearly horizontal central portion and gently rounded rims. The maximum slope angles of talus-like slopes appeared to be 33 to 35°. Subsequent observations by Orbiters and Surveyors are compatible with these findings for the maria areas of the moon.

Choate determined the proportion of the impact areas covered by slopes of different inclination. The results of this analysis in the form of slope angle versus percentage of slopes greater than that angle are shown in Fig. 2-1. Subsequent analyses of observations from Surveyors and Orbiters are, in general, compatible with these findings for the maria areas of the moon. Slope angle distribution relationships are discussed more fully in Volume 3, Chapter 1, this report, in connection with trafficability on the lunar surface and models for terrain characterization.

IV. LUNAR SOIL PROPERTIES

Data from the Surveyor program have shown the soil to be quite similar in appearance and properties at all five landing sites (Surveyors I, III, V, VI, VII). It is significant to note that these sites are separated from each other by considerable distances. Four are in maria areas and one is in the lunar highlands (Tycho rim). The evidence suggests that the properties of the surface soils may be quite similar over the surface of the moon. Current estimates of the properties of the surface material are summarized in the following paragraphs and in Table 2-2.

A. Composition

Both remote (radar and optical measurements) and direct (γ-ray, apha scattering, magnetic) observations indicate the lunar surface material to be basic in composition and similar to terrestrial iron-rich basalt. Measurements on a rock fragment during the Surveyor VII experiments gave a density range of 2.4 to 3.2 with a most probable value of 2.8 to 2.9 gm/cm^3 for the solid material.

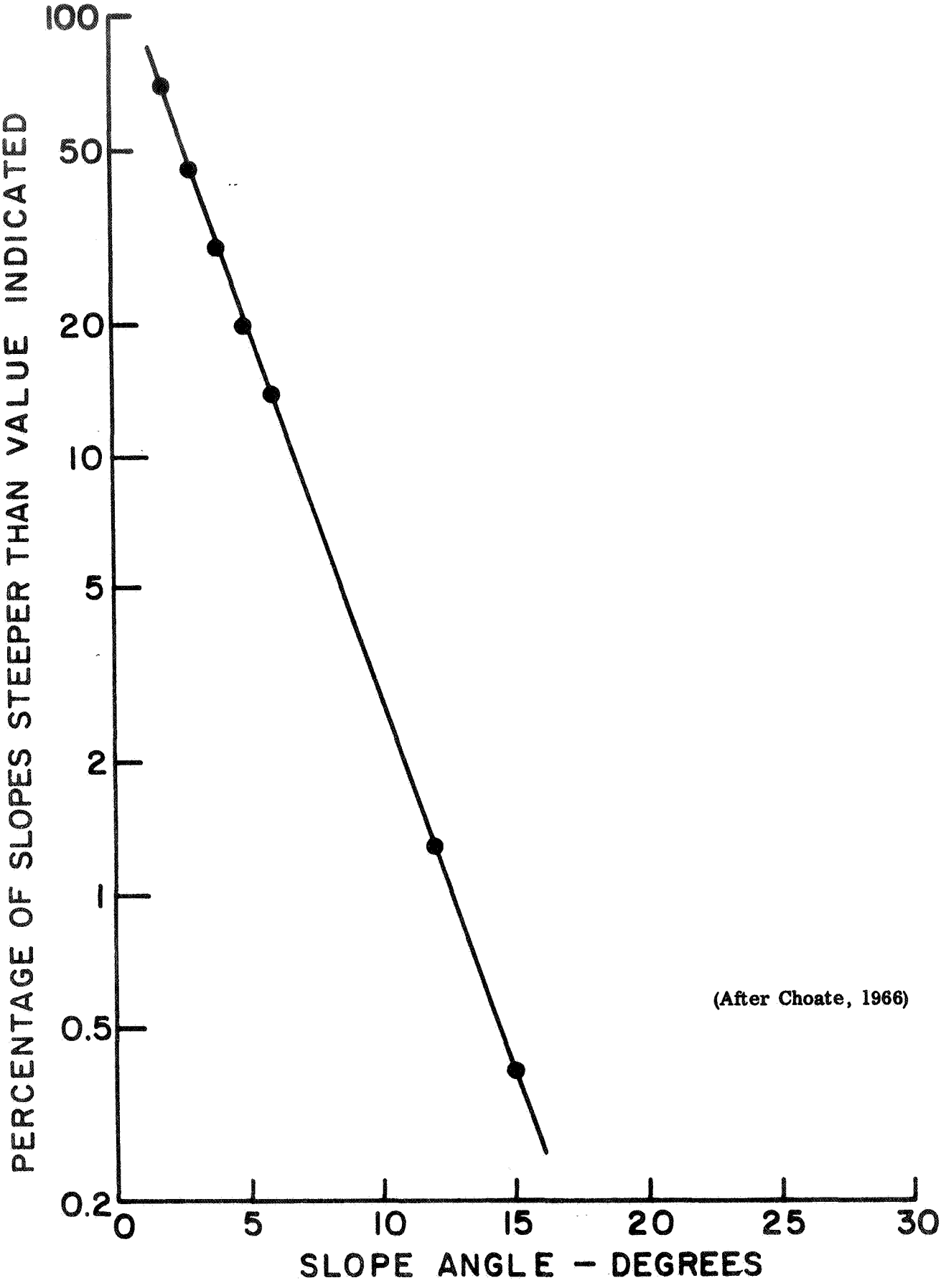

FIG. 2-1. Distribution of Lunar Slope Angles.

TABLE 2-2

SUMMARY OF LUNAR SOIL PROPERTY VALUES

PROPERTY OR CHARACTERISTIC	PROBABLE VALUE	
	THIS REVIEW	JPL ESTIMATE*
SOIL AND SURFACE PROFILE	Fragmental layer of variable thickness. Max. slopes of 33 – 35° (crater sides)	Max. slopes of 34 – 35°
COMPOSITION	Similar to terrestrial iron-rich basalt	–
PARTICLE SIZES	Size Range: boulders to 2μ; bulky particles; varying angularity	2μ – 60μ (fine friction) 50% < 10μ Distribution curves available for 1 mm – 10 m, Surveyor sites
DENSITY		
UPPER FEW MILLIMETERS	0.6 – 1.2 gm/cm^3	0.7 – 1.2 gm/cm^3
BELOW TOP FEW MILLIMETERS	1.0 – 2.0 gm/cm^3	1.5 gm/cm^3
COMPRESSIBILITY	Relatively incompressible below top few millimeters (under spacecraft and SMSS loadings)	–
STRENGTH PARAMETERS		
COHESION	0.02 – 0.5 psi	0.07 – 0.26 psi (0.048 – 0.180 N/cm^2)
ANGLE OF INTERNAL FRICTION	33 – 37°	37 – 39°
BEARING CAPACITY	Increases with depth and breadth of loaded area. A few psi near surface. See text.	Variable with depth Static (average) – 5 psi Upper few mm – 0.15 psi 2 cm depth – 2.7 psi 5 cm depth – 8.2 psi
DYNAMIC PROPERTIES		
EFFECTIVE SPRING CONSTANT (MODULUS)	7000 psi	–
PERMEABILITY	$1 \times 10^{-8} - 7 \times 10^{-8}$ cm^2 (Reasonable, but assumptions needed for determination)	$1 \times 10^{-8} - 7 \times 10^{-8}$ cm^2

*Bank, H. (see text).

B. Grain Size, Shape, and Distribution

Photographs of the lunar surface provide the only unambiguous data concerning the particle size and shape characteristics of the lunar soil. Unfortunately conclusions based on estimates of permeability (Surveyor V surface erosion experiment), thermal properties, and optical properties involve assumptions that cannot be verified, and in several cases the data do not yield unique answers.

Camera resolution limits the fineness of particle that can be distinguished to the order of 1 mm. It seems clear, however, that a significant proportion of the soil at the Surveyor sites is finer than this, probably extending down to 1 or 2 microns. Simulations have shown that more than 50 per cent of the particles must be finer than about 60 microns in order to account for the honeycomb pattern retained on the lunar surface after impression by the Surveyor III footpads. Those particles that can be clearly distinguished are bulky in character and exhibit varying degrees of angularity, probably reflecting the extent to which they have been subjected to lunar "weathering" processes. A well-graded size distribution is observed with sizes ranging up to boulders in some areas.

C. Density and Porosity

Estimates of lunar soil density and porosity have been based on remote observations (thermal, optical, radar), tactile measurements (γ-ray, failure mode under Surveyor footpads, landing dynamics) and simulations. Unfortunately data obtained with these methods are capable of several interpretations dependent upon assumptions in the analysis, and definite values remain to be determined. It does appear, however, that density increases and porosity decreases with depth below the surface. From the available data it would appear that the density at the surface may range from 0.6 to 1.2 gm/cm^3 increasing to 1.5 or 2.0 gm/cm^3 at depth. Bearing capacity analyses of Surveyor data indicate an average density of 1.5 to 1.7 gm/cm^3 to a depth of about 10 cm; with a value of 1.5 gm/cm^3 being the most probable.

Porosity estimates range from 35 to 80% or more. The nature of this porosity is important from an engineering property standpoint and is as yet undetermined. If particles are vesicular then a high porosity may not be indicative of high compressibility under moderate stress application. If particles are vesicular with sealed pores, then the permeability characteristics of the soil will differ from those of a material with the same porosity but open pores.

D. Compressibility

Photographs of the Surveyor footpad imprint areas show that deformation of the soil during landing was accompanied by some heave of the surface adjacent to the footpad, thus suggesting that the soil deforms more in shear than by densification. This is characteristic of a material with low compressibility under loads of the magnitude involved. Deformation patterns accompanying the Soil Mechanics Surface Sampler operations during the Surveyor VII mission also are consistent with what is observed for relatively incompressible terrestrial soils. A great number of well defined boulder tracks have been found in Orbiter photographs, clearly indicating either compression or displacement of soil under the rolling boulders. Detailed study of boulder tracks would appear desirable to ascertain whether an uplifted ridge has formed parallel to the track which would also be compatible with low compressibility. On the other hand if the volume of the track cannot be accounted for in this manner, then it would appear that the soil compressed under the weight of the boulder.

E. Strength Parameters

Estimates of strength parameters for unconsolidated lunar soil indicate the material to be predominantly frictional in nature but to possess a small amount of cohesion, as indicated both by the ability of the soil to stand on vertical slopes and by the appearance of tensile cracks on the surface adjacent to the point of application of bearing pressures. Estimates of cohesion range from 0.002 to 2 psi, although 0.05 to 0.1 psi is typical for the Surveyor landing areas. An upper bound on the value of cohesion of 0.1 psi has been established at the

Surveyor VI and VII sites* using the results of (1) the surface erosion experiment, (2) stress analysis on the surface adjacent to SMSS bearing tests, and (3) measurement of the load required to cause failure of a SMSS trench wall.

Studies of slopes on the moon show that the angle of repose is seldom greater than 35 to 40°. Choate (1966) studied slope angles from Ranger data and concluded that the angle of repose of lunar surface material, as indicated by the angle of repose of crater slopes, is in the range of 33 to 35°. In the absence of significant cohesion these values might represent a lower bound on the angle of internal friction. In the presence of cohesion the significance of these values is less certain. Analyses of the failure geometry (lateral distance over which soil has heaved) adjacent to Surveyor footpads and to the SMSS when used in the plate bearing test mode indicate friction angles of 35 to 37°.* Jaffe (1967b) has estimated friction angles as high as 55°, however, his estimate was based on the assumption of a completely compressible soil as opposed to one that is incompressible during shear. Thus 35° — 37° would appear reasonable for analysis purposes.

An attempt was made to crush a piece of lunar rock during tests with the Soil Mechanics Surface Sampler (Surveyor III) and was unsuccessful, thus indicating the rock capable of withstanding a compressive stress of at least 2×10^7 dynes/cm^2.

F. Bearing Capacity

Bearing capacity is not a basic soil property; but depends on density and strength parameters. Since it is considered as one of the lunar surface mechanical properties in much of the literature, however, it has been included in Table 2-1. Table 2-1 indicates that estimates of bearing capacity have been made using a variety of techniques. The data clearly indicate that the bearing capacity increases with depth and breadth of loaded area. These results support the concept of a frictional soil layer. Static analysis of boulders and blocks resting on the lunar

---

*Scott, R. F., personal communication.

surface would seemingly provide reasonable lower bound estimates of bearing capacity, but in each case an assumption of boulder density is required. Bearing capacities of 0.72, 0.73, and 0.74 psi (0.50 — 0.51 N/cm^2) are obtained as lower bound bearing capacities required to support the dead weight of Surveyors I, III, and V, respectively. A compressible soil model has been assumed for landing dynamics analysis by Jaffe (1967b) and Christensen et al. (1967c), but evidence favors at most only partial compression during shear, thus making these estimates of bearing capacity questionable. SMSS bearing tests (Surveyor III) indicated a bearing capacity on a 5 × 2.5 cm bearing area of 3 psi (2×10^5 dynes/cm^2) at 5 — 7.5 cm depth.

It appears, therefore, that while the bearing capacity at the surface may be as low as a few tenths of a lb per sq in. and increase to several lb per sq in. at depths of several centimeters, exact values corresponding to specific values of sinkage cannot be established from the data available for this review. Now that the rather reliable values of $\phi = 35 - 37°$ and $c = 0.05 - 0.1$ psi have been determined, a reasonable calculation of ultimate bearing capacity can be made for specific loading conditions. Load vs penetration data were obtained with the SMSS on Surveyor VII, which when available may proved useful for estimation of the load-settlement relationship for lunar soil.

G. Dynamic Properties

Few data are yet available on the dynamic properties of the lunar surface. The relationships used for the landing dynamics analyses of Surveyors have been in terms of inertia and momentum transfer between the footpad and the deforming soil mass. Dynamic properties such as dynamic modulus and damping coefficient do not form a part of the relationship used. One analysis has been made, however, by Christensen et al. (1967b) based on Surveyor III strain gage records during landing. They deduced that the soil possessed an effective spring constant of about 7000 psi (4.9×10^8 dyne/cm^2). If this constant is considered analogous to a dynamic modulus in compression, it is of the same order of magnitude as observed for terrestrial compacted silty or sandy soils with some cohesion.

H. Permeability

An estimate of permeability was made from the results of the surface erosion experiment during the Surveyor V mission (Christensen et al., 1967c).* It was concluded that the absolute permeability should be in the range of $1 \times 10^{-8} - 7 \times 10^{-8}$ cm^2 to a depth of 25 cm. This value is consistent with the permeability of a silty soil.

I. Erodability

The vernier engine firing experiment (Surveyor V) indicated that the lunar surface material could be eroded by the rocket exhaust blast. Particles appear susceptible to movement by both viscous erosion and diffusion erosion (blowout).

V. SUMMARY

As a result of this review of available information on the properties of lunar soil, tentative values for use in the analysis of engineering problems have been selected. These values are listed in Table 2-2. Subsequent to preparation of this summary, Bank** has summarized linear surface property data as determined from the results of landing impact analyses and science experiments on Surveyors III, V, VI, and VII. Bank's listing reflects the results of studies by R. F. Scott of the Surface Sampler Experiment (Surveyor III) and the Lunar Mechanical Properties Working Group at the Jet Propulsion Laboratory (JPL). Results from Surveyor missions VI and VII were included in arriving at the values indicated. These results were not available to us during the review of soil property data conducted to arrive at the values listed in Table 2-2. A listing of the JPL values is also presented in Table 2-2. It may be seen that in general the values corroborate each other, which, of course, is not unreasonable since the conclusions in each case were based on the same data sources (with the exception of Surveyors VI and VII).

---

*Method used described by Scott, R. F. and Ko, H. Y., "Transient Rocket-Engine Gas Flow in Soil," in press J. AIAA.

**Bank, H., Letter to O. H. Vaughen and N. C. Costes, MSFC, March 21, 1968.

TABLE 2-1: Recent Estimates of Lunar Surface Materials Properties

GENERAL PROFILE

REFERENCE	BASIS	TECHNIQUE	VALUE
JAFFE, L. D. (1966a)	COMPARISON OF PICTURES OF CRATERS FROM RANGER 7 WITH LABORATORY CRATERS	REMOTE AND SIMULATED	MARE COGNITUM OVERLAIN WITH AT LEAST 5 METERS OF GRANULAR MATERIAL
RENNILSON, J. J., ET AL. (1966)	SURVEYOR I PHOTOGRAPHS SHOWING ANGULAR SHAPES OF EJECTED BLOCKS	DIRECT	SHALLOW SUB-SURFACE IS RELATIVELY STRONG ROCK
JAFFE, L. D. (1966b)	COMPARISON OF PICTURES OF CRATERS FROM RANGERS VIII AND IX WITH LABORATORY CRATERS	REMOTE AND SIMULATED	AT LEAST 5 METERS OF SURFACE GRANULAR MATERIAL PROBABLY MORE ON MARE TRANQUILLITATIS, ALPHONSUS, AND NEARBY HIGHLANDS
OBERBECK, V. R., ET AL. (1967)	LUNAR ORBITER I PHOTOGRAPHS AND LABORATORY IMPACT STUDIES	REMOTE AND SIMULATED	FRAGMENTAL SURFACE THICKNESS AT SURVEYOR I SITE: 85% IS 5 - 15 METERS THICK MODAL THICKNESS IS 5 - 6 METER AVERAGE THICKNESS IS 8 - 9 METERS
SCOTT, R. F., ET AL. (1967)	RESULTS OF EMSS ON SURVEYOR III	DIRECT	SOIL FIRMER BELOW 5 - 7.5 CM. AND THERE APPEARS TO BE NO DUST LAYER
CHRISTENSEN, E. M., ET AL. (1967d)	SURVEYOR V TELEVISION DATA AND ASSUMING LANDING SITE CRATER IS A FISSURE	DIRECT	SHOCK-COMPRESSED AGGREGATES BELOW 10 CM RANGING FROM FEW MILLIMETERS TO 3 CM IN DIA. SET IN MATRIX OF LESS COHERENT, FINER PARTICLES. ROCKY CHIPS AND FRAGMENTS LARGER THAN 1 MM DISPERSED AS SUBORDINATE CONSTITUENT
FILICE, A. L. (1967b)	COMPARISON OF ALBEDO MEASUREMENTS OF SURVEYOR I SITE TO SIMULATED BASALT	DIRECT AND SIMULATED	THIN MANTLE OF VERY FINE PARTICLES, POSSIBLY < 10 μ, EXISTS AT SURFACE AND IS PROBABLY ABSENT IN POTS
SHOEMAKER, E. M., ET AL. (1967)	SURVEYOR V PHOTOGRAPHS OF NEARBY BLOCKY-RIMMED CRATER AND ASSUMING DEPTH TO DIAMETER RATIOS BETWEEN 1:3 AND 1:4	DIRECT	DEPTH TO BLOCKY OR COHERENT MATERIAL NOT GREATER THAN 5 METERS AT SURVEYOR V SITE
HEUZÉ, F. E. (1968)	COMPARATIVE AND DIRECT STUDIES OF RANGER, ORBITER, AND SURVEYOR PHOTOGRAPHS MATHEMATICAL MODEL OF CRATER EROSION	REVIEW	SUMMARY TABLE PRESENTED FOR ALL SITES INVESTIGATED

TABLE 2-1 CONT.

COMPOSITION

REFERENCE	BASIS	TECHNIQUE	VALUE
LIPSKIY, Y. N., ET AL. (1967)	LUNA 13 PHOTOGRAPHS	DIRECT	COMPOSITION OF STONES IS ANALOGOUS TO SOIL. THEY ARE NOT METEORITES. SOURCE OF STONES EITHER VOLCANIC OR EJECTA FROM PRIMARY CRATERS
ROELOF, E. C. (1967)	LUNA 10 γ - RAY EXPERIMENT	DIRECT	BASALT TYPE ROCK
DE WYS, J. N. (1967b)	COMPARISON OF PICTURES OF LUNAR SOIL ADHERING TO MAGNET ON SURVEYOR V WITH SIMULATED LABORATORY PHOTOS	DIRECT AND SIMULATED	UPPER 10 CM SIMILAR TO A TERRESTRIAL PLATEAU BASALT, 37 - 50 μ
TURKEVICH, A. L., ET AL. (1967b)	PRELIMINARY RESULTS OF SURVEYOR V ALPHA-SCATTERING EXPERIMENT	DIRECT	CLOSE AGREEMENT TO BASALTIC ACHONDRITES AND TERRESTRIAL BASALT ON EARTH
FILICE, A. L. (1967b)	COMPARISON OF LABORATORY TO OBSERVED SPECTRAL DATA FROM THE MOON	REMOTE AND SIMULATED	VISIBLE PORTION OF MOON IS BASIC-ULTRABASIC COMPOSITION
TURKEVICH, A. L., ET AL. (1967a)	COMPARISON OF SURVEYOR V ALPHA-SCATTERING RESULTS WITH DIFFERENT ROCKS	DIRECT	LUNAR SURFACE IS A SILICATE ROCK SIMILAR TO BASALTIC ACHONDRITE AND TERRESTRIAL BASALT
DE WYS, J. N. (1967a)	SURVEYOR V MAGNET EXPERIMENT	DIRECT	IRON PRESENT ON SURFACE IN FORM OF MAGNETITE PURE IRON, METEORITE NI-FE, OR SOME COMBINATION OF THESE
O'KEEFE, J. A., ET AL. (1967)	MEASUREMENT OF RADAR REFLECTIVITY ASSUMING POROSITY RANGE 0.35 - 0.45	REMOTE	ACIDIC ROCK OR POSSIBLY VESICULAR BASALT
HAPKE, B. (1968)	COMPARISON OF OPTICAL CHARACTERISTICS OF SURFACE WITH THOSE OF ROCK AND METEORITE PWODERS	REMOTE	LUNAR CRUST SIMILAR IN COMPOSITION TO TERRESTRIAL IRON-RICH BASALTS

TABLE 2-1 CONT.

GRAIN SIZE, SHAPE AND DISTRIBUTION

REFERENCE	BASIS	TECHNIQUE	VALUE
MOLUCHOWSKI, R. (1966)	VARIOUS THERMAL AND OPTICAL PROPERTIES INDICATE HIGH POROSITY STRONG LOCAL BONDS COULD CAUSE HIGH POROSITY AND AGGLOMERATION	REMOTE	POSSIBLY HIGHLY IRREGULAR, ELONGATED QUASI PARTICLES AND AGGLOMERATES
LUCAS, W., ET AL. (1966)	VALUE OF THERMAL PARAMETER PREDICTED FROM EARTH AND CALCULATED FROM SURVEYOR I INDICATE A PROBABLE FINE GRANULAR MATERIAL	REMOTE AND DIRECT	SOIL AROUND SURVEYOR I IS FINE AND GRANULAR
JAFFE, L. D. (1967b)	TELEVISION PICTURES FROM SURVEYOR I "5 μ" AND "POROUS" ARE UNFOUNDED STATEMENTS	DIRECT	BULK OF MASS < 100 μ, PERHAPS 5 μ. FEW > 1 MM DISTRIBUTION EXTENDS TO GREATER THAN 1 M ROCKS PARTICULATE, INDIVIDUAL PARTICLES THAT MAY BE POROUS
LUM, P., ET AL. (1967)	OBSERVATION OF BASALT GROUND INTO FINE AGGREGATE IN HIGH VACUUM	SIMULATED	DIVERSE AND ANGULAR SHAPES
CHRISTENSEN, E. M., ET AL. (1967b)	SURVEYOR III TELEVISION DATA	DIRECT	MOST LUNAR SOIL PARTICLES < 1 MM AND WELL GRADED
CHRISTENSEN, E. M., ET AL. (1967b)	SURVEYOR III TELEVISION DATA AND FOOTPAD IMPRINT SIMULATIONS	DIRECT AND SIMULATED	MECHANICAL PROPERTIES SIMILAR TO MOIST TERRESTRIAL SOIL CONTAINING > 10% FINE SILT OR < 10% CLAY-SIZE PARTICLES SUGGESTS SUBSTANTIAL AMOUNT FINER THAN .06 MM
SHOEMAKER, E. M., ET AL. (1967)	SURVEYOR V TELEVISION DATA	DIRECT	SIZE FREQUENCY DISTRIBUTION OF FRAGMENTAL LAYER AT SURVEYOR V SITE SIMILAR TO SURVEYOR I AND III SITES
CHRISTENSEN, E. M., ET AL. (1967c)	CONCLUDED FROM ESTIMATED LUNAR PERMEABILITY ($1 \times 10^{-8} - 7 \times 10^{-8}$ CM^2) SEVERAL ASSUMPTIONS INVOLVED IN ANALYSIS	DIRECT	MOST PARTICLES IN 2 - 60 μ RANGE

TABLE 2-1 CONT.

DENSITY

REFERENCE	BASIS	TECHNIQUE	VALUE
SMOLUCHOWSKI, R. (1966)	VARIOUS THERMAL AND OPTICAL PROPERTIES	REMOTE	POROSITY AT SURFACE $\geq$ 80% AT DEPTH OF PERHAPS 1 METER, POROSITY $\simeq$ 30%
HALAJIAN, J. D. (1966)	MODE OF FAILURE UNDER SURVEYOR I FOOTPAD	DIRECT	BULK DENSITY 1 GM/CM^3 (60 - 70% POROSITY)
JAFFE, L. D. (1967a)	RADAR AND THERMAL EMMISSION MEASUREMENTS	REMOTE	TOP FEW CENTIMETERS 0.6 - 0.7 GM/CM^3 10 CENTIMETERS 1 GM/CM^3 OR MORE 1 - 10 METERS 2 - 3 GM/CM^3
LIPSKIY, Y. N., ET AL. (1967)	LUNA 13 γ - RAY EXPERIMENT	DIRECT	SURFACE NOT EXCEEDING 1 GM/CM^3
NORDMEYER, E. F. (1967)	SURVEYOR I FOOTPAD DATA FOR A BEARING CAPACITY OF 4 PSI WITH 2 INCH PENETRATION	DIRECT	1.56 GM/CM^3
CHRISTENSEN, E. M., ET AL. (1967b)	SURVEYOR III LANDING DYNAMIC ANALYSIS COMPRESSED DENSITY ASSUMED 1.7 - 2.0 GM/CM^3	DIRECT	UPPER 0.5 CENTIMETERS 1.2 - 1.1 GM/CM^3 OR LOWER
CHERKASOV, I. I., ET AL. (1967)	LUNA 13 γ - RAY EXPERIMENT	DIRECT	NOT LESS THAN 5 CENTIMETERS, 0.8 GM/CM^3 OR SOMEWHAT LESS
CHRISTENSEN, E. M., ET AL. (1967c)	LANDING SIMULATION COMPUTER MODELS OF SURVEYOR V BEARING CAPACITY ASSUMED 2.7 N/CM^2	DIRECT AND SIMULATED	SURFACE MATERIAL 1.1 GM/CM^3
O'KEEFE, J. A., ET AL. (1967)	CROSS SECTION OF SOIL THROWOUT AT SURVEYOR I, FOOTPAD 2	DIRECT	POROSITY OF .35 - .45 (EXCLUDING THE CLOSED VESICULAR VOIDS)
CAMPBELL, M. J., ET AL. (1968)	LUNAR RADAR AND RADIOTHERMAL OBSERVATIONS ELECTRICAL PROPERTIES OF BASALT ASSUMED	REMOTE	SURFACE 0.6 $\pm$ .2 GM/CM^3 FEW CENTIMETERS 1.0 GM/CM^3

TABLE 2-1 CONT.

COMPRESSIBILITY

REFERENCE	BASIS	TECHNIQUE	VALUE
CHRISTENSEN, E. M., ET AL. (1967a)	PHOTOGRAPHS OF SURVEYOR I FOOTPAD	DIRECT	SURFACE MATERIAL COMPRESSIBLE TO SOME EXTENT
CHRISTENSEN, E. M., ET AL. (1967b)	PHOTOGRAPHS OF SURVEYOR III FOOTPAD THROWOUT	DIRECT	LOW COMPRESSIBILITY OF SURFACE MATERIAL
O'KEEFE, J. A., ET AL. (1967)	CROSS SECTION THROUGH SURVEYOR I, FOOTPAD 2	DIRECT	RELATIVELY INCOMPRESSIBLE SURFACE MATERIAL

STRENGTH PARAMETERS

REFERENCE	BASIS	TECHNIQUE	VALUE
NORDMEYER, E. F. (1967)	SURVEYOR I FOOTPAD DATA FOR MINIMUM CAPACITY OF 4 PSI WITH 2 INCH PENETRATION	DIRECT	ϕ 33° C .05 PSI
JAFFE, L. D. (1967b)	STRAIN GAGE AND TELEVISION DATA FROM SURVEYOR I	DIRECT	C PROBABLY .02 PSI, BUT TOTAL RANGE .002 - 2 PSI ϕ 55°
SCOTT, R. F., ET AL. (1967)	SMS TESTS, DENSITY ASSUMED 1.5 GM/CM^3	DIRECT	STRENGTH OF LUNAR ROCK AT LEAST 2×10^7 DYNES/CM^2 C = .02 - .2 PSI ϕ 35°
CHRISTENSEN, E. M., ET AL. (1967c)	PRELIMINARY RESULTS OF SURVEYOR V MISSION	DIRECT	SURFACE MATERIAL AT SURVEYOR V SITE SOMEWHAT WEAKER THAN SURVEYOR I AND III SITE

TABLE 2-1 CONT.

BEARING CAPACITY

REFERENCE	BASIS	TECHNIQUE	VALUE
JAFFE, L. D., ET AL. (1966)	STATIC ANALYSIS OF LUNA 9 MANY ASSUMPTIONS	DIRECT	AT LEAST 0.05 N/CM^2 (0.07 PSI)
CHRISTENSEN, E. M., ET AL. (1968)	ANALYSIS OF SURVEYOR I IMPACT DATA	DIRECT	DYNAMIC CAPACITY AT LEAST 4 - 7 N/CM^2 (5.8 - 10 PSI)
JAFFE, L. D. (1967a)	DERIVED FROM PROPERTIES NEEDED FOR STABILITY OF SLOPES OBSERVED IN RANGER VII, VIII, AND IX IMAGERY	REMOTE	BEARING WIDTH / NO SINKAGE / SINKAGE=BEARING WIDTH 0.1 METER / 0.1 N/CM^2 / 0.3 N/CM^2 1.0 METER / 1.0 N/CM^2 / 10 N/CM^2
HALAJIAN, J. D., ET AL. (1967)	THEORETICAL EXPRESSIONS OF THERMAL CONDUCTIVITY AND BEARING STRENGTH OF POROUS MEDIA IN VACUUM	SIMULATED	BEARING STRENGTH INCREASES WITH LUNAR MIDNIGHT TEMPERATURE INCREASE
JAFFE, L. D. (1967b)	R. F. SCOTT'S EQUATION FOR LOCAL SHEAR FAILURE AND LANDING FORCES FROM SURVEYOR I	DIRECT	4 N/CM^2 (6 PSI) ON 25 CM FOOTPAD WITHOUT SINKAGE. STRENGTH INCREASES WITH SINKAGE
FILICE, A. L. (1967a)	CAPACITY OF SOIL NECESSARY TO SUPPORT 13 METER BOULDER THAT ROLLED DOWN SLOPE (ASSUMED DENSITY OF BOULDER 3 GM/CM^3)	REMOTE	+0 N/CM^2 (58 PSI) AT 35 CM DEPTH
SCOTT, R. F., ET AL. (1967)	OBSERVATION AND MEASUREMENTS OF SURVEYOR III SMSS BEARING TESTS	DIRECT	2 N/CM^2 (3 PSI) AT 5 - 7.5 CM DEPTH ON 5 x 2.5 CM BASE
CHRISTENSEN, E. M., ET AL. (1967b)	LANDING INTERACTIONS OF SURVEYOR I AND SURVEYOR III	DIRECT	2 - 5.5 N/CM^2 (3 - 8 PSI)
CHRISTENSEN, E. M., ET AL. (1967b)	LANDING DYNAMIC ANALYSES OF SURVEYOR III	DIRECT	0.7 N/CM^2 (1.0 PSI) FOR TOP 0.5 CM

TABLE 2-1 CONT.

BEARING CAPACITY, CONT.

SHOEMAKER, E.M., ET AL. (1967)	SURVEYOR V PHOTOGRAPHS OF TRACKS LEFT BY SMALL FRAGMENTS	REMOTE	< 0.1 N/CM^2 (0.15 PSI) UPPER FEW MILLIMETERS ON AREA ABOUT 1 CM^2.
CHRISTENSEN, E. M., ET AL. (1967c)	COMPUTER SIMULATION OF SURVEYOR V LANDING USING COMPRESSIBLE SOIL MODEL	DIRECT	2.7 N/CM^2 (4 PSI)
LANGLEY WORKING PAPER (1968)	ORBITER V PHOTOGRAPHS AND CALCULATIONS USING STATIC ANALYSES FOR THREE BLOCKS	REMOTE	1.6 - 16 N/CM^2 (2.3 - 23 PSI)

DYNAMIC PROPERTIES

REFERENCE	BASIS	TECHNIQUE	VALUE
CHRISTENSEN, E. M., ET AL. (1967a)	SURVEYOR I STRAIN GAGE RECORDS UPON LANDING	DIRECT AND SIMULATED	RIGID SURFACE LANDING SIMULATION AGREES WELL WITH SURVEYOR I DATA
SCOTT, R. F., ET AL. (1967)		DIRECT	LITTLE CONCLUDED FROM IMPACT TESTS OF SMSS ON SURVEYOR III
CHRISTENSEN, E. M., ET AL. (1967b)	SURVEYOR III STRAIN GAGE RECORDS UPON LANDING	DIRECT	K ≃ 7,100 PSI (4.9×10^3 N/CM^2) (K EFFECTIVE SPRING CONSTANT)

PERMEABILITY

REFERENCE	BASIS	TECHNIQUE	VALUE
CHRISTENSEN, E. M., ET AL. (1967c)	CALCULATED FROM FIRING OF VERNIER ENGINES ON THE SURVEYOR V	DIRECT	1×10^{-8} - 7×10^{-8} CM^2 TO DEPTH OF 25 CM

TABLE 2-1 CONT.

ERODABILITY

REFERENCE	BASIS	TECHNIQUE	VALUE
CHRISTENSEN, E. M., ET AL. (1966)	SURVEYOR I WOULD HAVE BEEN AFFECTED BY DEPOSITION OF LUNAR MATERIAL BUT WAS NOT	DIRECT	NO SOIL DISTURBANCE OBSERVED UPON FIRING SURVEYOR I CONTROL JET
CHRISTENSEN, E. M., ET AL. (1967b)	SURVEYOR III FIRED VERNIERS CLOSE TO LUNAR SURFACE DURING LANDING BUT NOT AFFECTED BY DEPOSITION OF DUST	DIRECT	EROSION HAZARD DURING LANDING OF FUTURE SPACECRAFT NOT AS SEVERE AS HAD BEEN ANTICIPATED
CHRISTENSEN, E. M., ET AL. (1967d)	PARTICLES MOVED BY DIFFUSED GAS BLOWOUT AND VISCOUS EROSION (PREDOMINANTLY BY BLOWOUT)	DIRECT	SOME SOIL MOVEMENT WHEN VERNIER ENGINES ON SURVEYOR V WERE FIRED, BUT NO FUNCTIONAL EFFECTS WERE OBSERVED ON SPACECRAFT

REFERENCES

1. "A Preliminary Geologic Evaluation of Areas Photographed by Lunar Orbiter V Including an Apollo Landing Analysis of One of the Areas," Langley Working Paper, Langley Research Center Langley Station, Hampton, Va., LWP-506, February 1968.

2. Blum, P., et al. (1967), "Properties of Powder Ground in Ultra High Vacuum," NASA CR-66276, March.

3. Campbell, M. J., et al. (1968), "Density of Lunar Surface," Science, v. 159, n. 3818, March 1.

4. Cherkasov, I. I., et al. (1967), "First Panoramas of Luna 13," NASA, ST-LPS-LSL-10640, August 25.

5. Choate, R. (1966), "Lunar Slope Angles and Surface Roughness from Ranger Photographs," Proc. Fourth Symposium on Remote Sensing of Environment, U. of Michigan, p. 411-432, June. (Also published as JPL Technical Report 32-994).

6. Christensen, E. M., et al. (1966), "Lunar Surface Mechanical Properties," Surveyor I Mission Report — Part II: Scientific Data and Results, NASA, TR 32-1023, September 10.

7. Christensen, E. M., et al. (1967a), "Lunar Surface Mechanical Properties — Surveyor I," Journal of Geophysical Research, v. 72, n. 2, January 15.

8. Christensen, E. M., et al. (1967b), "Lunar Surface Mechanical Properties," Surveyor III — A Preliminary Report, NASA, SP-146, June.

9. Christensen, E. M., et al. (1967c), "Lunar Surface Mechanical Properties," Surveyor V Mission Report — Part II: Science Results, NASA TR 32-1246, November 1.

10. Christensen, E. M., et al. (1967d), "Surveyor V," Science, v. 158, n. 3801, November 3.

11. de Wys, J. N. (1967a), "Lunar Surface Electromagnetic Properties: Magnet Experiment," Surveyor V Mission Report — Part II: Science Results, NASA TR 32-1246, November 1.

12. de Wys, J. N. (1967b), "Surveyor V," Science, v. 158, n. 3801, November 3.

13. Filice, A. L. (1967a), "Lunar Surface Strength Estimate from Orbiter II Photograph," Science, v. 156, n. 3781, June 16.

14. Filice, A. L. (1967b), "Observations on the Lunar Surface Disturbed by the Footpads of Surveyor I," Journal of Geophysical Research, v. 72, n. 22, November 15.

15. Halajian, J. D. (1966), "Mechanical, Optical, Thermal, and Electrical Properties of the Surveyor I Landing Site," Grumman Aircraft Engineering Company, Report No. AS 424-4, November.

16. Halajian, J. D., et al. (1967), "Correlation of Thermal and Mechanical Properties of Lunar Surface," Transactions American Geophysical Union, v. 48, n. 1, March.

17. Hapke, B. (1968), "Lunar Surface: Composition Inferred from Optical Properties," Science, v. 159, n. 3810, January 5.

18. Heuzé, F. E. (1968), "Lunar Stratigraphy as Revealed by Crater Morphology. A Critical Review," NASA CR-61219, April.

19. Jaffe, L. D. (1966a), "Lunar Dust Depth in Mare Cognitum," NASA, TR 32-896, March 30.

20. Jaffe, L. D. (1966b), "Lunar Overlay Depth in Mare Tranquillitatus, Alphonsus, and Nearby Highlands," NASA, TR 32-1021, September.

21. Jaffe, J. D., et al. (1966c), "Lunar Surface Strength: Implications of Luna 9 Landing," Science, v. 153, n. 3734, July 22.

22. Jaffe, L. D. (1967a), "Lunar Surface Stength," Icarus, International Journal of the Solar System, v. 6, n. 1, January.

23. Jaffe, L. D. (1967b), "Surface Structure and Mechanical Properties of Lunar Maria," Journal of Geophysical Research, v. 72, n. 6, March 15.

24. Lipskiy, Y. N., et al. (1967), "Luna 13 Is on the Moon," NASA, ST-PR-LPS-10 545, January 4.

25. Mitchell, J. K. (1964), "Current Lunar Soil Research," Journal of the Soil Mechanics and Foundation Division, ASCE, v. 90, n. SM3, p. 53-83, May.

26. Nordmeyer, E. F. (1967), "Lunar Surface Mechanical Properties Derived from Track Left by Nine Meter Boulder," MSC Internal Note No. 67-Th-1, NASA, February.

27. Oberbeck, V. R., et al. (1967), "Estimated Thickness of a Fragmental Surface Layer of Oceanus Procellarum," Journal of Geophysical Research, v. 72, n. 18, September.

28. O'Keefe, J. A., et al. (1967), "Chondrite Meteorites and the Lunar Surface," Science, v. 158, n. 3805, December 1.

29. Rennilson, J. J., et al. (1966), "Lunar Surface Topography," Surveyor I Mission Report — Part II: Scientific Data and Results, NASA, TR 32-1023, September 10.

30. Scott, R. F., et al. (1967), "Soil Mechanics Surface Sampler: Lunar Surface Tests and Results," Surveyor III — A Preliminary Report, NASA, SP-146, June.

31. Shoemaker, E. M., et al. (1967), "Television Observations from Surveyor V," Surveyor V Mission Report — Part II: Science Results, NASA, TR-1246, November 1.

32. Smoluchowski, R. (1966), "Structure and Coherency of the Lunar Dust Layer," Journal of Geophysical Research, v. 71, n. 6, March 15.

33. Turkevich, A. L., et al. (1967a), "Chemical Analysis of the Moon at Surveyor V Landing Site: Preliminary Results," Surveyor V Mission Report — Part II: Science Results, NASA, TR 32-1246, November 1.

34. Turkevich, A. L., et al. (1967b), "Surveyor V," Science, V. 158, n. 3801, November 3.

C H A P T E R 3

MATERIALS PROPERTIES EVALUATIONS

FROM BOULDER TRACKS ON THE LUNAR SURFACE

by

James K. Mitchell and Scott S. Smith

CHAPTER 3

MATERIALS PROPERTIES EVALUATIONS FROM BOULDER TRACKS ON THE LUNAR SURFACE

(James K. Mitchell and Scott S. Smith)

I. INTRODUCTION

Photographs provided by Lunar Orbiters have shown that a number of areas show distinct tracks formed as a result of large boulders rolling and sliding on the lunar surface. To data several hundred tracks have been identified. These tracks appear to be of three different types, i.e. (1) regular, continuous tracks such as might be formed by an approximately spherical boulder rolling over a compressible and/or displaceable surface layer, Fig. 3-1; (2) segmented tracks suggestive of boulder movement by a bouncing or skipping action, Fig. 3-2; and (3) relatively short tracks suggestive of a plowing or skidding action, Fig. 3-3.

Study of these tracks is of interest from two standpoints which may be stated in the form of two questions:

1. What processes set the boulders in motion?
2. What information can be deduced about the physical properties of the boulders and soils over which they rolled?

Although no attention has as yet been directed by us to the study of the first question, possible mechanisms might include:

1. The boulders forming the tracks are ejecta from primary and secondary craters.
2. The boulders, originally resting on lunar slopes, were set in motion by ground motions caused by seismic or meteorite impact events.
3. Motion of the boulders, originally at rest on the lunar surface, was initiated through loss of support resulting from some type of lunar "erosion" or "weathering" process.

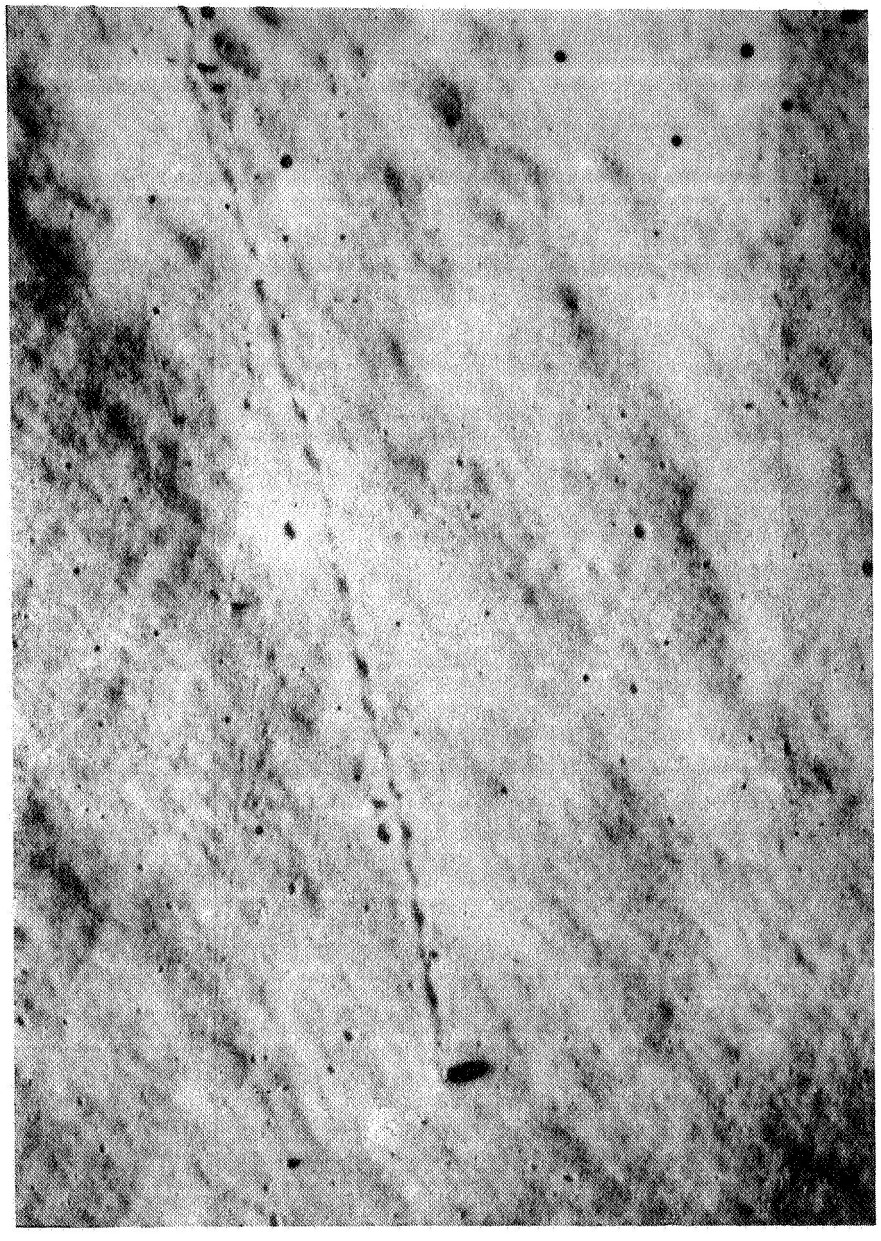

FIG. 3-1. Continuous Boulder Track

FIG. 3-2. Segmented Boulder Track

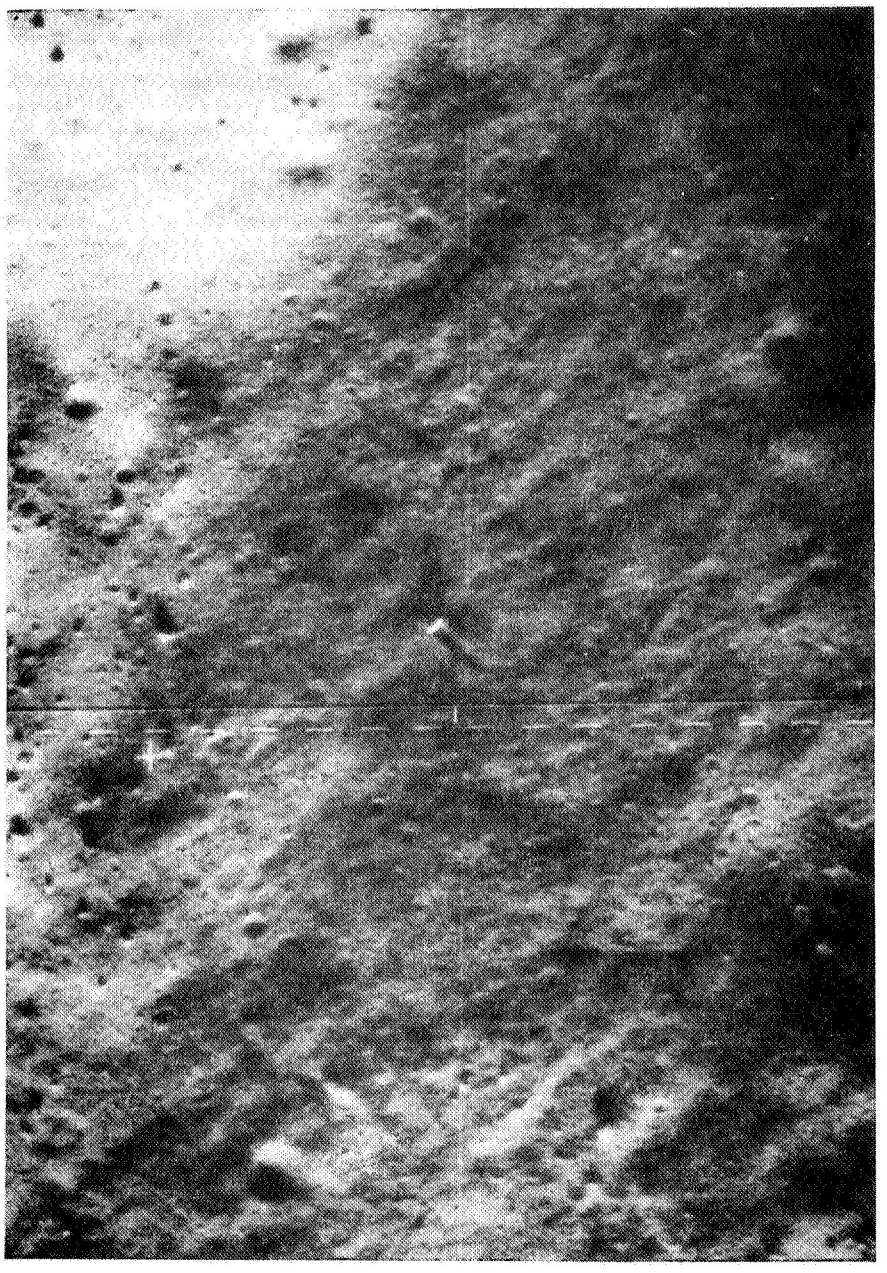

FIG. 3-3. Boulder Track Caused by Plowing or Skidding

With respect to the second question, the deduction of soil and boulder properties, a few analyses have been published (Nordmeyer, 1967; Filice, 1967; Eggleston, 1967) and some additional analysis has been made by us. Attention has been directed only at the regular and continuous type of track. The nature of these analyses, the results obtained, and the potential for meaningful determination of soil and boulder properties through study of boulder track records are discussed in this section.

II. ANALYSIS DIFFICULTIES

Insofar as we are aware a rational theoretical solution to the problem of the rolling of an essentially rigid spherical body on the surface of a deformable material has not yet been made. In the case of highly compressible surface materials, it might be anticipated that both sinkage and bulldozing deformations would result from the action of the rolling boulder. For incompressible soils both displacement along a line parallel to the track as a result of bearing capaity failure and bulldozing action might be important. Track cross sections corresponding to the first type of deformation should be as shown by Fig. 3-4(a), whereas, those for the second type should appear as in Fig. 3-4(b). Thus careful study of whether or not the tracks visible in Orbiter photographs have raised rims should be indicative of the compressibility characteristics of lunar soils. Based on Surveyor results it would be anticipated that raised rim tracks should be the rule provided the surface material in the boulder track areas is similar to that at the Surveyor sites. While some tracks with raised rims have been identified, no systematic study has yet been made.

Proper theoretical description of the boulder-surface interaction process could be expected to require specific knowledge of the following variables and parameters:

1. Boulder size and shape
2. Track cross section profile
3. Surface slope
4. Boulder velocity
5. Boulder density
6. Soil density

FIG. 3-4 (a). Cross Section of Boulder Track in Highly Compressible Soil

FIG. 3-4 (b). Cross Section of Boulder Track in Incompressible Soil

7. Soil compressibility
8. Soil strength and stress-deformation characteristics

It is conceivable that, with the aid of appropriate experimentation and theoretical analysis, relationships could be developed which would provide a quantitative description of the mechanisms of track formation. The application of these relationships to lunar boulder tracks could then provide quantitative information on boulder and/or soil properties. The theory so obtained would also be of use for study of the general problem of wheel-soil interaction.

If it is assumed that development of such relationships is an attainable objective, then their application to the study of Lunar Orbiter photographs will still be limited rather severely because:

1. The resolution of Orbiter photographs is insufficient to provide highly accurate values of boulder size and shape or of track cross section characteristics.
2. Slope angles cannot be determined with high precision.
3. The number of soil and rock properties will exceed the number of independent relationships so that computation of any one property will require assumptions for other properties.

It appears, therefore, that as applied to Lunar Orbiter data, boulder tracks analyses can best be used for assessment of the uniformity of different areas and the variability in properties from location to location on the moon. For this purpose use of the same method of analysis and assumed values for soil and rock properties is required for all sites. On the other hand tracks left by rolling stones at Surveyor sites and those that may be encountered during Apollo missions may be useful for more specific quantitative study. This is so because of greater photographic resolution, more precise knowledge of slope angles, and more specific knowledge of pertinent properties and stratigraphy that will be available.

III. ANALYSIS OF THE SABINE D ROLLING BOULDER

The boulder track that has been given the most study in an effort to determine properties is that found in the high resolution Orbiter II photography of the Sabine D crater (Nordmeyer, 1967; Filice, 1967; Eggleston, 1967). A review of the published analyses as well as some further analysis done by us is useful for illustration of (1) the variability in answers that may be obtained when different theories are applied to analysis of the same data, (2) the necessity for assuming a number of properties in order to estimate some other property, and (3) the types of analysis methods that might be useful.

A photograph of the Sabine D track is shown in Fig. 3-1. A profile of the slope, determined using photoclinometry, is given in Fig. 3-5. The average slope angle along the path of the boulder is approximately 30°. The boulder was determined to be approximately nine meters in diameter and nearly spherical in shape. The track width averaged five meters and was nearly uniform along its length. Lunar gravity is taken as 1/6 that of the value for earth; i.e. 5.4 ft per sec^2 = 163 cm per sec^2. These values are used in the following analyses. It should be noted that the estimates of the boulder size and shape, the track width, and the slope angle cannot be considered precise, and, in fact, may be in error by a significant amount. Dimensions are probably no closer than ± 0.5 m.

A. Static Bearing Capacity Method

Nordmeyer (1967) assumed that the boulder was supported by the forward half of the buried segment of the boulder as it slowly rolled downhill; i.e., by the segment AB shown in Fig. 3-6. Values of soil properties were assumed as follows:

Cohesion, $c = 0.05$ psi

Angle of friction, $\phi = 33°$

Density, $\rho = 1.55$

The Terzaghi bearing capacity equation for a square or circular footing,

$$Q_{ult} = \pi R^2 (1.3\ cN_c + z\rho gN_q + 0.6\ \rho gRN_\gamma) \qquad (3\text{-}1)$$

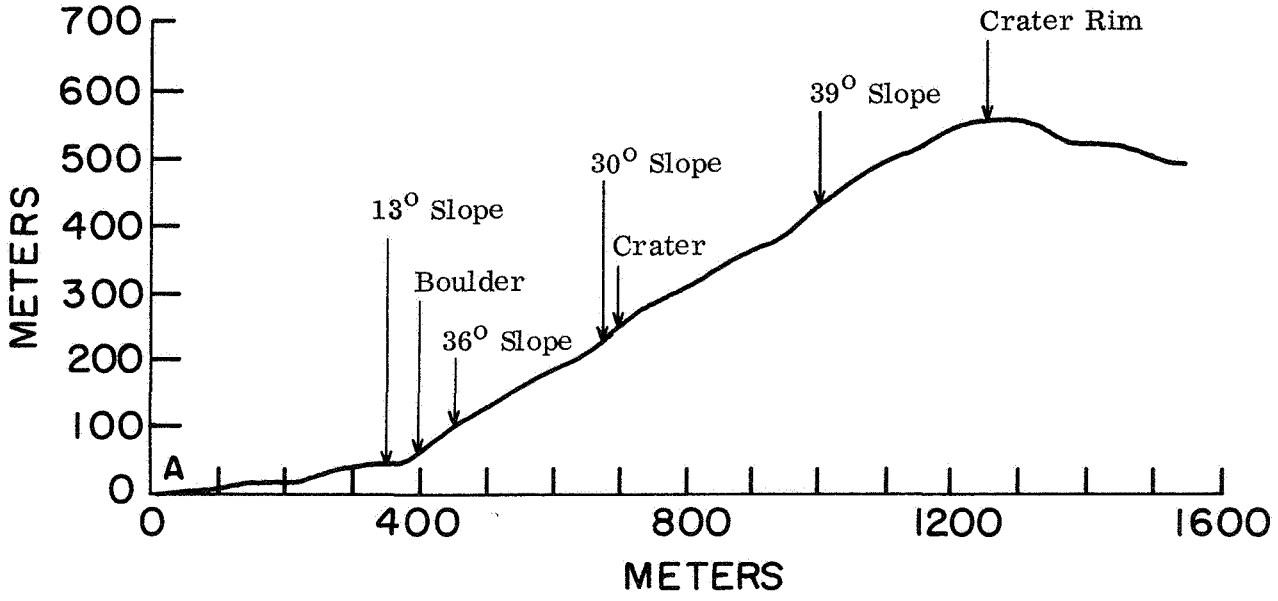

FIG. 3-5. Profile Down Wall of Crater Sabine D Along Track of Boulder

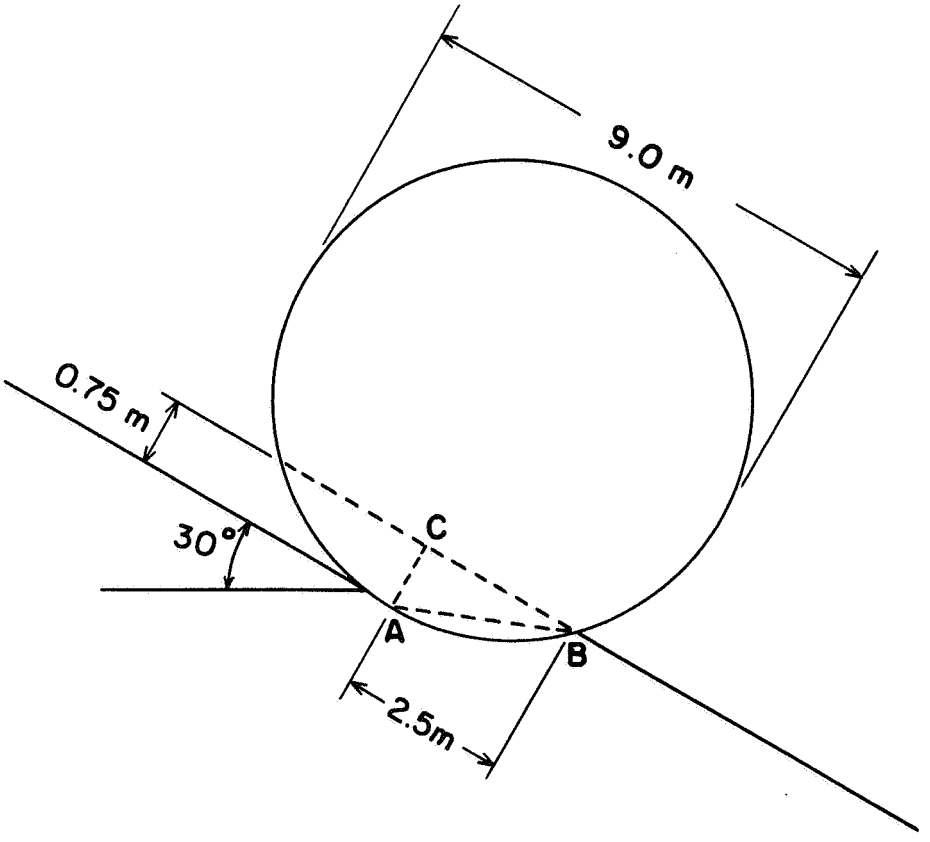

AB - Cord of Segment in Contact with Surface AC - Depth of Track

FIG. 3-6 . Boulder Rolling Down Crater Wall

where R = radius of footing and N_c, N_q, and N_γ are bearing capacity factors, was used to estimate the supported weight of the boulder Q_{ult}. Then using the known volume of boulder, a boulder density of 2.6 gm/cm^3 was calculated for the boulder considered to be lying on a horizontal surface; whereas, 2.7 gm/cm^3 was obtained for a surface inclined at 30°.

An alternative analysis was made by us considering the boulder to represent a loaded footing located on the face of a slope and using the analysis presented by Meyerhof (1957). According to Meyerhof the ultimate unit bearing capcity for a rough strip footing is given by

$$q_{ult} = cN_{cq} + \rho g \frac{B}{2} N_{\gamma q} \qquad (3\text{-}2)$$

where N_{cq} and $N_{\gamma q}$ are bearing capacity factors dependent on the depth of footing, the angle of internal friction and the slope inclination, and B is the width of footing. Reference to Fig. 3-6 indicates that distance AB may be a reasonable assumption for the width of footing. Since the base of the boulder represents a circular rather than a strip footing, Equation 3-2 should be modified to

$$q_{ult} = 1.2\ cN_{cq} + 0.6\ \rho g B\ N_{\gamma q} \qquad (3\text{-}3)$$

From later Surveyor results it is now known that values of c - 0.1 psi and $\phi = 37°$ are more reasonable than those used by Nordmeyer. Unfortunately Meyerhof (1957) only gives values of $N_{\gamma q}$ for the case of c = 0 and values of N_{cq} for the case of $\phi = 0$ for footings on slopes. However since the cohesion is relatively small the first term in Equation 3-3 can probably be neglected without too great a loss in accuracy.

With these assumptions and further assuming that the boulder is supported by a circular area with $\overline{AB}$ (Fig. 3-6) as a diameter* and that

---

*This is not strictly correct since the bearing area under conditions shown by Fig. 3-6 will be elongate normal to the plane shown.

the sinkage to diameter ratio is 0.3, then the bearing capacity may be computed. For $\phi = 37°$, a slope angle of 30°, $N_{\gamma q} = 38$, and $\overline{AB} = 289$ cm, we obtain

$$q_{ult} = 0.6 \times 289 \times 38 \times (\rho g) = 6600\ \rho g\ gm/cm^2$$

The value of ρg, the unit weight of the soil, may be taken the same as used by Nordmeyer (1); i.e., 1.55 gm/cm^3 (earth gravity) or 0.258 gm/cm^3 (lunar gravity). Thus the bearing capacity becomes 1700 gm/cm^2 in the lunar gravity field. The total force that can be supported by the soil is given by this unit capacity times the bearing area or 11.2×10^7 gm. The volume of a sphere nine meters in diameter is 382×10^6 cm^3, thus the maximum unit weight of boulder of this size that could be just supported by the soil on a 30° slope would be

$$\gamma = \frac{11.2 \times 10^7}{38.2 \times 10^7} = 0.293\ gm/cm^3$$

Such a boulder would have a specific gravity of only 1.76, a value that appears unreasonably low, at least by comparison with terrestrial rocks.

On the other hand it could more rationally be argued, since the boulder is known to have rolled down the 30° slope rather than to have been supported as assumed in the analysis, that the Meyerhof analysis simply shows that a boulder of more reasonable specific gravity, say 2.5 — 3.0, would not be expected to be stable on the 30° slope.

The profile in Fig. 3-5 indicates that the boulder came to rest on a 13° slope. For this slope angle the value of $N_{\gamma q}$ is 80. For this condition the soil could support 23.6×10^7 gm, and the corresponding value of boulder specific gravity becomes 3.70. This value is high compared with the specific gravity of terrestrial rocks. Unfortunately values of $N_{\gamma q}$ are very sensitive to small variations in both the friction

angle of the soil and the slope angle. It is evident, therefore, that any type of boulder track analysis based on bearing capacity factors can be only approximate at best unless the track dimensions, bearing areas, and soil or boulder properties are quite accurately known.

Felice (1967) made a lower bound extimate of the bearing capacity of the soil under the boulder by assuming that the average width of track approximates the diameter of a circle, the front half of which supports the boulder. He assumed a boulder density of 2.7 gm per cm^3. On this basis a minimum bearing capacity of 25 pounds force per sq in. (17.2 newtons per sq cm) is obtained. This value represents the absolute minimum required to support a boulder of the assumed density and bearing area. From the Meyerhof theory, however, if the soil has Surveyor soil properties, then more reasonable bearing capacity values of 20.9 and 44.0 psi are obtained for 30° and 13° slopes, respectively.

Eggleston (1967) also made a static analysis. However, the weight of the boulder was assumed supported by the full surface area of the spherical segment on which the boulder rests. On this basis an even lower value of bearing capacity for a boulder density of 2.7 gm per cm^3 is estimated.

B. Work of Compression Method

Nordmeyer (1967) assumed the boulder to be rolling downhill slowly at constant velocity, and that the work done as it rolls downhill is equal to the work done in compressing the soil. With the same soil property assumptions as used in his analysis of the static bearing capacity, he obtained a value of boulder density of 1.2 gm per cm^3. This value appears unreasonably low in the light of data now available on lunar soil and rock properties.

C. Constant Rolling Velocity Analysis

Recent tests carried out at the University of Michigan reported by Gray (1967) have established unique empirical relationships between track dimensions, soil properties, rolling sphere characteristics, and the slope angle of a bed of sand necessary to obtain constant velocity

rolling of the sphere. Fig. 3-7 shows the slope angle, sin α, required for constant sphere velocity as a function of the parameter $(2/3\ \pi)\ \sin^{-1}\left(\frac{b}{D}\right)$ where b is the track width and D is the sphere diameter. It may be seen that this relationship is independent of the sand density. It is not, however, independent of friction angle or sphere density, as would appear at first glance, since α depends on these variables; i.e., the slope angle must be varied to obtain a constant velocity for different sands or sphere densities.

Fig. 3-8 shows the relationship between slope angle for constant velocity, sand friction angle, and specific gravity of sphere. It should be noted that while these relationships appear unique and well established by the data, they are empirical.

These figures may be used to estimate the density of the Sabine D rolling boulder. For a track width of 5 meters and boulder diameter of 9 meters, Fig. 3-7 yields a value of about 0.46 for sin α, and the slope angle for constant rolling velocity would be 27.5°. Thus the boulder should have accelerated on slopes greater than 27.5°, and decelerated on slopes flatter than 27.5°. If velocity was constant and the track width was 5 meters as the boulder passed along a 27.5° region of the slope, then from Fig. 3-8, assuming Surveyor soil (ϕ = 37°), the boulder density would have to be of the order of 3.0 gm/cm^3. This value is quite reasonable, and further study of relationships such as shown in Figs. 3-7 and 3-8 would appear desirable for application to the lunar rolling stone problem.

D. Analysis by Trafficability Methods

Another approach to the analysis of the rolling boulder — soil interaction problem is within the framework of existing methods of trafficability analysis by considering the boulder analogous to a rolling wheel. Three such methods were examined in terms of their suitability for deducing soil properties.

1. Rigid wheel analysis. An empirical relationship has been developed by the U. S. Army Engineer Waterways Experiment Station (Freitag, 1965) which relates the drawbar pull to wheel and soil parameters for a rigid wheel in a frictional soil; i.e.,

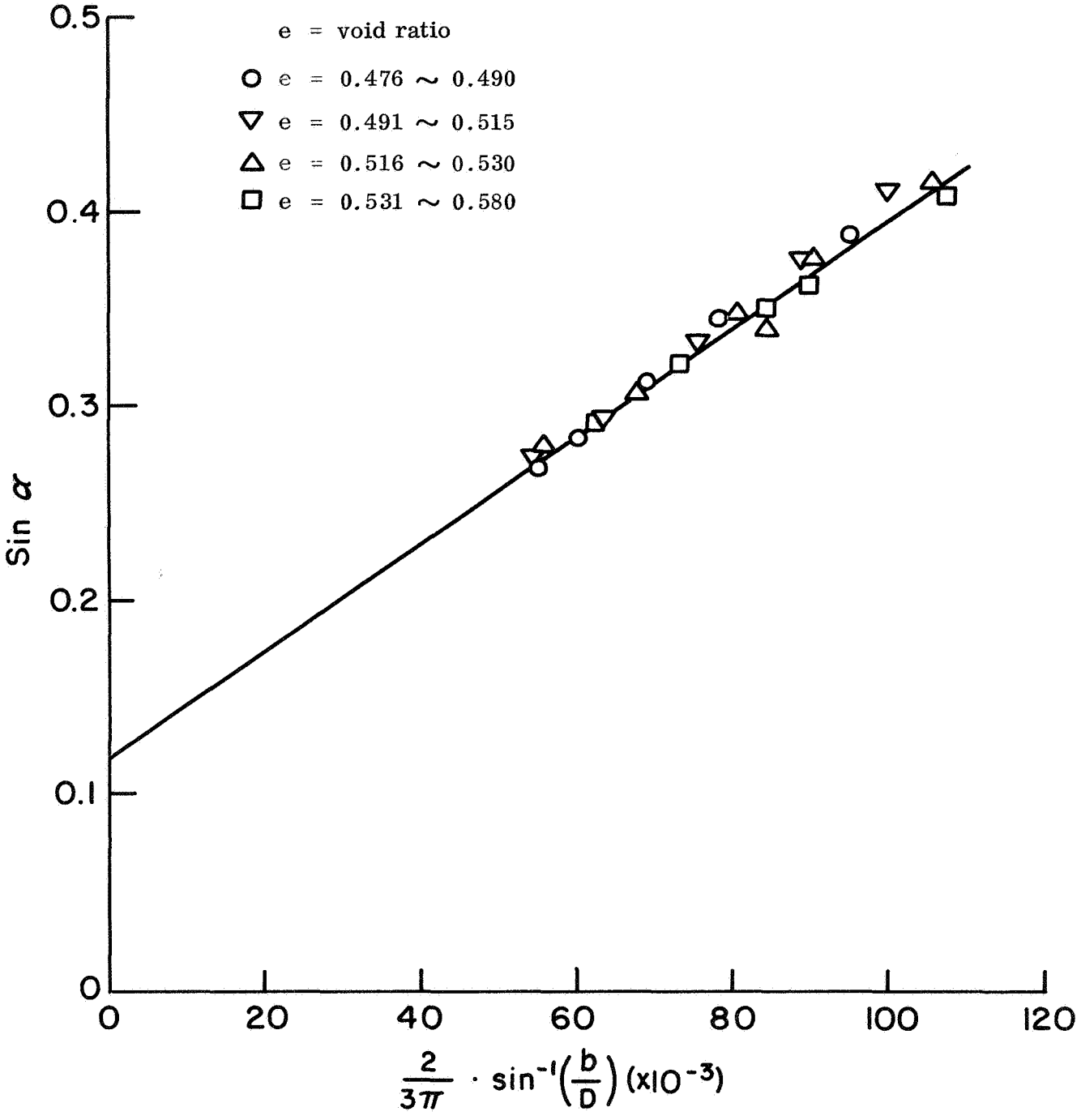

FIG. 3-7. Slope Angle as a Function of Track Width for Constant Velocity Rolling of Sphere on Sand

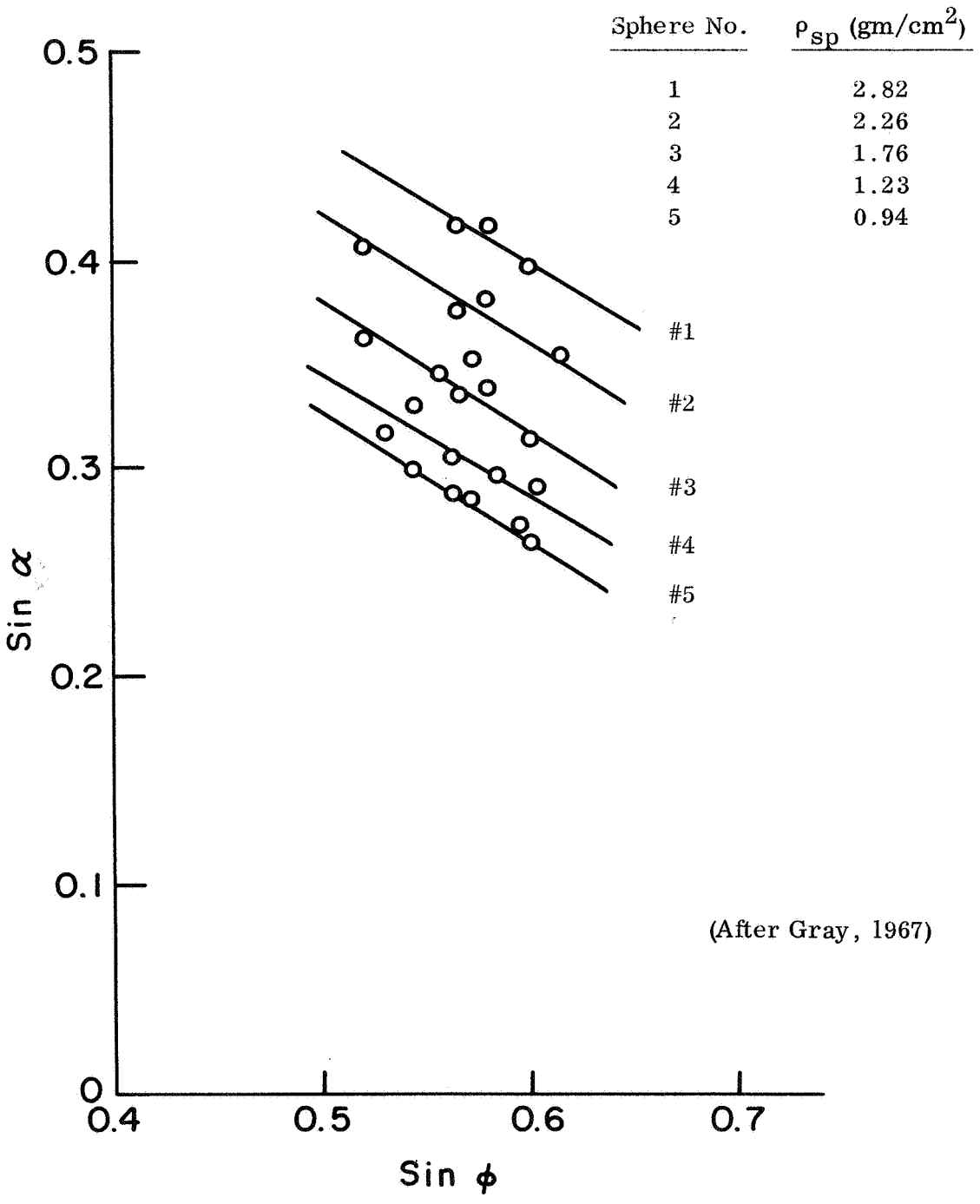

FIG. 3-8. Slope Angle, Friction Angle, Sphere Density Relationship for Constant Velocity Rolling on Sand

$$\frac{P_T}{W} = \frac{8}{G}\left(\frac{W^{1/2}}{b^{1/2}d}\right) \qquad (3\text{-}4)$$

where:

P_T = pull on wheel
W = load on wheel
G = cone index gradient
b = wheel section width
d = wheel diameter

For application to the rolling boulder problem the wheel section width to wheel diameter ratio must be considered. Only when the sinkage of the wheel is such that its soil contact area approximates in shape that of the soil contact area of the boulder is the analysis of the rigid wheel developed by the WES approximately comparable to the boulder problem. The contact area geometries for a rigid wheel and for a spherical boulder are compared in Fig. 3-9.

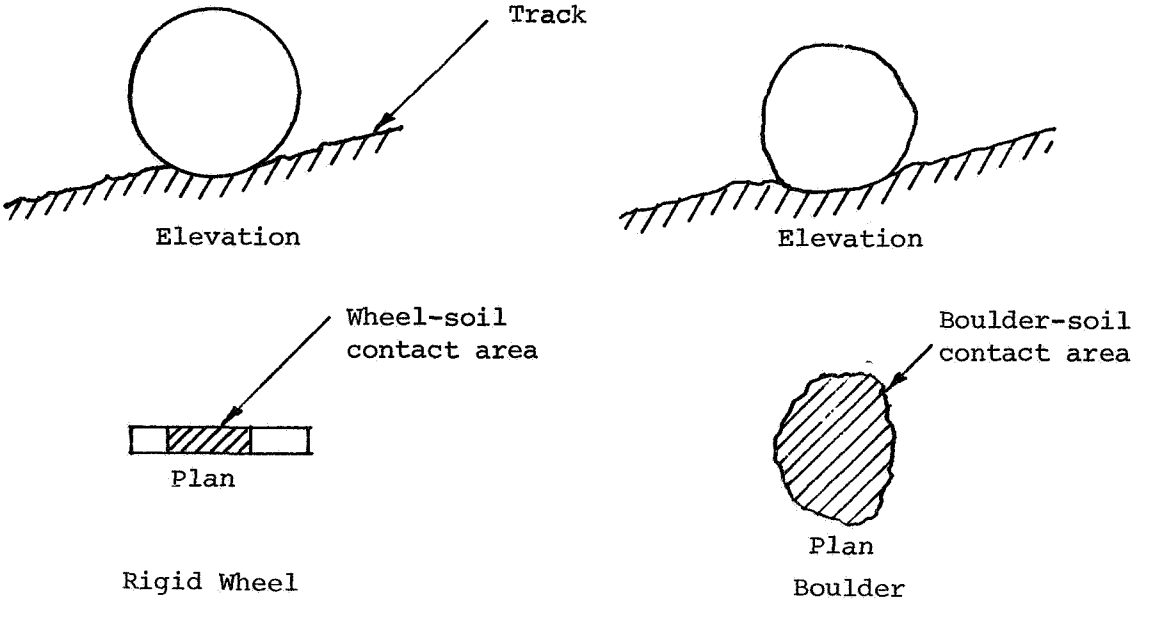

FIG. 3-9. Comparison of Contact Area Geometry for Rigid Wheel and Spherical Boulder.

Assuming that the contact areas are approximately equal and that P_T is the component of boulder weight parallel to the slope, W is the component of boulder weight normal to the slope, b is the track width and d is the boulder diameter, the cone index gradient for the lunar soil can be estimated by means of Equation (A-6), Chapter 1, Volume III, if it is noted that G = C/Z. For the Surveyor soil conditions n = 1, k_ϕ = 5, and k_c = 0 have been suggested by Scott;* thus G is computed to be 5 lb/in.^{3} (earth gravity). If the boulder weight is denoted by W_B, Equation 3-4 becomes, for any slope angle, α

$$\frac{W_B \sin \alpha}{W_B \cos \alpha} = \frac{8}{5} \frac{\left(W_B \cos \alpha\right)^{1/2}}{\left(\frac{500}{2.54}\right)^{1/2} \frac{900}{2.54}}$$

which reduces to

$$W_B = 9.6 \times 10^6 \frac{\tan^2 \alpha}{\cos \alpha} \qquad (3\text{-}5)$$

With the aid of this relationship and the known boulder volume, the boulder density (specific gravity) required for constant velocity rolling down a slope of any inclination may be computed. The results of this computation are shown in Fig. 3-10. It may be seen that the nature of this empirical relationship is such that the higher the density, the greater is the slope angle needed for constant velocity rolling, probably because of the greater sinkage accompanying the density increase. Since Equation 3-4 was developed for wheels rather than spherical bodies, it is not likely that it should hold exactly for the rolling boulder. Nonetheless, it is significant to note from Fig. 3-10 that for Surveyor type soil and an average slope angle of 30°, as for the Sabine D crater, a boulder density of 4.4 gm/cm^3 is obtained. This value appears to be unreasonably high. If constant velocity rolling is

---

*Scott, R. F., Personal communication, May 1968.

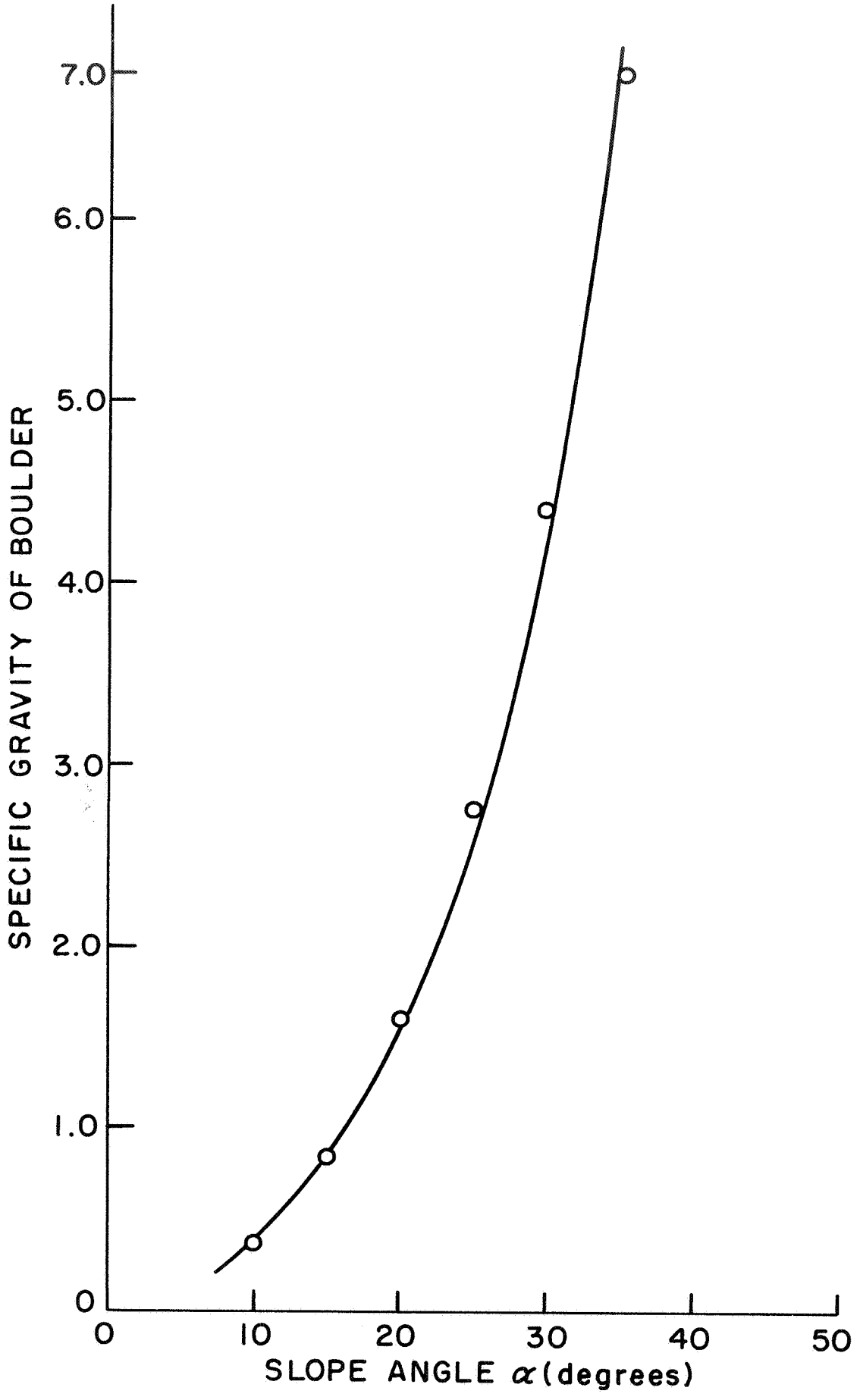

FIG. 3-10. Relation Between Boulder Density and Slope Angle for Constant Velocity Rolling According to WES Empirical Equation

developed at a slope angle of 27.5°, as suggested by Analysis 3, then a value of about 3.5 gm/cm^3 is obtained, which is still somewhat high in comparison with values reported from Surveyor test results.

2. Soil value system analysis. The Bekker soil value system may be used to estimate the boulder density. With the aid of Equation 3-1, Bekker (1960) has developed the following equation:

$$N = \frac{bK\sqrt{dZ}}{3} Z^n(3 - n) \qquad (3\text{-}6)$$

where:

N = force normal to soil

$K = \left(\frac{k_c}{b} + k_\phi\right)$

d = wheel diameter

b = wheel section width

Z = sinkage

n = soil constant

Again assuming the Surveyor soil properties as estimated by Scott, $k_c = 0$, $k_\phi = 5$, and $n = 1$, and noting that for the boulder, $b = 500$ cm, $Z = 75$ cm, and $d = 900$ cm, Equation 3-b becomes

$$W_B \cos \alpha = \left(\frac{1}{3}\right) \frac{500}{2.54} (5) \sqrt{\frac{900 \times 75}{2.54 \times 2.54}} \left(\frac{75}{2.54}\right) \times 2$$

$$W_B \cos \alpha = 1.98 \times 10^6 \text{ lb force}$$

For a 30° slope $W_B = 2.29 \times 10^6$ lb and the corresponding density of boulder (specific gravity) is 2.72. This value is very reasonable. The value, however, is sensitive to the value chosen for n. If, for

example, n had been taken as 0.5, then a value of boulder density of only 0.392 would be computed. Thus this method can be expected to be reliable only if accurate values of n are available.

3. Similitude analysis. In Volume III, Chapter 1, of this report, a similitude approach to analysis of soil-wheel interaction was outlined. It was noted that a dimensionless number could be used to characterize behavior. For sands the sand mobility number was used, $G(bd)^{3/2}(\delta/h)/W$. Such a relationship cannot be used directly because the (δ/h) term, tire deflection divided by section height, does not have meaning when applied to a rolling boulder. On the other hand Green (1967) has presented correlations between the sand loading number, $G(bd)^{3/2}/W$, and various performance factors for single wheels. The correlations were developed from the results of tests on one sand (Yuma sand) using different tires inflated to give different deflections. The sand was placed at different densities so that values of cone index gradient in the range of 0.7 to 8.3 could be studied. Fig. 3-11 shows the sinkage coefficient vs δ/h for several values of $G(bd)^{3/2}/W$. These curves can be extrapolated to $\delta/h = 0$ and corresponding values of sand loading number and sinkage number read off to give the relationship shown in Fig. 3-12.

The results in Fig. 3-12 may be applied to the Sabine D boulder by noting that from the boulder track and boulder size, $Z/d = 0.75/9.0 = 0.0833$. Thus the corresponding value of sand loading number is 175. Knowing that G = 5, b = 197" (500) cm), and d = 354" (900 cm) the weight of boulder normal to the slope is computed as 0.525×10^6 lb. For a 30° slope the boulder weight would then be 0.606×10^6 lb. From the known volume of boulder, a specific gravity of 0.72 is obtained. This value is inordinantly low and casts doubt on the applicability of the method. It is not surprising, however, that a questionable result is obtained since the correlations used were based on the results of tests with pneumatic tires. It was shown in Volume III, Chapter 1, that the similitude correlations developed for pneumatic tires were not adequate to account for the behavior of proposed lunar vehicle wheels. It appears that they are equally invalid when applied to rolling boulders.

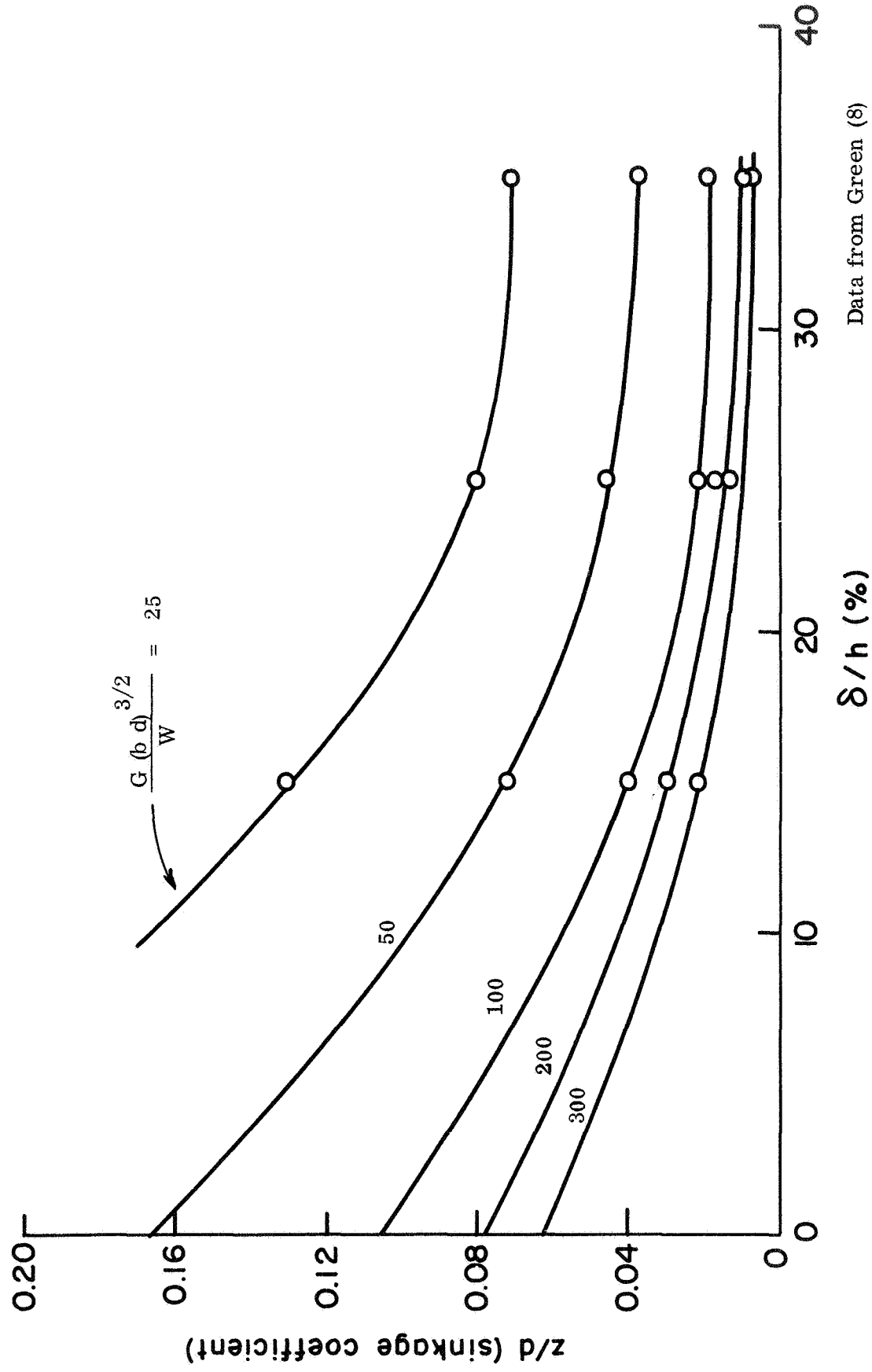

FIG. 3-11. Sinkage Coefficient versus Tire Deflection for Single Wheels on Yuma Sand

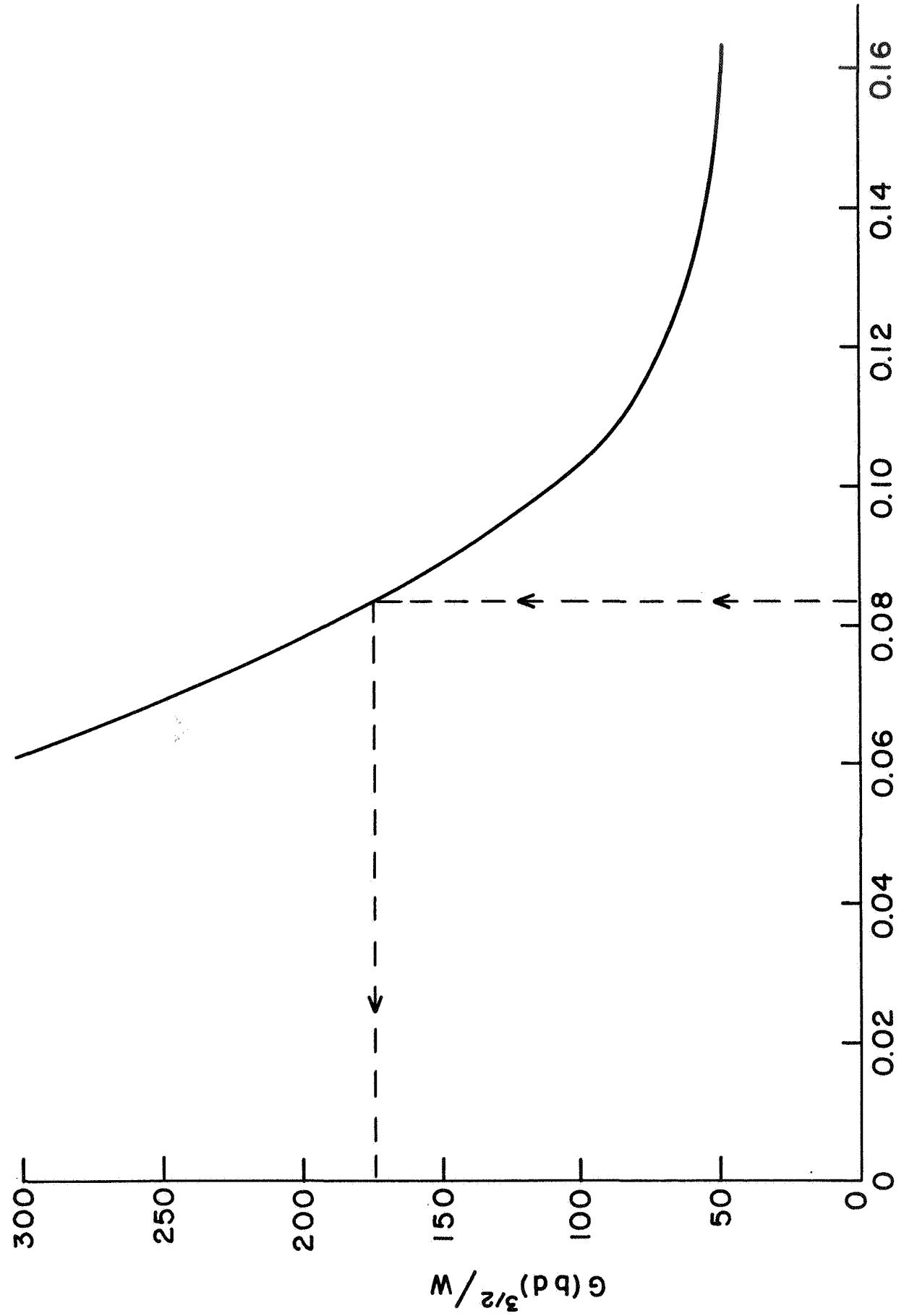

FIG. 3-12. Sand Loading Numbers versus Sinkage Coefficient for $\delta/h = 0$

IV. CONCLUSION

The analysis of boulder tracks on the lunar surface should be potentially rewarding in terms of yielding information on soil and rock variability in the areas covered by Orbiter photography. Reasonable quantitative determinations should be possible in those cases where relatively accurate values of boulder size, track shape and sinkage, and slope angle can be obtained, as should be the case for some of the Surveyor results, and as will be possible during Apollo missions. Theoretical and experimental studies are desirable in order that a rational analytical framework may be developed. The results will be useful not only for boulder track analysis, but also for study of the trafficability problem.

The Sabine D boulder track has been analyzed using several methods in addition to those already presented in the literature (Nordmeyer, 1967; Filice, 1967; Eggleston, 1967). The results of these analyses are summarized in Table 3-1. It is shown by means of Meyerhof's bearing capacity factors (Meyerhof, 1957) for footings on sand slopes that a boulder of specific gravity similar to that for terrestrial rocks; i.e., 2.7 – 3.0, would be unstable on a 30° slope having Surveyor soil characteristics. On the other hand it would be stable on a 13° slope, the estimated slope on which the Sabine D boulder finally came to rest.

Analysis of the boulder within the framework of empirical correlations developed for constant velocity rolling of spheres down slopes of cohesionless soil (Gray, 1967) led to the very reasonable boulder density estimate of 3.0. From application of an empirical equation developed to describe the rolling resistance of a rigid wheel in sand (Freitag, 1965), a boulder density of 3.5 was obtained. An estimate obtained using trafficability relationships based on the soil value system (Bekker, 1960) gave a density of 2.7 for an assumed value of n equal to 1. An analysis based on similitude relationships for trafficability (Green, 1967) gave an unrealistically low value for density. In all cases the estimates involved a number of approximations and assumptions. Whatever the final methods selected for boulder track analysis, it will be imperative that the same method be applied in the same manner to all tracks if meaningful comparative

TABLE 3-1

ANALYSIS RESULTS — SABINE D BOULDER TRACK

Investigator	Analysis Method	Measured Input Data	Assumed Input Data	Derived Quantities
Nordmeyer (1967)	Static bearing capacity: $Q_{ult} = \pi R^2\left(1.3\ cN_c + d\rho g\ N_q + 0.6\ \rho g\ RN_\gamma\right)$	Bearing area, Boulder volume	c = 0.05 psi, ϕ = 33° soil density = 1.55	Boulder density = 2.6 (horizontal surface) Boulder density = 2.7 (30° slope)
Authors	Footing on slope (Meyerhof, 1957) $q_{ult} = cN_{cq} + \rho g \frac{B}{2} N_{\gamma g}$	Footing width, Bearing area	c = 0, ϕ = 37°, $(\rho g)_{soil}$ = 1.55 gm/cm^2	Boulder density = 1.76 on 30° slope Boulder density = 3.70 on 13° slope (Analysis shows that boulder of specific gravity ∿ 3.0 will roll on a 30° slope and come to rest on a 13° slope)
Filice (1967)	Lower bound bearing capacity. Front half of circular area under boulder supports boulder.	Bearing area	Boulder density = 2.70 gm/cm^3	Bearing capacity = 25 lb/in.^{2} (17.2 N/cm^2)
Eggleston (1967)	Static bearing capacity. Boulder supported by circular segment	Bearing area	Boulder density = 2.70 gm/cm^3	Bearing capacity
Nordmeyer (1967)	Work done in rolling = work of soil compression	Track dimensions, Boulder volume	c = 0.05 psi, ϕ = 33°, soil density = 1.55	Boulder density = 1.2 gm/cm^3
Authors	Empirical correlations by Gray (1967) between track dimensions, soil properties, sphere characteristics, sand slope angle for constant velocity rolling	Track width, Boulder diameter, Boulder sinkage	ϕ = 37°	Constant rolling velocity on 27.5° Slope of boulder density = 3.0 gm/cm^2
Authors	Rigid wheel in frictional soil. Freitag (1965) equation: $\frac{P_T}{W} = \frac{8}{G}\left(\frac{W^{1/2}}{b^{1/2}\ D}\right)$	Surveyor soil conditions, Boulder volume	Cone index gradient = 5 lb/in^3	Boulder density vs slope angle for constant rolling velocity
Authors	Bekker (1960) soil value system $N = \frac{bK\sqrt{DZ}}{3}\ Z^n(3-n)$	Track width, Boulder sinkage, Boulder diameter	$k_c = 0$, $k_\phi = 5$, n = 1	Boulder density = 2.72 for 30° slope
Authors	Similitude (Green, 1967) Sand loading number = $\frac{G(bD)^{3/2}}{W}$	Boulder sinkage, Boulder density	Boulder deflection = 0, Cone index gradient = 5 lb/in^3	Boulder density = 0.72 gm/cm^3

results are to be obtained. It is recommended that a rational theory for description of the mechanics of boulder track formation be developed for this purpose.

Finally, it should be noted that only regular, continuous tracks have been considered herin. Tracks formed by bouncing, skipping, and skidding boulders must be analyzed separately.

REFERENCES

1. Bekker, M. G. (1960), Off-the-Road Locomotion, University of Michigan Press.

2. Eggleston, J. M., et al. (1967), "Preliminary Investigation of a Lunar Rolling Stone," NASA, TMX-58007, March.

3. Filice, A. L. (1967), "Lunar Surface Strength Estimate from Orbiter II Photograph," Science, Vol. 156, No. 3781, pp. 1486-1487, June 16.

4. Freitag, D. R. (1965), "Wheels on Soft Soils — An Analysis of Existing Data," U. S. Army Waterways Experiment Station, T. R., No. 3-670, January.

5. Gray, D. H. (1967), Status Report to Land Locomotion Division, U. S. Army Tank-Automative Command, October 27 (letter report), on Contract DA-20-018-AMC-0980T.

6. Green, A. J. (1967), "Performance of Soils Under Tire Loads," U. S. Army Engineer Waterways Experiment Station, TR 3-666, Report 5, July.

7. Meyerhof, G. G. (1957), "The Ultimate Bearing Capacity of Foundations on Slopes," Proc. 4th Int. Conf. Soil Mech. and Found. Eng., Vol. 1, pp. 384-386, London.

8. Nordmeyer, E. F. (1967), "Lunar Surface Mechanical Properties Derived from Track Left by Nine Meter Boulder," NASA, MSC Internal Note No. 67-TH-1, February 28.

List of Symbols

b	track width
B	width of footing
c	cohesion
C	cone index
d	wheel diameter
D	sphere diameter
e	void ratio
g	acceleration at gravity
G	cone index gradient
h	tire section height
k_c, k_ϕ	soil parameters
K	coefficient = $k_c/b + k_\phi$
n	soil constant
N	force normal to soil
N_c, N_γ, N_q	bearing capacity factors
N_{cq}, $N_{\gamma q}$	bearing capacity factors
P_T	pull on wheel
q_{ult}	ultimate unit bearing capacity
Q_{ult}	ultimate bearing capacity as weight of boulder
R	radius
W	load on wheel
W_B	boulder weight
z	depth
Z	sinkage

α	slope angle
γ	unit weight
δ	tire deflection
ρ	density
ϕ	angle of friction

C H A P T E R 4

IMPACT RECORDS AS A SOURCE OF LUNAR SURFACE MATERIAL PROPERTY DATA

by

James K. Mitchell, Donald W. Quigley, and Scott S. Smith

CHAPTER 4

IMPACT RECORDS AS A SOURCE OF LUNAR SURFACE MATERIAL PROPERTY DATA

(James K. Mitchell, Donald W. Quigley, and Scott S. Smith)

I. INTRODUCTION

The use of impact penetrometers for remote determination of soil properties has been under study for some time, for both terrestrial and extra-terrestrial applications. A number of studies have been made to investigate the mechanics of dynamic penetration into soil and rock materials. Tests have been carried out for determination of characteristic signatures of instrumented penetrometers into soils of different types, and it appears feasible to determine in some detail the soil profile characteristics from the time-acceleration history recorded during a penetration event. Recent contributions to this subject, which deal with various aspects of penetrometer design and instrumentation, analysis of impact events, and analysis of data for determination of soil properties, have been made by McCarty and Garden (1968) and Womack and Cox (1967). These investigators have concerned themselves mainly with the development and application of instrumented penetrometers for remote area investigation.

The possibility exists as well that the results of certain natural lunar phenomena might be used for inference of surface material property data. Moore (1967) recognized from Lunar Orbiter photographs that many secondary impact craters exist which were formed by ejecta blocks thrown out during formation of primary craters. These observations led him to a study of the characteristics of these secondary craters and the development of a relationship between penetration depth and characteristics of the surface material and penetration. Naturally, in the analysis of this type of a record a number of assumptions are required. The data available are block size and shape, penetration depth (both limited in accuracy by photographic resolution), and the approximate range from the primary impact crater to the secondary impact point.

An analysis of existing soil penetration equations has been made in an effort to arrive at the most suitable equation for analysis of secondary impact craters. It is important to note that for this study only relationships that could be applied without knowledge of the deceleration history during penetration were investigated. Following this work a study was initiated of the penetration process based on analysis of deformation patterns under the base of an impacting penetrometer. The analyses presented by Scott (1962), which have been used in part for study of Surveyor footpad penetrations, are used as a starting point. This section reports the results of the study of existing penetration equations; results of the analysis of deformation mechanics during penetration will be reported subsequently.

II. SECONDARY IMPACT CRATER ANALYSIS

A. Moore's Analysis

H. J. Moore (1967) attempted to analyze quantitatively the data obtained from Lunar Orbiter photographs showing secondary impact craters caused by ejecta blocks spewn out from meteor explosion craters.* He noted that the depth of penetration of a block was roughly proportional to its distance from the meteor crater. This suggested a relationship between depth of penetration and impact velocity, since range and velocity are related by simple ballistics equations. A semi-theoretical soil penetration prediction equation was derived which could be used for the analysis of the secondary impact crater data. The equation was developed with the aid of tests on the penetration of rods into granular soils. The following assumptions were made:

1. Penetration resistance is proportional to the density of the soil;
2. Penetration resistance is proportional to the acceleration of gravity;
3. Penetration resistance is proportional to depth of penetration;

---

*Ejecta blocks impact the lunar surface at velocities of about 50 — 200 ft/sec based on the range from the primary to secondary crater. These are considered low velocities for the purposes of this report.

4. Energy available for penetration is proportional to the kinetic energy of the penetrator.

By equating the work required for penetration to the energy available for penetration, Moore arrived at the following relationship:

$$\frac{P}{L} = c\left(\frac{\rho_p}{\rho_t}\right)^{1/2} \frac{1}{g^{1/2}} \frac{V_0}{L^{1/2}} \qquad (4\text{-}1)$$

in which P = depth of penetration of the projectile, L = length of projectile, c = constant, ρ_p = mass density of the projectile, ρ_t = mass density of the soil, g = gravitational constant, V_0 = vertical component of the impact velocity of the projectile.

The assumptions used for development of this equation appear reasonable for penetration into granular (frictional) soil materials. A direct proportionality between penetration resistance and density probably does not exist, but in the absence of specific data it may be a good first approximation. If a soil is considered which derives its strength only from friction, if penetration resistance is directly proportional to shear strength, and if density does not vary with depth, then assumptions (2) and (3) will be satisfied. Assumption (4) depends on the partition of energy between penetration and other losses, e.g., heat, as a function of initial penetrator energy, and says, in effect, that this partition will be the same for all impacts regardless of penetrator size, shape, mass, or velocity. An experimental value of c was determined from the results of low velocity penetration tests into a dense fine sand.* Moore then used the equation to evaluate secondary impact crater data from Lunar Orbiter photographs, with the results shown in Fig. 4-1, where the different symbols represent boulder impacts on different areas of the moon. From the scatter of the data, Moore concluded that the lunar surface is inhomogeneous over the areas investigated.

---

*The coefficient c is given by the value of $\left(\frac{P}{L}\right)$ for $\left(\frac{\rho_p}{\rho_t}\right)^{1/2} \frac{V_0}{L^{1/2}g^{1/2}} = 1.$

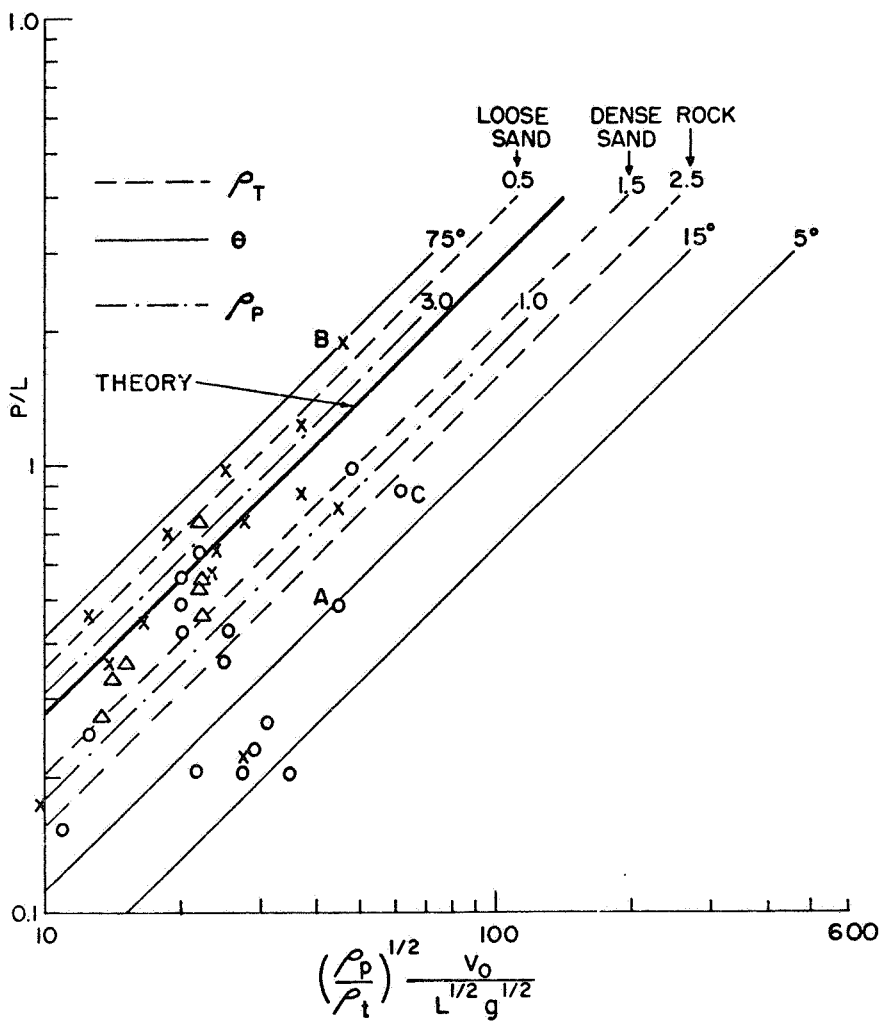

FIG. 4-2. Influence of Parameter Variation on Penetration Values

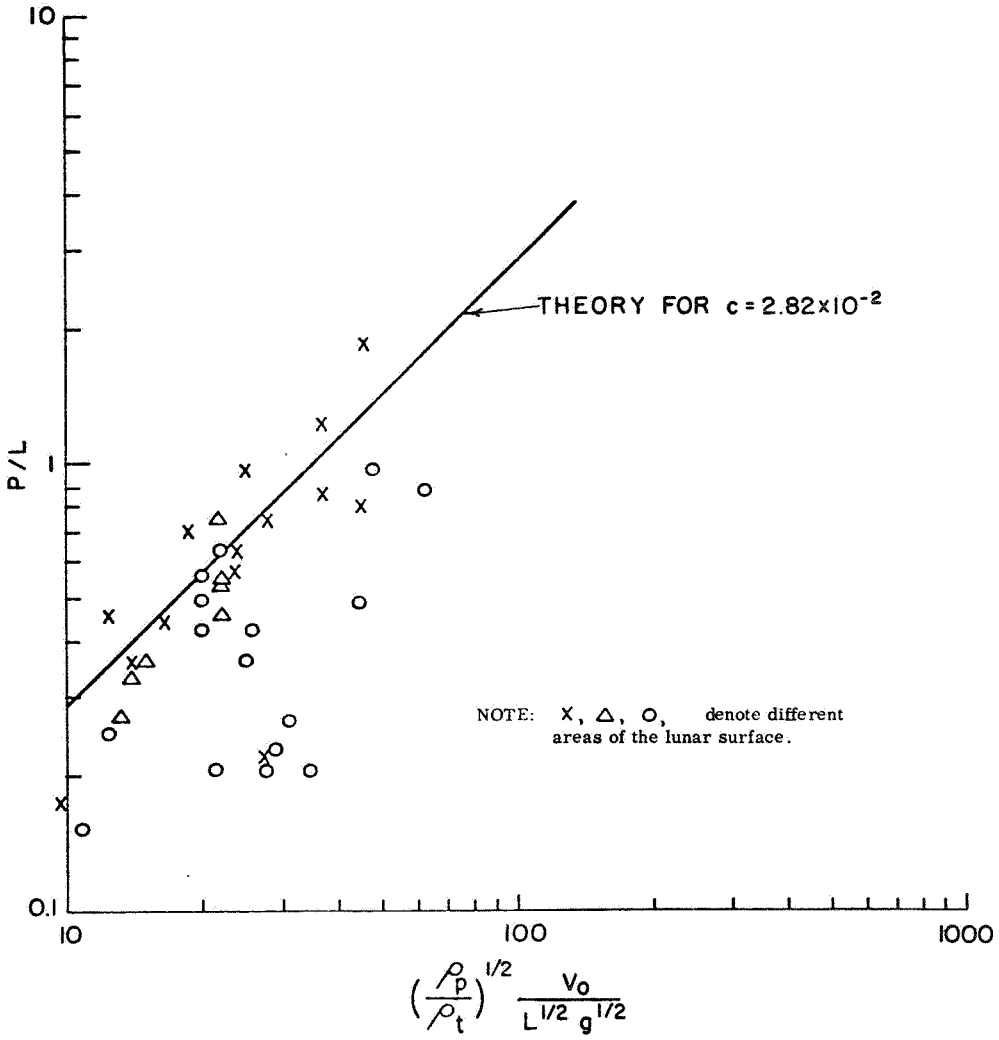

FIG. 4-1. Moore's Analysis of Secondary Impact Craters on the Lunar Surface

Since this conclusion is at variance with the findings at the five Surveyor landing sites, and because Orbiter data are now available for a number of other areas on the lunar surface, further study has been made of relationships that might be used for study of secondary impact craters. In the analysis certain assumptions must be made for the values of ρ_p, ρ_t, and θ, the boulder ejection angle. Moore used $\rho_p = 2.4$ gm/cc, $\rho_t = 0.8$ gm/cc, and $\theta = 60°$. Fig. 4-2 shows that all the scatter in the secondary impact crater data can be accounted for by appropriate choices of the values of ρ_p, ρ_t, and θ. The line on the figure labeled "Theory" corresponds to the assumed values of $c = 2.82 \times 10^{-2}$, ρ_p, ρ_t, and θ. The other lines on the figure correspond to values of the above variables which would make data points falling on these lines correspond with the theory by appropriate choice of ρ_p, ρ_t, and θ.

For example, the data point marked "A" in Fig. 4-2 can be made to correspond to Moore's theoretical line if the boulder were ejected from the main meteor crater at an angle of 15° rather than at 60° as Moore assumed. Similarly, point "B" would correspond to the theoretical line if the boulder were ejected at an angle of about 75°, and point "C" would shift to the theoretical line if the surface mass density were slightly greater than 2.5 rather than 0.8 gm/cc as assumed.

If the values of the variables assumed by Moore are reasonable,* then the scatter in the data must be accounted for by other means. The most likely cases of such data scatter are (1) the Moore equation for projectile penetration does not represent the process of dynamic penetration on the lunar surface and/or (2) the equation does not take into account certain factors neglected in the derivation of the projectile penetration equation on earth, but which will be encountered on the lunar surface.

---

*In the light of Surveyor data obtained since Moore's original analysis an assumed value for ρ_t of 1.5 gm/cc would appear more reasonable than 0.8 gm/cc. An assumption of this value would shift the theoretical line and all data points in Figs. 1 and 2, but the scatter would not be reduced.

B. Soil Penetration Equations

In an attempt to resolve some of the uncertainty associated with the above findings, Moore's equation was examined in more detail, and its ability to account for dynamic penetration data beyond those used in its derivation was studied. In addition other equations developed for penetration depth prediction were examined. It must be noted, however, that all of the equations to be discussed are earth-derived and earth-oriented. The problem of their applicability to soil penetration on the moon is discussed later.

Equation 4-1 can be put in a more convenient form by the following rearrangement of terms:

$$P = c \frac{L^{1/2}}{\rho_t^{1/2}} \frac{\rho_p^{1/2} g^{1/2}}{g^{1/2} g^{1/2}} V_0 \qquad (4\text{-}2)$$

The weight-to-area ratio of the projectile (Q) is defined as

$$Q = W/A \qquad (4\text{-}3)$$

W = weight of penetrator,

A = gross cross-sectional area of the penetrator,

Therefore

$$Q = \frac{L A \rho_p g}{A} \qquad (4\text{-}4)$$

$$Q = L \rho_p g \qquad (4\text{-}5)$$

The unit weight of the target soil (γ_t) is by definition

$$\gamma_t = \rho_t g \tag{4-6}$$

Therefore

$$P = c \frac{Q^{1/2}}{\gamma_t^{1/2} g^{1/2}} V_0 \tag{4-7}$$

For a given value of g (32.2 ft/sec^2 for the Earth):

$$P = K' \frac{Q^{1/2}}{\gamma_t^{1/2}} V_0 \tag{4-8}$$

in which

$$K' = c \frac{1}{g^{1/2}} \tag{4-9}$$

Taking into account the nose shape of the penetrator, the equation can be written

$$P = K'' n \frac{Q^{1/2}}{\gamma_t^{1/2}} V_0 \tag{4-10}$$

in which K'' = a proportionality constant, and N = a relative projectile nose shape constant. Young (1967) has determined empirical values of n from low-velocity (V_0 < 200 ft/sec) projectile penetration tests in various soils. Typical values of n are given in Table 4-1.

TABLE 4-1

Values of Projectile Nose-Shape Coefficient, n

Nose Shape	n
Flat nose	0.56
Hemispherical nose	0.72
2.2 crh tangent ogive*	0.82
6.0 crh tangent ogive	1.00
9.25 crh tangent ogive	1.11

*A $\left(\frac{r}{h}\right)$ crh tangent ogive is a geometrical form as shown below:

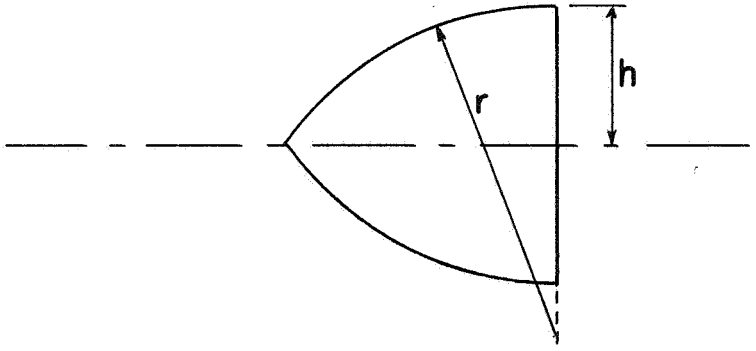

The form of Equation 4-10 can be seen from the data plotted in Fig. 4-3. These data, taken from low velocity (V_0 < 200 ft/sec) impact studies conducted by the Sandia Corporation (Thompson, 1967), show that the value of K'' is not a constant, but is different for each soil.

For these tests solid mild steel penetrators were used for tests in soils, and hardened steel penetrators were used for drops into rock. With the exception of paint abrasion observed on penetrators dropped into fine-grained soils, the penetrators were undamaged. Heavy striation marks were observed after penetration into granular soils.

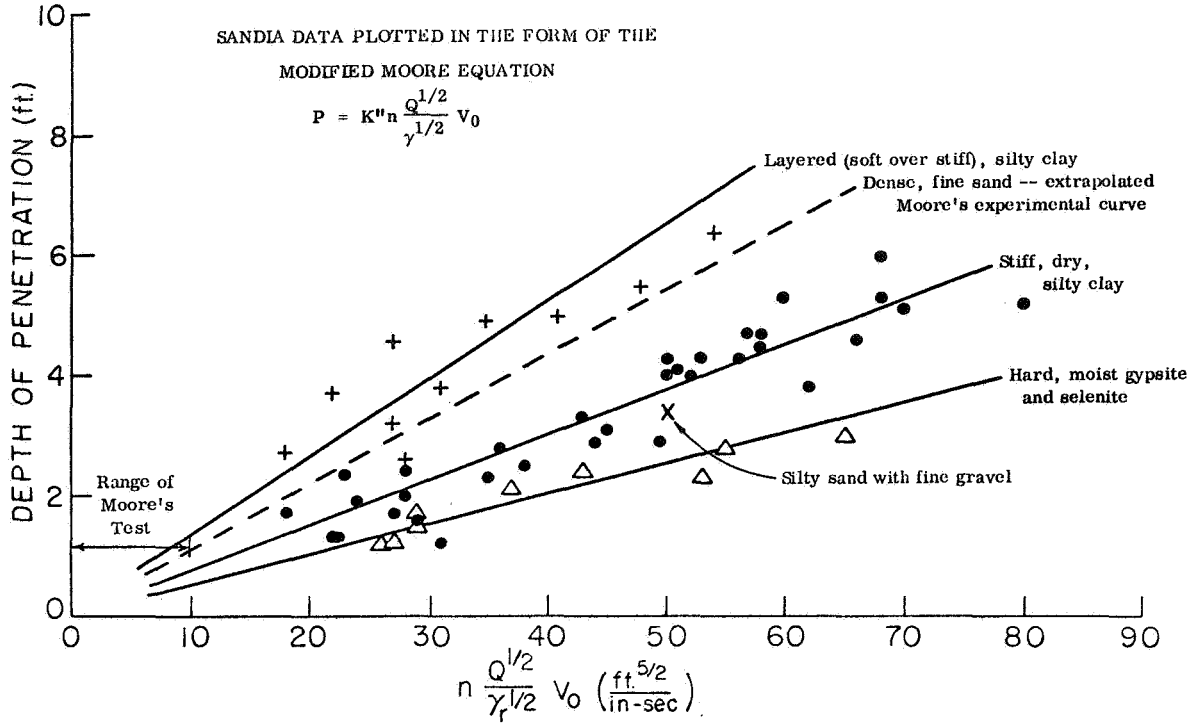

FIG. 4-3. Sandia Data Plotted in the Form of the Modified Moore Equation

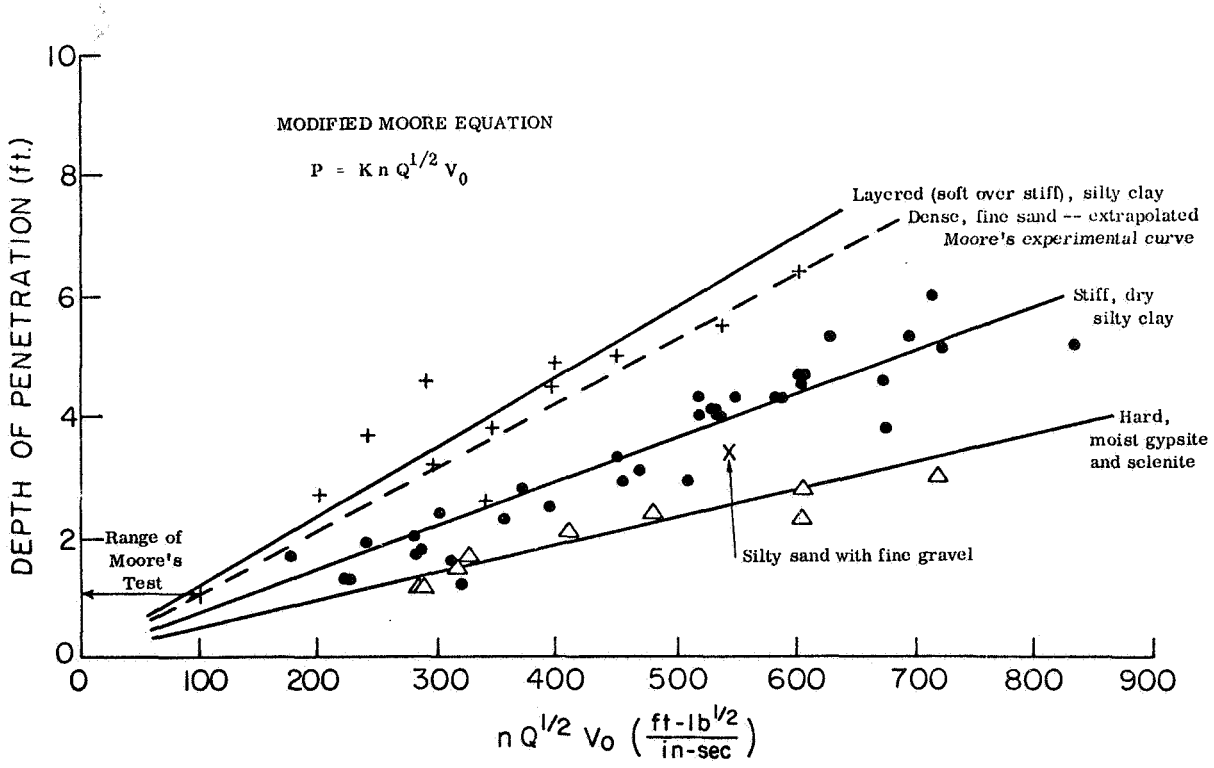

FIG. 4-4. Sandia Data Plotted in the Form of the Modified Moore Equation.

For comparison the relationship determined by Moore from his tests is also shown on Fig. 4-3. This is an extrapolated relationship, however, because the range of values of $\left(n \frac{Q^{1/2}}{\gamma_t^{1/2}} V_0\right)$ for Moore's tests is much less than that for the Sandia tests. Since K'' depends upon the soil, it can be combined with $\left(1/\gamma_t^{1/2}\right)$ to form a "soil constant," K. The Modified Moore Equation thus becomes

$$p = K\, n\, Q^{1/2} V_0 \tag{4-11}$$

By plotting the data as shown in Fig. 4-4, values of K can be determined for the different soil types. A summary of typical values thus determined is given in Table 4-2.

TABLE 4-2

Values of Soil Constant, K

Description of Soil	K(in. − sec/lb$^{1/2}$)
Dense, fine sand	10.5×10^{-3}
Hard, moist gypsite and selenite (clear, transparent gypsum)	4.7×10^{-3}
Stiff, dry, silty clay	7.3×10^{-3}
Layered (soft over stiff) silty clay	11.6×10^{-3}

The constants are consistent with the following units: p = feet, Q = psi, and V_0 = ft/sec.

The accuracy of the modified Moore Equation can be seen from Fig. 4-5 in which actual depths of penetration are compared with predicted depths for the Sandia data. The accuracy of the equation as a function

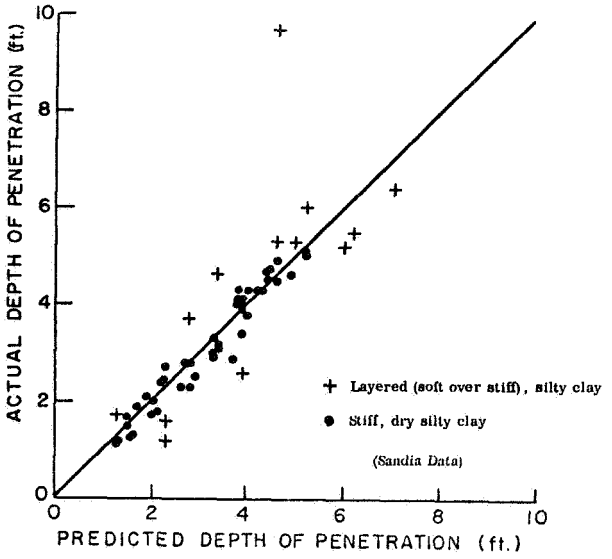

FIG. 4-5. Accuracy of the Modified Moore Equation

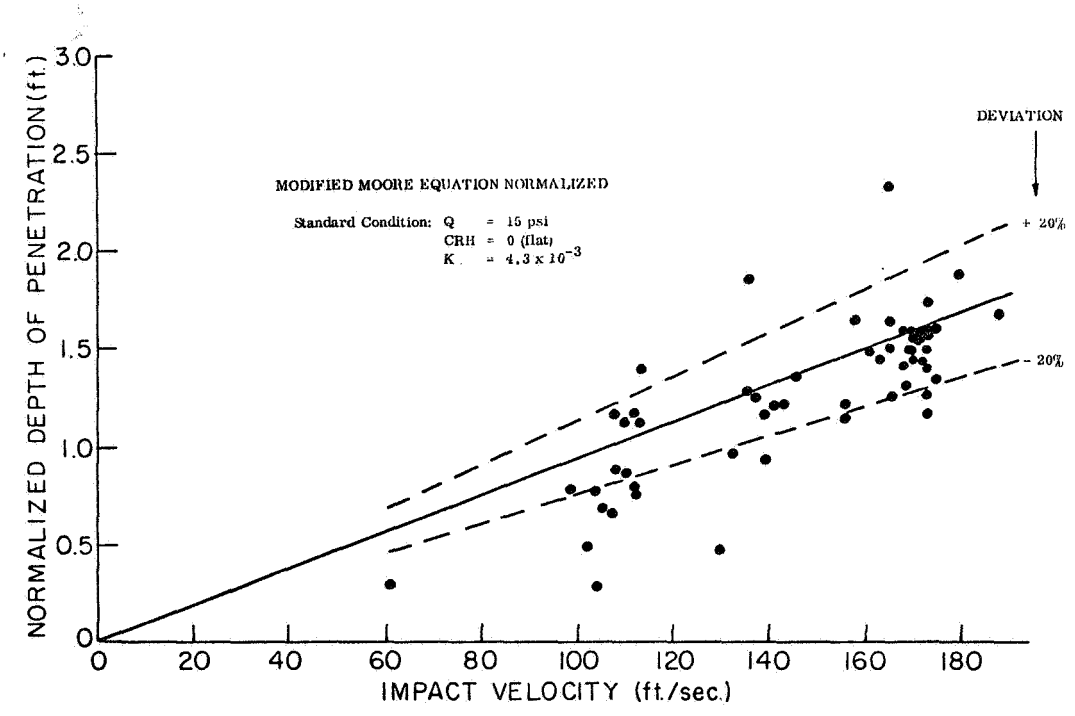

FIG. 4-6. Modified Moore Equation Normalized

of impact velocity can be determined by normalizing all the Sandia data to that of a standard condition (Q = 15 psi, crh = 0 [flat nose], $K = 4.3 \times 10^{-3}$) by the following equation:

$$P_N = P_A \left(\frac{4.3 \times 10^{-3}}{K}\right)\left(\frac{0.56}{n}\right)\left(\frac{15}{Q}\right)^{1/2} \tag{4.12}$$

where P_N = normalized depth of penetration, P_A = actual depth of penetration for a data point, and K, n, Q = the appropriate values for a data point.

The normalized data are shown in Fig. 4-6. From this graph it may be seen that, while the data are rather spread out in the range of lower velocities, most of the points fall within ± 20% deviation lines.

The Sandia Corporation has conducted a large number of instrumented projectile penetration tests into a variety of soils over a wide range of impact velocities. Their early data were used by Young (1967) to develop the following empirical penetration prediction equation for impact velocities less than 200 ft/sec:

$$P = 530\ S\ n\ Q^{1/2}(10^{-3})\ \ln\ (1 + 20 \times 10^{-6}\ V_0^2) \tag{4-13}$$

where

S is a soil constant

Typical values of S for the soils studied are given in Table 4-3.

Woodward-Clyde and Associates (1962-1967) have analyzed the Sandia data in an effort to correlate depths of penetration, for a given projectile and impact velocity, with the average standard blow count* and total unit weight of the soil. The equations developed were

---

*Obtained from the standard penetration test — see Terzaghi and Peck (1967).

TABLE 4-3

Values of Soil Constant, S

Soil	$S\left(\frac{\text{in-ft}}{\text{lb}^{1/2}}\right)$
Soft, saturated clay	50.0
Soft San Francisco Bay Mud	22.2
Layered (soft over stiff) silty clay	9.1
Loose-to-medium dense moist sand	6.5
Stiff, dry, silty clay	5.0
Hard, moist gypsite and selenite	2.43
Rock	1.07 – 1.30

based on tests covering a range of impact velocities from 100 to 1400 ft/sec. The equations are empirical in nature but are in the form of the Resal and Poncelet equations (early historical penetration equations) as shown below:

Resal Equation

$$P = \frac{1}{\alpha} \ln \left(1 + \beta V_0\right) \tag{4-14}$$

where

$$\alpha = \frac{(80 + N)\ \gamma_t C}{625{,}000\ \ell Q} \tag{4-15}$$

$$\beta = 1.26\ A \times 10^{-6} \tag{4-16}$$

$$\ell = 0.042\ (crh) + 0.942 \tag{4-17}$$

$$C = 1 + 3/2 \text{ sech } (N/10) - 5/2 \exp (- N^2/52) \quad (4\text{-}18)$$

in which

N = the average standard blow count over the depth of penetration

γ_t = the average total unit weight of the soil over the depth of penetration

A = cross-sectional area of the penetrator.

The units used are P = feet, V_0 = ft/sec, Q = psi, γ_t pcf, and A = sq in.

Poncelet Equation

$$P = \frac{1}{a} \ln(1 + bV_0^2) \quad (4\text{-}19)$$

where

$$a = \frac{(85 + N)(1.29 - 350 \times 10^{-6} V_0) \gamma_t C}{14400 \ell Q} \quad (4\text{-}20)$$

$$b = 0.431 \times 10^{-6} A \quad (4\text{-}21)$$

The accuracy of the equations 4-13, -14, -19 — Young, Resal, and Poncelet — was assessed by using only the Sandia low velocity data (V_0 < 200 ft/sec). It can be seen from Figs. 4-7, -8, -9 that only the Young equation approaches adequate prediction of depths of penetration for this velocity range. This is understandable, however, since only the Young equation was derived expressly for low impact velocities (V_0 < 200 ft/sec). On the other hand, the Resal and Poncelet equations give very good results in the higher range of velocities from 200 to 1400 ft/sec.

Because of the inadequate results obtained from these equations, it was decided to change the constants of the equations in an attempt to obtain a better fit to the low velocity data. In addition, the Resal and Poncelet equations were simplified as will be shown below.

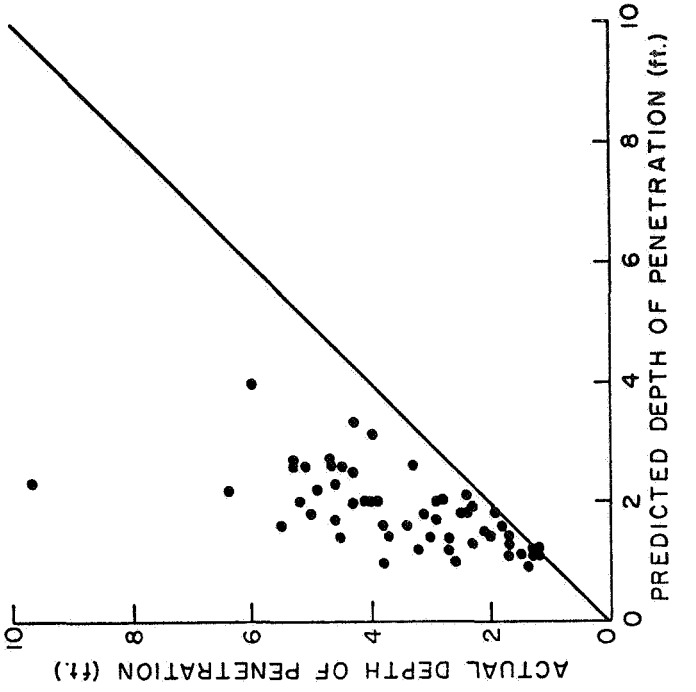

FIG. 4-8. Accuracy of the Resal Equation (V_o < 200 ft/sec)

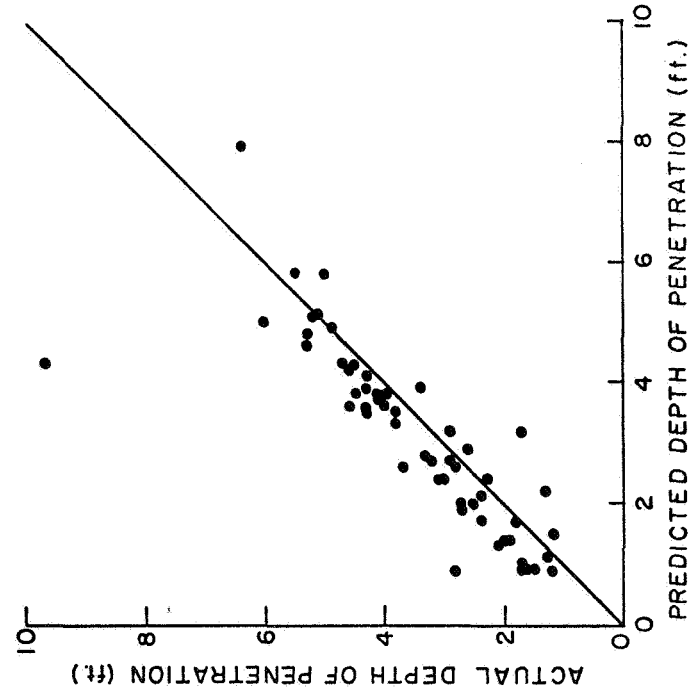

FIG. 4-7. Accuracy of the Young Equation (V_o < 200 ft/sec)

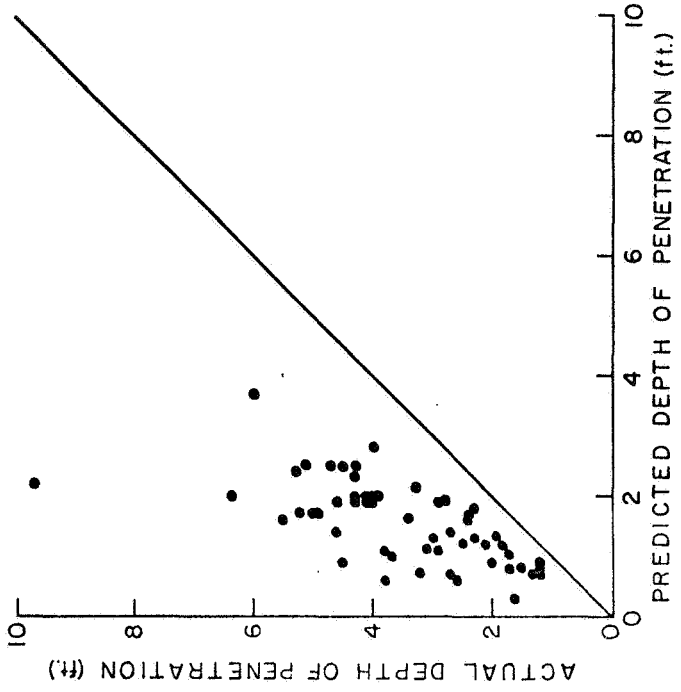

FIG. 4-9. Accuracy of the Poncelet Equation (V_o < 200 ft/sec)

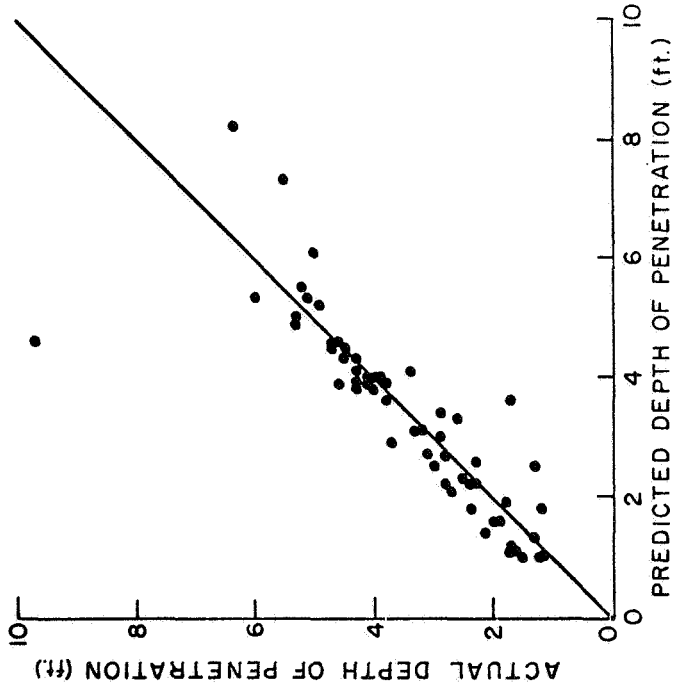

FIG. 4-10. Accuracy of the Modified Young Equation (V_o < 200 ft/sec)

The Young equation can be rewritten as

$$P = K_1 S\ n\ Q^{1/2}\ \ln(1 + K_2 V_0^2) \tag{4-22}$$

where

K_1, K_2 = constant coefficients

and the Resal equation may be rewritten as

$$P = \frac{C_2 \ell Q}{(C_1 + N)\gamma_t C} \ln(1 + C_3 A\ V_0) \tag{4-23}$$

where

C_1, C_2, C_3 = numerical constants.

Since ℓ depends upon the nose shape of the penetrator and $(C_1 + N)\gamma_t C$ depends upon the soil, the Resal equation can be simplified and rewritten as follows:

$$P = K_3 S' n' Q \ln(1 + K_4 A\ V_0) \tag{4-24}$$

where

K_3, K_4 = constant coefficients

S' = soil constant

n' = projectile nose-shape coefficient.

The Poncelet equation can be rewritten as

$$P = \frac{D_4 \ell Q}{(D_1 + N)\gamma_t C(D_2 - D_3 V_0)} \ln(1 + D_5 A\ V_0^2) \tag{4-25}$$

where

D_1, D_2, D_3, D_4, D_5 = constants.

By the same reasoning given above for the Resal equation, the Poncelet equation becomes

$$P = K_5 S'' n'' Q \frac{\ln(1 + K_6 A V_0^2)}{1 - K_7 V_0} \tag{4-26}$$

where

K_5, K_6, K_7 = constant coefficients

S'' = soil constant

n'' = projectile nose-shape coefficient

It has been advantageous to assume that S, S', S'' are equal as are also n, n', and n''. Strictly speaking this is not correct; however, the respective S and n values should be proportionally related between different soils and penetrator nose shapes. Therefore, actual differences in magnitude of these values can be accounted for by appropriate choices of the K-constants in the equations. Thus the modified equations can be finally rewritten as follows:

Modified Young Equation

$$P = K_1 S\ n\ Q^{1/2} \ln(1 + K_2 V_0^2) \tag{4-27}$$

Modified Resal Equation

$$P = K_5 S\ n\ Q \ln(1 + K_6 V_0) \tag{4-28}$$

Modified Poncelet Equation

$$P = K_5 S\ n\ Q \frac{\ln(1 + K_6 V_0^2)}{1 - K_7 V_0} \tag{4-29}$$

The constant coefficients for these equations have been determined by finding a "least-squares" fit to the Sandia low velocity data. The values of the constants thus determined are given in Table 4-4. (The units are those needed for consistency with those of the variables.)

TABLE 4-4

Constant Coefficients of Modified Sandia Equations

Coefficient	Value
K_1	3.52×10^{-1}
K_2	3.61×10^{-5}
K_3	9.02×10^{-2}
K_4	3.29×10^{-4}
K_5	-8.00×10^{1}
K_6	-3.76×10^{-9}
K_7	9.17×10^{-3}

The accuracy of the modified equations can be seen from the results plotted in Figs. 4-10, -11, -12. The variation of the experimental data between actual and predicted penetration depths can be seen to be the smallest for the Modified Young Equation, and the greatest for the Modified Poncelet Equation. The effect of impact velocity can be seen in Figs. 4-13, -14, -15, where the data have been normalized to a standard condition (Q = 15 psi, crh = 0 (flat nose), S = 2.0, nose diameter = 9 in.) in the following manner:

Modified Young Equation

$$P_N = P_A \left(\frac{2.0}{S}\right)\left(\frac{0.56}{n}\right)\left(\frac{15}{Q}\right)^{1/2} \qquad (4\text{-}30)$$

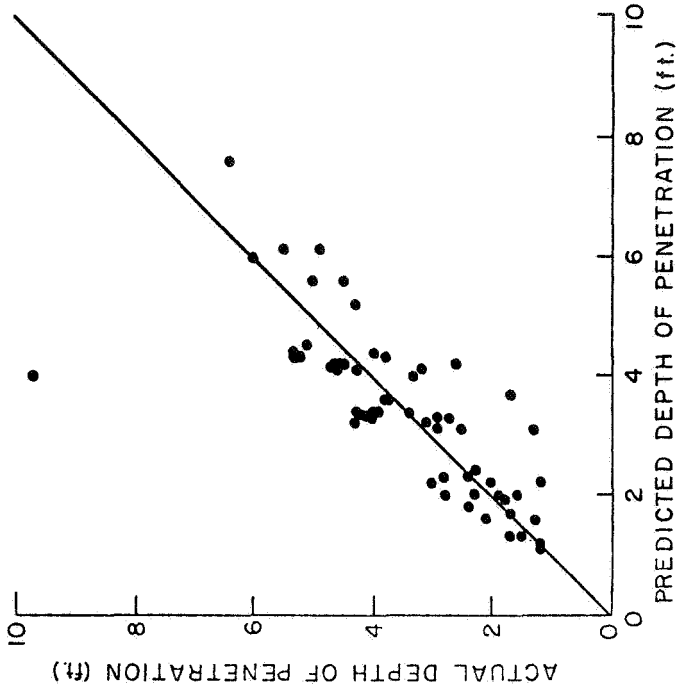

FIG. 4-11. Accuracy of the Modified Resal Equation (V_o < 200 ft/sec)

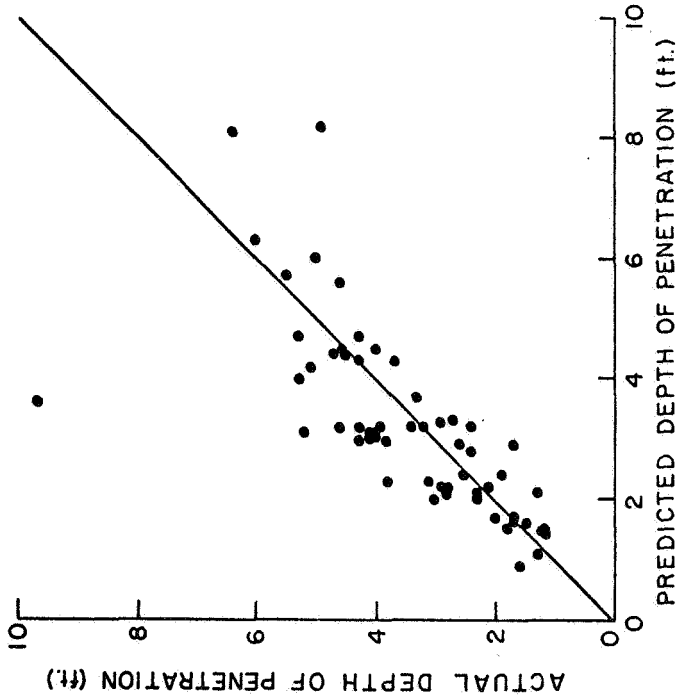

FIG. 4-12. Accuracy of the Modified Poncelet Equation (V_o < 200 ft/sec)

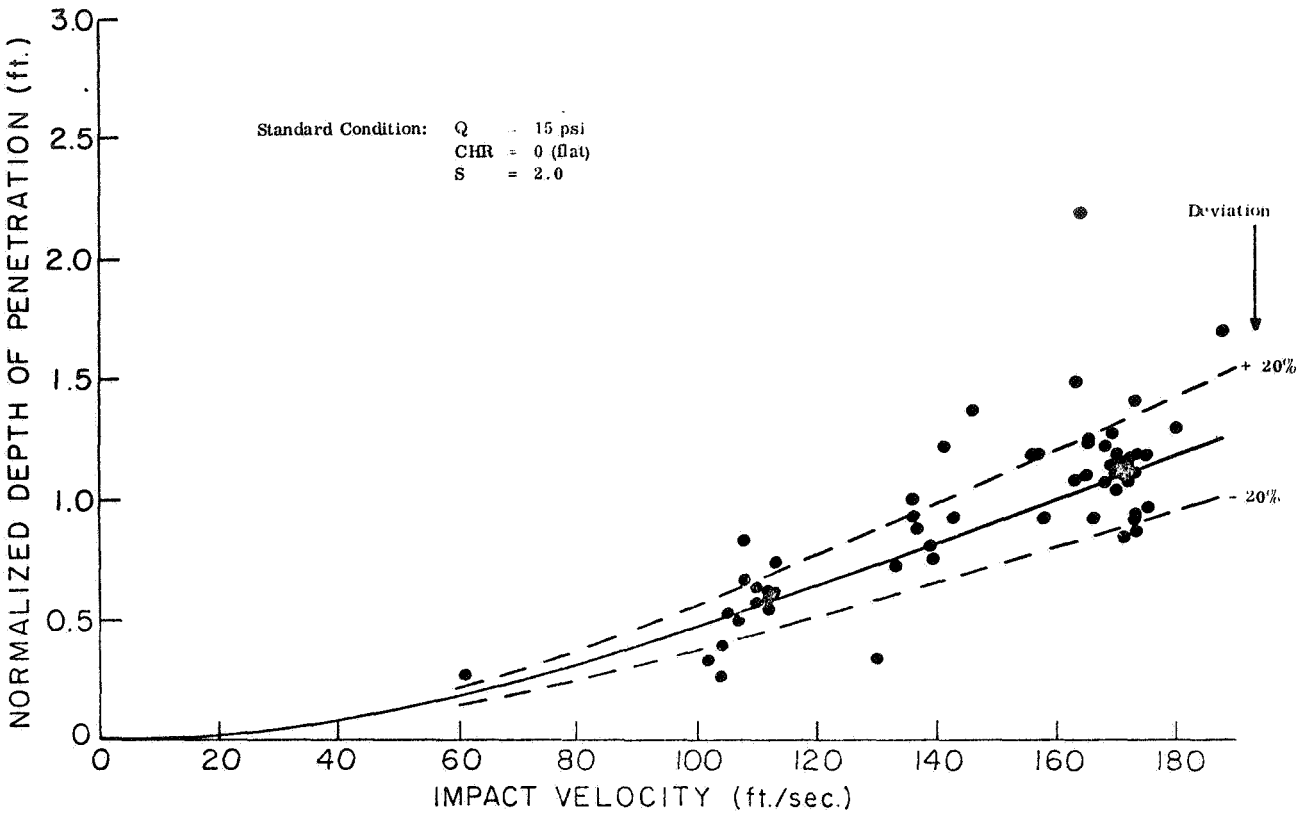

FIG. 4-13. Modified Young Equation Normalized

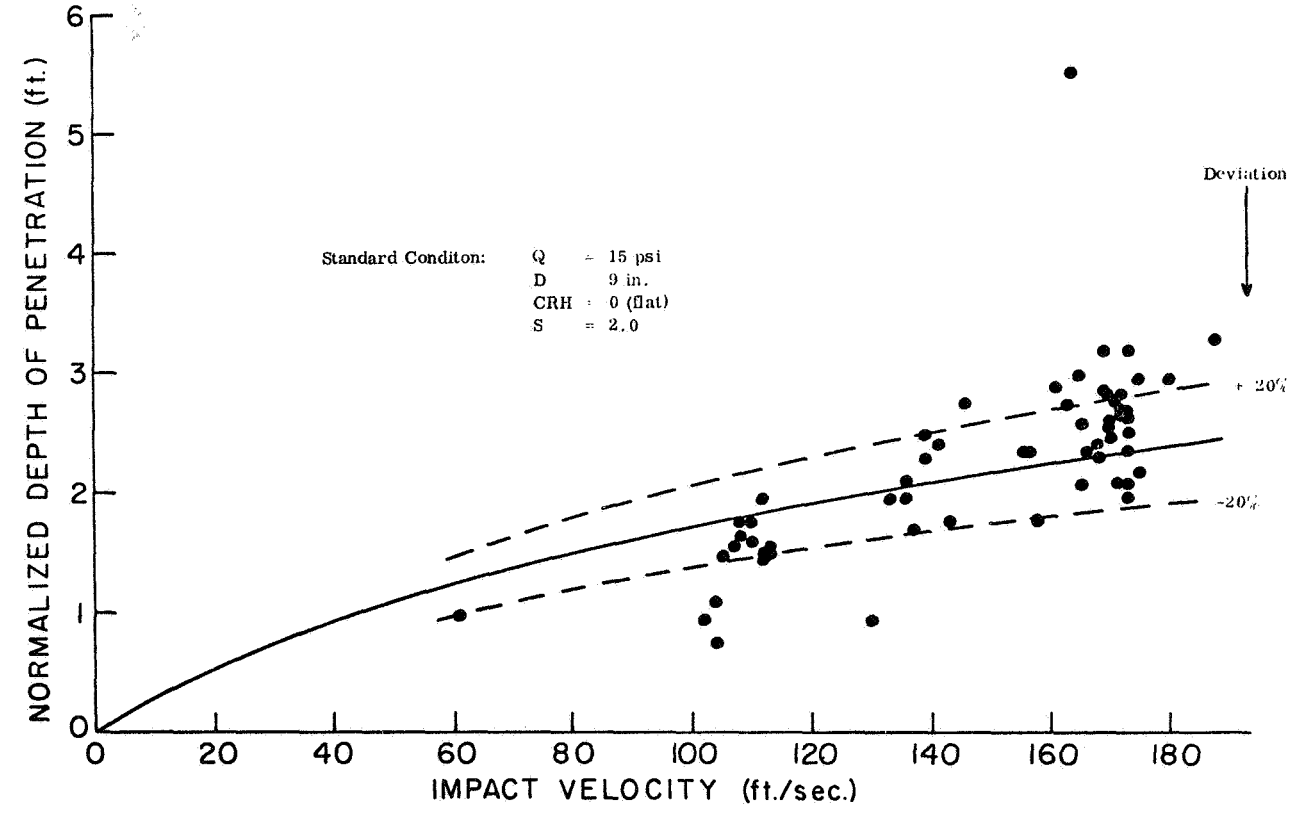

FIG. 4-14. Modified Resal Equation Normalized

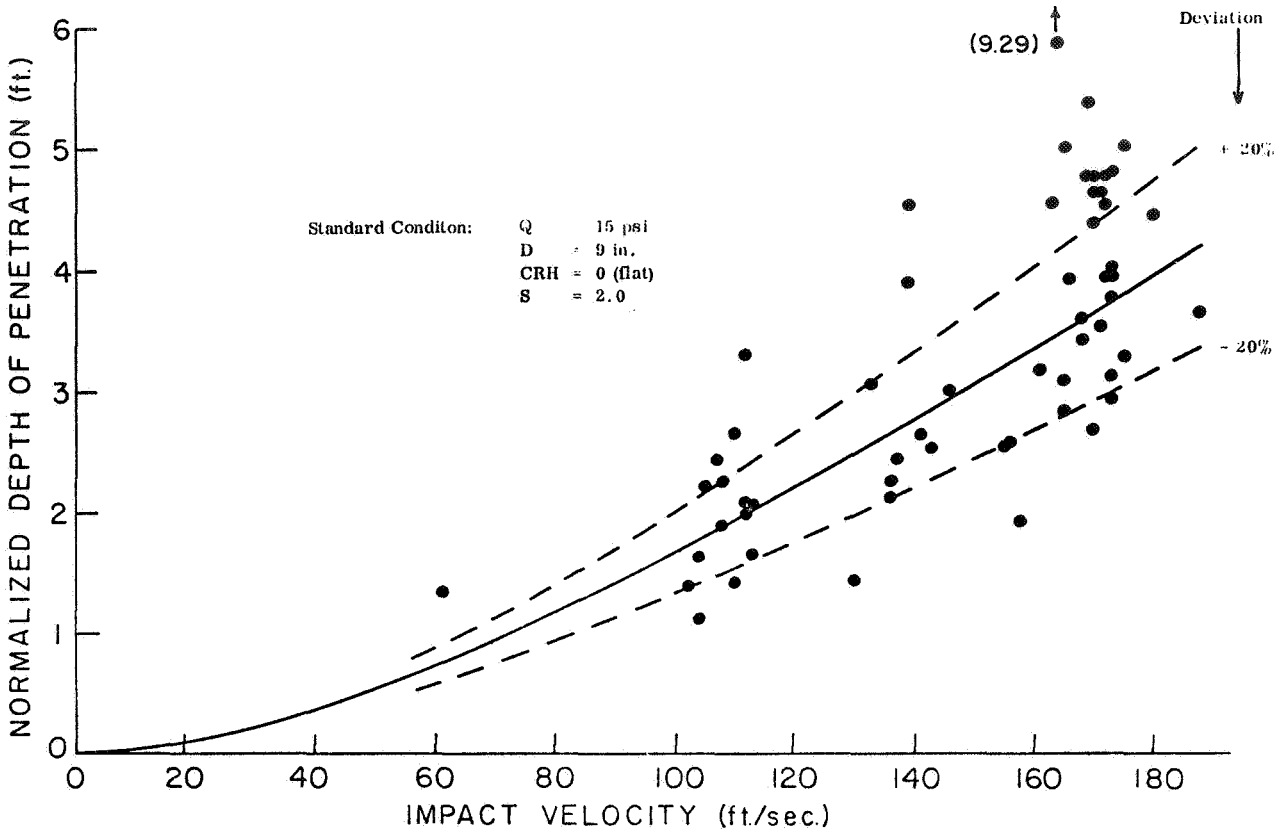

FIG. 4-15 . *Modified Poncelet Equation Normalized*

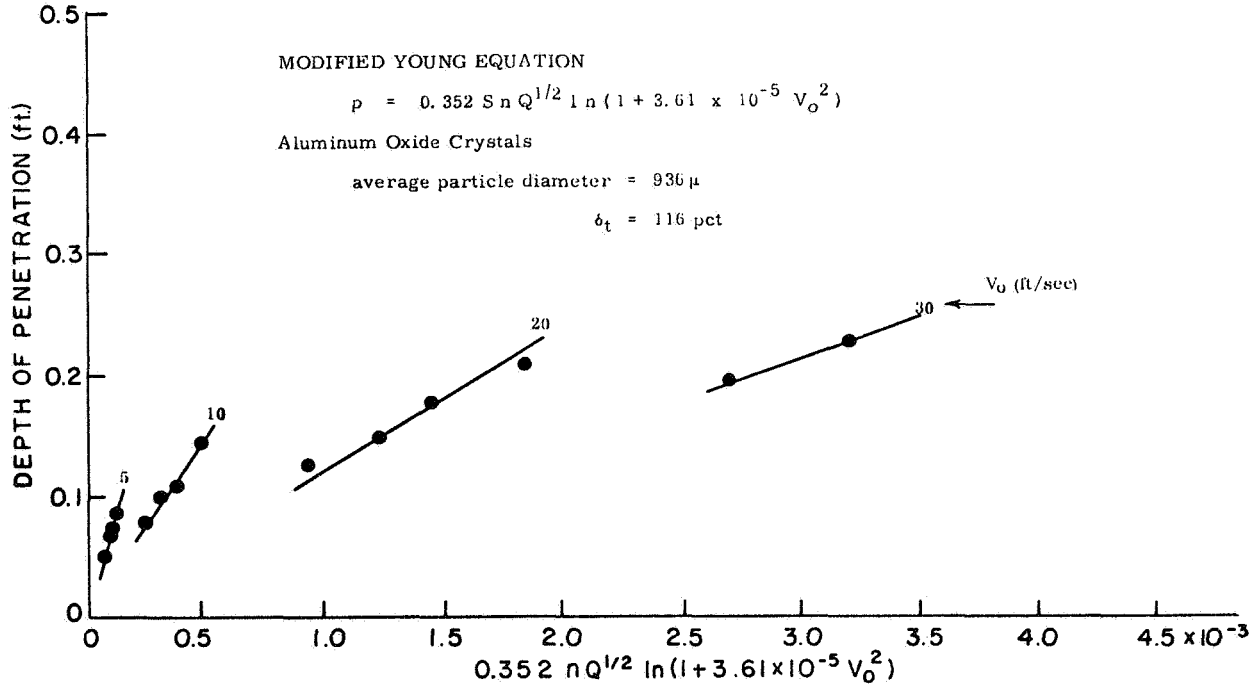

FIG. 4-16. Hank's and McCarty's Data Plotted According to the Modified Young Equation

Modified Resal Equation

$$P_N = P_A \left(\frac{2.0}{S}\right)\left(\frac{0.56}{n}\right)\left(\frac{15}{Q}\right) \frac{\ln(1 + 3.29 \times 10^{-4} \times 63.6\ V_0)}{\ln(1 + 3.29 \times 10^{-4} \times A\ V_0)} \qquad (4\text{-}31)$$

Modified Poncelet Equation

$$P_N = P_A \left(\frac{2.0}{S}\right)\left(\frac{0.56}{n}\right)\left(\frac{15}{Q}\right) \frac{\ln(1 - 3.76 \times 10^{-9} \times 63.6\ V_0^2)}{\ln(1 - 3.76 \times 10^{-9} \times A\ V_0)} \qquad (4\text{-}32)$$

$$\div\ (1 - 9.17 \times 10^{-3}\ V_0)$$

These graphs also show that the Modified Young Equation gives the best results, with a large majority of the data points falling within ± 20% of the predicted values.

As noted in the introduction a number of other investigators have also been studying the use of accelerometer-mounted projectiles for remote soil reconnaissance, especially on the lunar surface. McCarty and Carden (1962) showed that the depth of penetration for a given shape of projectile and with impact velocity less than 30 ft/sec could be predicted by the following equation:

$$P = k \frac{m^{1/2}}{D} V_0^{2/3} \qquad (4\text{-}33)$$

in which k = a soil constant, m = the mass of the projectile, and D = the diameter of the projectile. Because of the very low velocity range for which this equation is valid, it cannot be used for the analysis of secondary impact craters. But it has been advantageous to use low-velocity data to further evaluate the Modified Moore and Young equations — the most accurate of the available penetration equations studied thus far.

Data taken from Hanks and McCarty (1966) and shown in Fig. 4-16 indicate quite clearly that the Modified Young equation is extremely velocity dependent in the low velocity range. This is not unreasonable because the Modified Young equation is empirical and intended for greater velocities than those in question. It is thus obvious that the Modified Young Equation can not be extrapolated into velocity ranges for which it was not intended.

On the other hand, data from Carden (1967), McCarty and Carden (1962) and Hanks and McCarty (1966) tend to support the Modified Moore Equation for impact velocities substantially less than 100 ft/sec, as may be seen from Figs. 4-17, -18, -19. However, these very low velocity data have also shown that the straight line relationship between P and $n \cdot Q^{1/2} \cdot V_0$ does not pass through the origin but intercepts the ordinate axis at a finite value of P. It might be concluded therefore that a better fit to the data would be obtained by the following form of the equation

$$P = K\, n\, Q^{1/2}\, V_0 + P_0 \qquad (4\text{-}34)$$

where

P_0 = the "static" depth of penetration.

However, it must be remembered that both the impact velocities and weight-to-frontal area ratios were relatively small for these tests. Therefore, little error should be involved in applying the regular Modified Moore Equation to heavier projectiles and greater impact velocities, because the intercept on the ordinate axis will be small compared to measured depths of penetration.

Further substantiation of the Modified Moore Equation can be provided by means of dimensional analysis. Assuming that

$$P = f(Q, \gamma_t, g, V_0) \qquad (4\text{-}35)$$

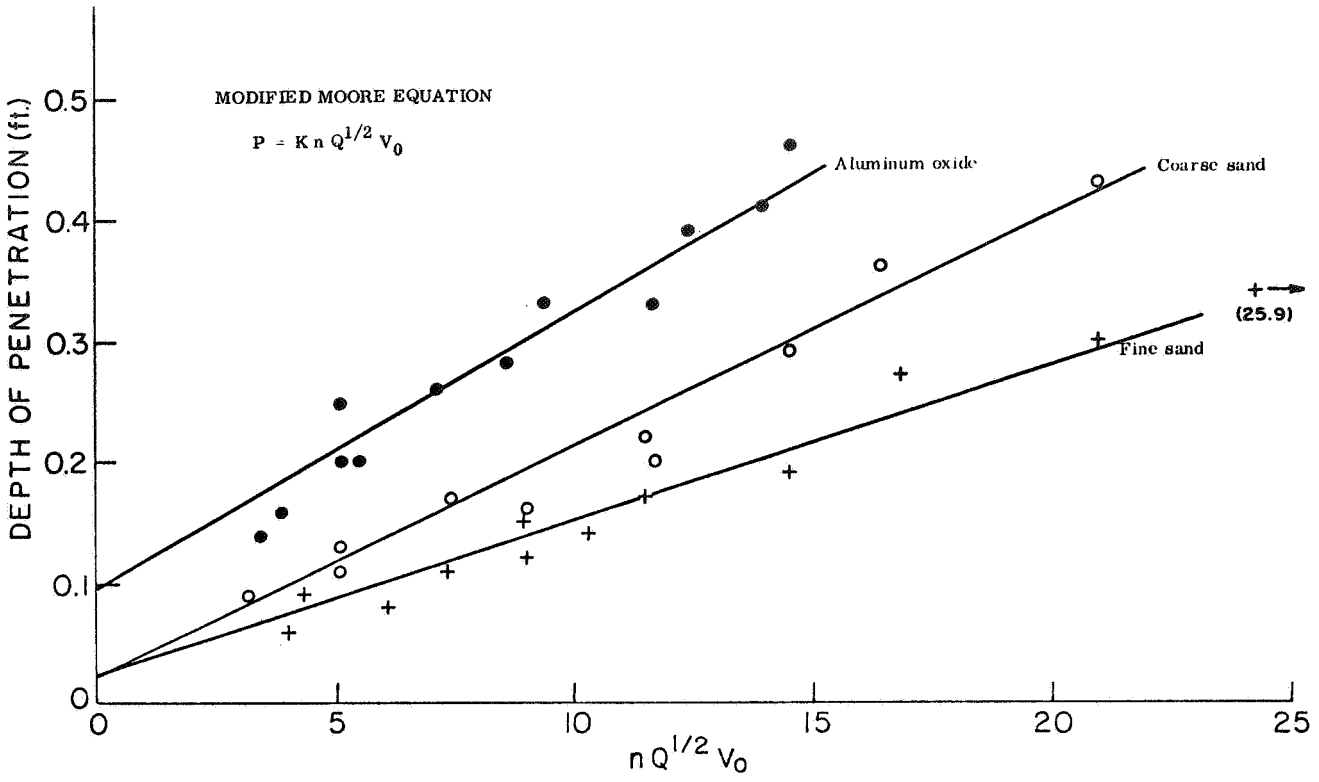

FIG. 4-17. Test Data from Carden (1967)

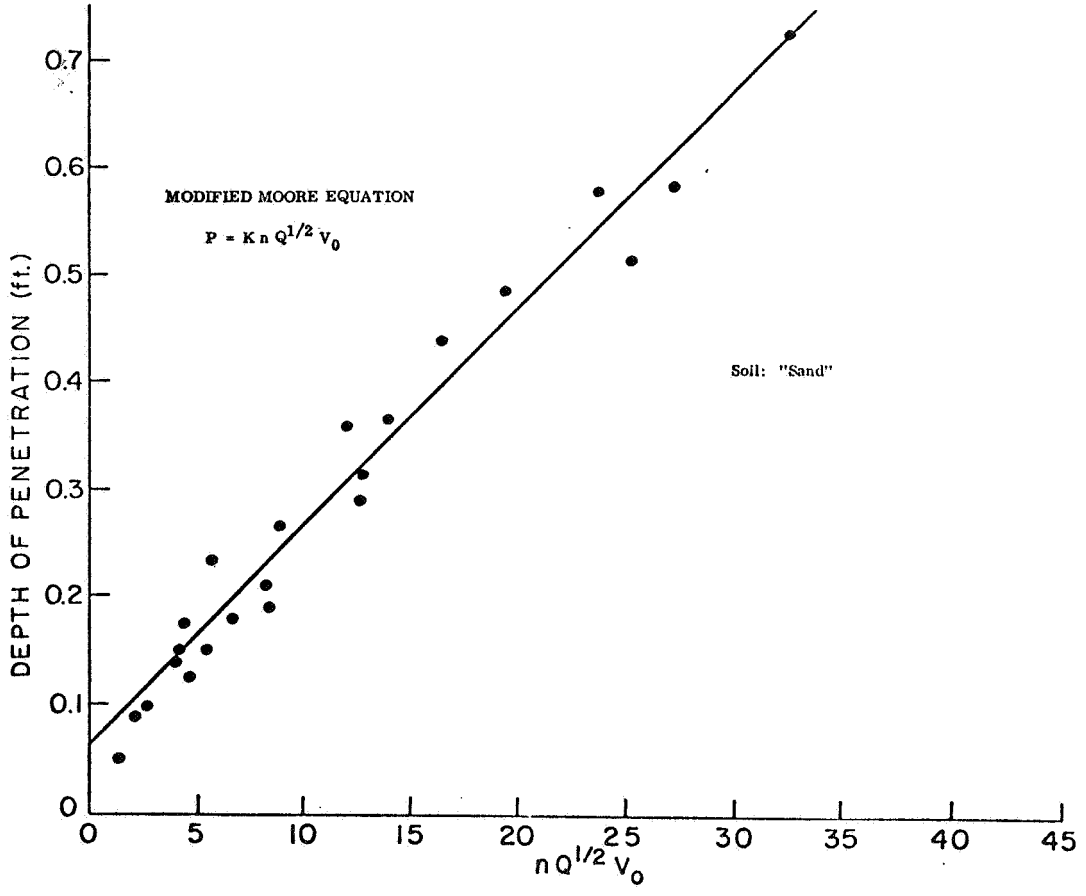

FIG. 4-18. Data from McCarty and Carden (1962).

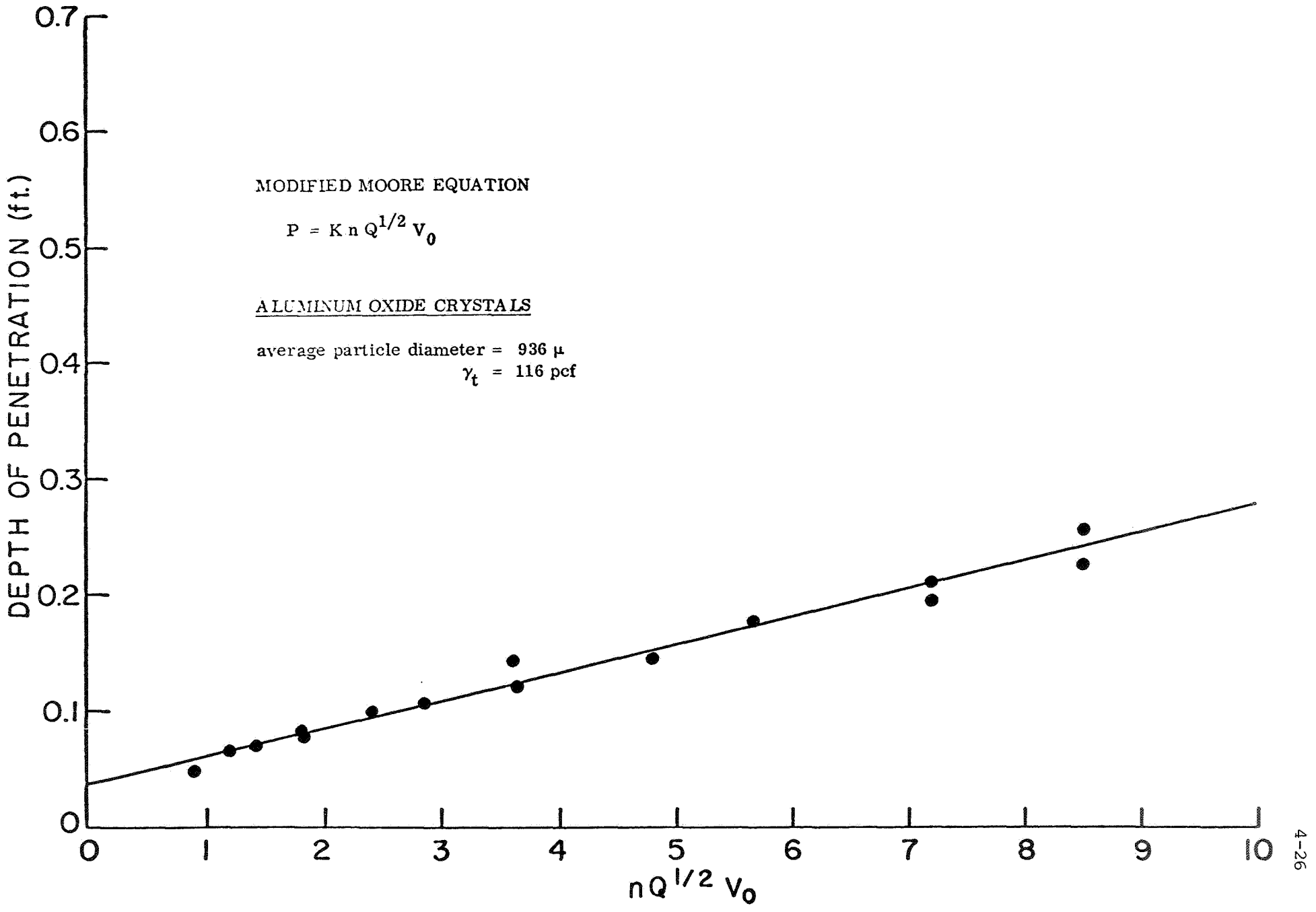
MODIFIED MOORE EQUATION
$P = K n Q^{1/2} V_0$
ALUMINUM OXIDE CRYSTALS
average particle diameter = 936 μ
γ_t = 116 pcf
DEPTH OF PENETRATION (ft.)
0.7
0.6
0.5
0.4
0.3
0.2
0.1
0
0
1
2
3
4
5
6
7
8
9
10
$nQ^{1/2} V_0$

use of the Buckingham Pi Theorem yields equations for two dimensionless parameters:

$$\pi_1 = Q^{x_1}\gamma_t^{y_1}V_0^{z_1}P = (ML^{-1}T^{-2})^{x_1}(ML^{-2}T^{-2})^{y_1}(LT^{-1})^{z_1}(L) \qquad (4\text{-}36)$$

$$\pi_2 = Q^{x_2}\gamma_t^{y_2}V_0^{z_2}g = (ML^{-1}T^{-2})^{x_2}(ML^{-2}T^{-2})^{y_2}(LT^{-1})^{z_2}(LT^{-2}) \qquad (4\text{-}37)$$

These relationships yield two sets of simultaneous equations:

$$x_1 + y_1 = 0 \qquad (4\text{-}38a) \qquad x_2 + y_2 = 0 \qquad (4\text{-}39a)$$

$$-x_1 - 2y_1 + z_1 + 1 = 0 \qquad (4\text{-}38b) \qquad -x_2 - 2y_2 + z_2 + 1 = 0 \qquad (4\text{-}39b)$$

$$-2x_1 - 2y_1 - z_1 = 0 \qquad (4\text{-}38c) \qquad -2x_2 - 2y_2 - z_2 - 2 = 0 \qquad (4\text{-}39c)$$

Solving, we obtain:

$$x_1 = -1 \qquad x_2 = 1$$

$$y_1 = 1 \qquad y_2 = -1$$

$$z_1 = 0 \qquad z_2 = -2$$

Therefore

$$\pi_1 = \frac{\gamma_t P}{Q} \tag{4-40}$$

$$\pi_2 = \frac{Qg}{\gamma_t V_0^2} \tag{4-41}$$

In other words

$$f\left(\frac{\gamma_t P}{Q}, \frac{QG}{\gamma_t V_0^2}\right) = 0 \tag{4-42}$$

Therefore, we can say

$$\frac{\gamma_t P}{Q} = f\left(\frac{\gamma_t V_0^2}{Qg}\right) \tag{4-43}$$

The form of this function is shown in Fig. 4-20 using Moore's laboratory data, where it may be seen that $\log \left(\frac{\gamma_t V_0^2}{Qg}\right) = 2 \log \left(\frac{\gamma_t P}{Q}\right) + \text{const.}$ Thus

$$\left(\frac{\gamma_t P}{Q}\right)^2 \alpha \frac{\gamma_t V_0^2}{Qg} \tag{4-44}$$

or

$$\frac{\gamma_t P}{Q} = k^1 \frac{\gamma_t^{1/2} V_0}{Q^{1/2} g^{1/2}} \tag{4-45}$$

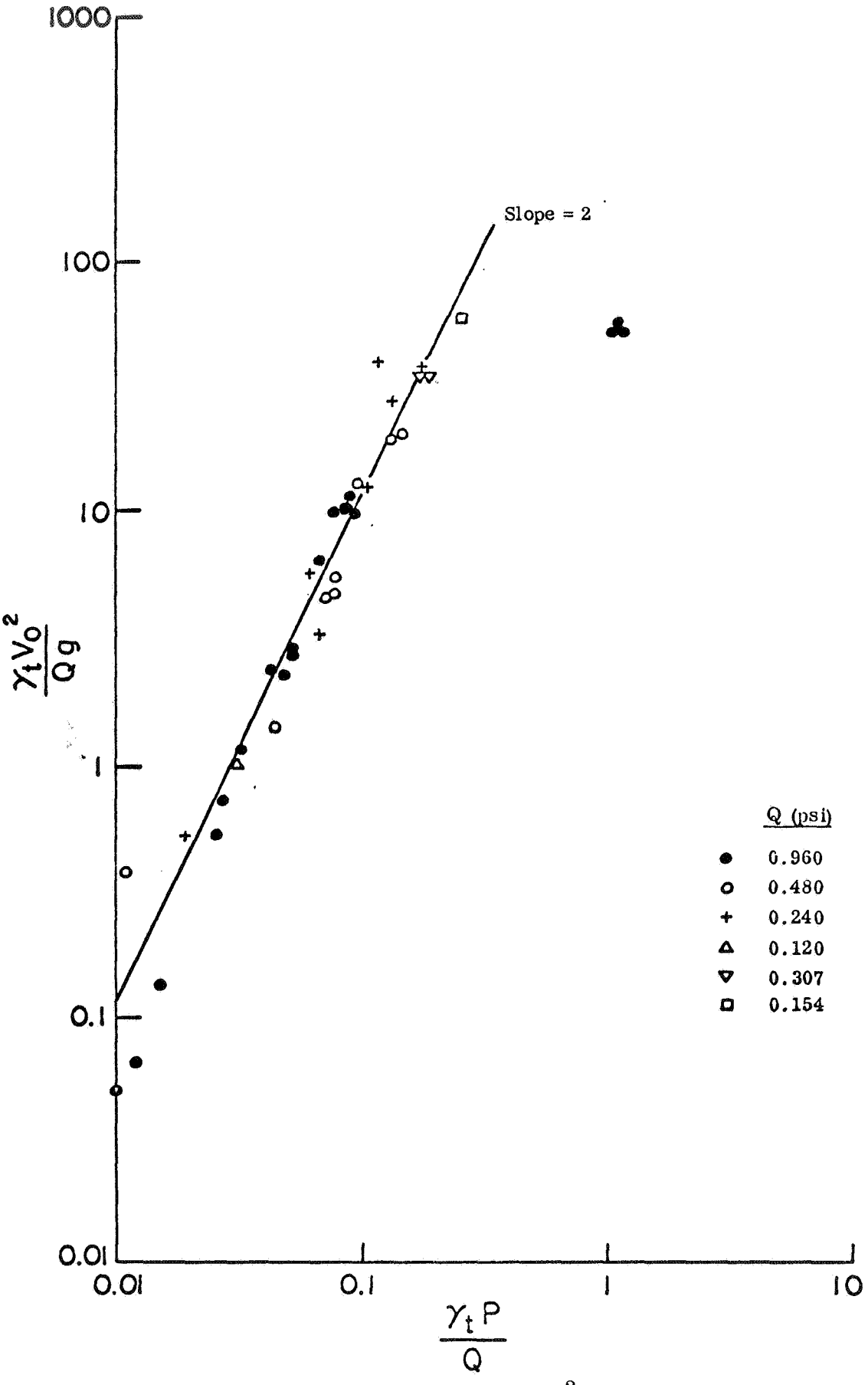

FIG. 4-20. γ_t P/Q versus $\gamma_t V_0^2$ / Q g

Therefore,

$$P = \frac{k^1}{\gamma_t^{1/2} g^{1/2}} Q^{1/2} V_0 \qquad (4\text{-}46)$$

For a given soil and known value of g

$$P = K Q^{1/2} V_0 \qquad (4\text{-}47)$$

Taking into account different projectile nose shapes:

$$P = K n Q^{1/2} V_0 \qquad (4\text{-}48)$$

Equation 4-48 is readily identified as the Modified Moore Equation. From the results of these analyses it is reasonable to conclude that the Modified Moore Equation provides quite an accurate basis for prediction of low velocity (< 200 ft/sec) projectile penetrated on earth.

C. Effects of Related Factors

Returning now to a consideration of lunar secondary impact craters, the scatter in Fig. 4-1, if not caused by material inhomogeneity, must be attributed to other factors which hinder the accurate use of the equation.

Because there is essentially no atmosphere on the moon, there can be no pore air pressures developed during dynamic penetration of lunar soils. This is in direct contrast to soils on Earth, where the dynamic strength can be greatly affected by excess pore air pressures. On Earth excess pore air pressures develop when soils are forced to either compress or dilate rapidly causing air to be forced out of or into the soil pores.

If the soil is fine grained, its air permeability may be quite low thereby restricting the flow of air. This results in either positive or negative excess pore air pressures. In a loose soil, which tends to compress during shearing (as in projectile penetration), the positive excess pore air pressures decrease intergranular pressures resulting in a loss of shear strength. This is shown clearly by Fig. 4-21, prepared from data of Hanks and McCarty (1966). When the average particle size falls below a value between 27 and 65 μ, the air permeability becomes too low to permit air to escape as the material attempts to compress. Excess pore air pressures develop, the strength is reduced, and the penetration is increased.

Conversely, in a dense soil which tends to dilate upon shearing, the negative excess pore air pressures increase intergranular pressures and lead to an increase in shear strength. Thus, when two soils — one loose and one dense — are placed in a vacuum, the effect is to reduce depths of projectile penetration into the loose soil and increase them for the dense soil as compared to values obtained from similar tests under atmospheric conditions. Nonetheless, the results of Clark and McCarty (1963) show that the relationship between depth of penetration and projectile and soil parameters remains in the form of the Modified Moore Equation when the soil is tested in-vacuo. However, the value of K for penetration in-vacuo can be greater or smaller than that for penetration under atmospheric conditions, depending upon whether the soil is dense or loose. Thus prediction of K values for the lunar soil cannot be made from the results of penetration tests on earth without some consideration being given to these effects. Surveyor results yield permeability values characteristic of silts and fine sands. These types of soils are likely to be the most susceptible to excess pore air pressure affects during dynamic loading. Thus, it appears that it is not possible at the present time (without the results of penetration tests of earth soils in-vacuo) to accurately predict the specific type and nature of lunar soil from the available secondary impact crater data, since the significance of lunar K values cannot yet be assessed. In addition, it should be noted that all of the analyses have assumed a homogeneous lunar soil profile.

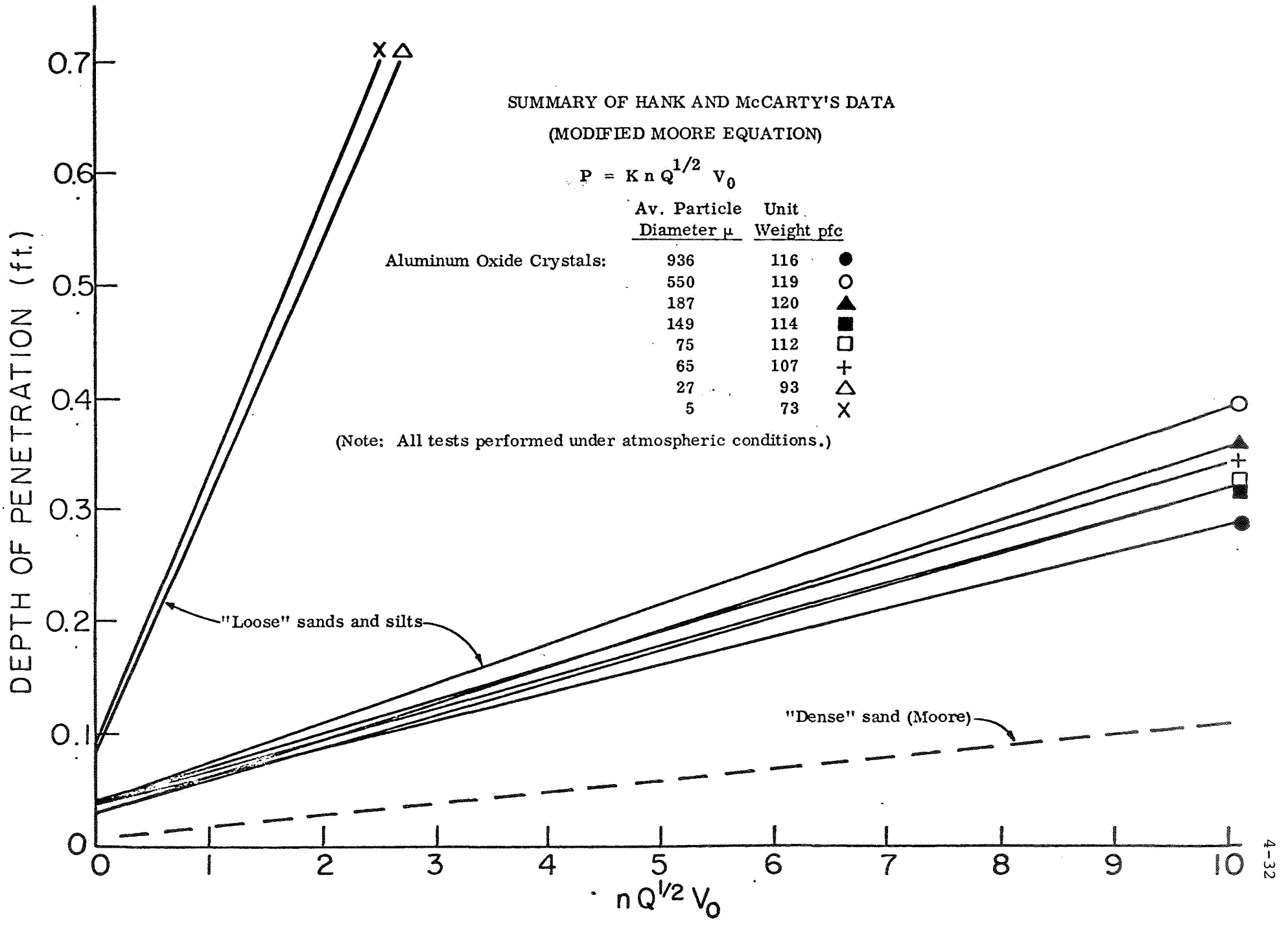

FIG. 4-21 Effect of Particle Size on Penetration Depth

It is likely, however, that the lunar soil is underlain by bedrock at different depths in different locations. The depth to bedrock, if within the depth of penetration, should have a pronounced effect on the depth of penetration.

On the other hand the investigation of secondary craters would still appear to be useful for the assessment of lunar soil variability since only relative values of parameters are needed. In this case any problems created by reduced gravity conditons on the moon need not be considered.

Various investigators have shown that the penetrator nose shape has an influence upon depths of projectile penetration. In fact, this is accounted for by the empirical constant, n, in the Modified Moore Equation. Values of n ranged from 0.56, for a flat-nosed projectile, to 0.725, for a hemispherical projectile. Higher values are obtained for more pointed nose shapes. Assuming that the nose shape of the boulders which created the lunar secondary craters ranged between flat and hemispherical, an error of ± 13% might be incurred in the calculated values of $n \cdot Q^{1/2} \cdot V_0$ if an average value of n = 0.643 is assumed for the lunar boulders. This amount of error is in addition to that caused by uncertainty as to how the boulder contacted the ground — whether on its "nose" (as we have assumed), on its long flat side, or in some other intermediate position. There is really no way of knowing with only the Lunar Orbiter data available.

All earth-based tests of low-velocity projectile penetration into soils have shown that the depth of penetration is independent of projectile diameter as long as Q remains constant. However, no tests have been conducted with projectiles of diameter greater than one foot — much less of diameters approaching 5 m as are those of the secondary impact crater boulders. But since the lunar boulders are of the same magnitude of diameter, we can hopefully conclude that the results will not be affected by this factor.

All of the secondary crater boulders that can be analyzed bounced upon impacting the lunar surface. This may have been due to their low angles of impact (assumed by Moore [1967] to be at 60° from the horizontal). In all of the analyses, it was assumed that boulder bouncing has a negligible effect upon depth of penetration, and only a very small portion

of the impacting energy is consumed by boulder bouncing. Furthermore, angles of impact less than 90° (vertical) are accounted for by using the normal component of velocity as the effective impact velocity which determines depth of penetration. To investigate these assumptions, a series of oblique impact tests was performed using spherical projectiles impacting an air-dry, powdered, medium dense, silty clay at velocities from 20 — 70 fps. Three different spherical projectiles were used, and for each the normal component of velocity, V_n, was kept constant while the angle of impact was varied from 30° to 90°.

The test results, shown in Fig. 4-22, indicate that there is a slight trend for depths of penetration to decrease with a decrease in impact angle. While there are probably other factors involved, one that seems most apparent is that projectile rebound caused less than the full amount of effective vertical kinetic energy to be used in the penetration process. In the tests described, the spherical projectiles invariably bounced out of their associated craters at impact angles of 60° or less. In some cases they bounced out for angles as high as 75°. It was noticed that the lower the impact angle, the greater was the distance (both horizontally and vertically) that the projectile bounced after impact. This would seem to account for the lesser and lesser depths of penetration as the angle of impact became smaller and smaller.

It would appear from these results that very little error is involved in assuming a single angle of impact (i.e. 60°) for all secondary impact crater boulders if the actual angles differ from the value by no more than ± 15% (45° — 75°). In such a case the error range would only be ± 3%, provided the vertical component of boulder velocity at impact is known. Unfortunately, however, as the analysis is applied, the impact velocity is computed using the range from the primary to secondary crater and a simple ballistics equation where it is assumed that the ejection angle is 60°. This component will range from 70.7% to 96.5% of the boulder velocity over an impact angle range of 45° to 75°.

As already noted, surface layering is a problem that may mask out the effects of weak, thin layers of soil over hard rock. The result would be to give an "average" hardness of the surface — a value that would be too great for the soil layer. The only way of avoiding this error is

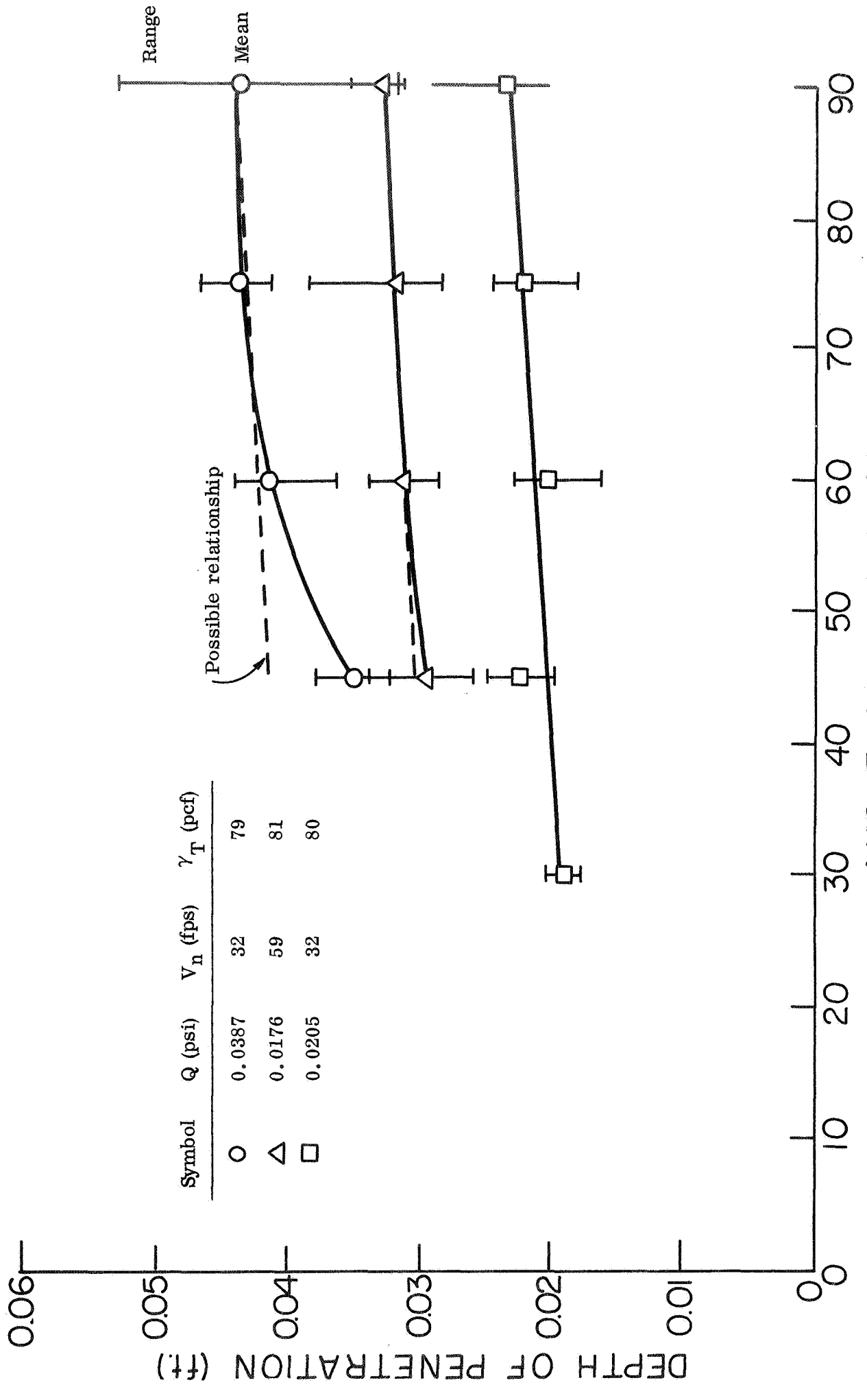

FIG. 4-22 Depth of Penetration versus Angle of Impact

to exclude from the analysis any secondary crater that is abnormally shallow as compared to its width. Such a crater would imply a hard surface at a very shallow depth. But on the other hand, the identification of such craters provides a valuable clue to lunar stratigraphy.

In analyzing the secondary craters, the density of the boulder must be assumed. Estimates of rock density on the moon have ranged from 1.0 to over 3.0 gm/cc. If a value of 2.0 gm/cc is assumed for calculations, it can be shown that errors in calculated values of $n \cdot Q^{1/2} \cdot V_0$ up to 30% may occur if the assumed value is incorrect. Of course, it is of no consequence if the assumed density is incorrect as long as all the boulders have the same density, since as has been stated the most feasible purpose of the analysis at this stage should only be to assess the variability of K values and not their absolute value and meaning.

It has also been customary to assume that the boulders' range is measured from the edge of the meteor crater. In fact, if it were spewn out from the center of the crater, the error in the calculated impact velocity may approach 15% and thus cause considerable scatter in the data.

Because of the many factors listed above and the possible errors involved, it does not seem prudent to attribute all the scatter in the secondary impact crater data to variability of the lunar surface materials. It must therefore be concluded that from the information available it is not possible to assess, with any confidence, absolute values of lunar soil properties by using secondary impact crater data from Lunar Orbiter photographs; however the determination of lunar soil variability at different locations may be possible.

III. CONCLUSIONS

Soil penetration equations have been presented which adequately relate depth of projectile penetration to soil type on earth. The Modified Moore Equation has been shown to give the best results of all the equations. Because of this and because of its relatively simple form, its use for further analysis of secondary impact craters is recommended in preference to the other equations examined.

However, analyses of the factors involved in the investigation of lunar secondary impact craters indicate that there exist great possibilities for error which can completely negate the purpose of the analysis if it is applied in the hope of determining absolute soil property values. It appears that at the present time conclusions can only be drawn concerning lunar soil variability on the basis of lunar secondary impact crater data.

In addition information on secondary impact craters has proved beyond any doubt that large areas of the moon's surface are covered by soil to a depth of at least one to two meters. Because the boulders bounced out of the secondary craters, it would appear that the lunar soil offers a significant resistance to penetration.

It is to be hoped that continued study of secondary cratering phenomena will lead to a reduction of the uncertainties in the analyses, and that more specific quantitative estimates of soil properties can be obtained.

REFERENCES

1. Carden, H. D. (1967), "Experimental Study of the Application of the Penetrometer Technique to the Lunar Surveying Staff Concept," NASA Tech. Note TN-D-3937, May.

2. Clark, L. V. and McCarty, J. L. (1963), "The Effect of Vacuum on the Penetration Characteristics of Projectiles into Fine Particles," NASA Tech. Note TN-D-1519, Jan.

3. Hanks, B. R. and McCarty, J. L. (1966), "Investigation of the Use of Penetrometers to Determine the Capability of Dust Materials to Support Bearing Loads," NASA Tech. Note TN-D-3200, Jan.

4. McCarty, J. L. and Carden, H. D. (1962), "Impact Characteristics of Viscous Materials Obtained by an Acceleration-Time-History Technique Applicable to Evaluating Remote Targets," NASA Tech. Note TN-D-1269, June.

5. McCarty, J. L. and Carden, H. D. (1968), "Response Characteristics of Impacting Penetrometers Appropriate to Lunar and Planetary Missions," NASA Technical Note TN D-4454, April.

6. Moore, H. J. (1967), "The Use of Ejected Blocks and Secondary Impact Craters as Penetrometers on the Lunar Surface," Appendix A of "Preliminary Geologic Evaluation and Apollo Landing Analysis of Areas Photographed by Lunar Orbiter III," NASA, June.

7. Scott, R. F. (1962), "Problem of the Penetration of a Projectile Into Soil, A Soil-Like Medium, or Compressible Rock (Pumice)," Series of 4 reports to Space-General Corporation.

8. Terzaghi, K. and Peck, R. B. (1967), Soil Mechanics in Engineering Practice, John Wiley, N. Y., 2nd. ed.

9. Thompson, L. J. (1967), "Dynamic Penetration of Selected Projectiles into Particulate Media," SC-RR-66-376, Sandia Laboratory, Albuquerque.

10. Womack, D. P. and Cox, W. R. (1967), "Measurement of Dynamic Characteristics of Soils with Penetrometers," NASA Contractor Report CR-849, August.

11. Woodward-Clyde & Associates (1962-67), Special Projects Division, Fifty-two reports to the Sandia Corporation on Soil Studies Associated with Sandia earth penetration tests.

12. Young, C. W. (1967), "The Development of Empirical Equations for Predicting Depth of an Earth-Penetrating Projectile," Sandia Corporation, SC-RR-67-60.

List of Symbols

a	grouping of certain terms in the Poncelet Equation
A	gross cross-sectional area of penetrator
b	constant depending on A in the Poncelet Equation
c	constant
C	constant depending on N
C_1, C_1, C_3	numerical constants in the Resal Equation
D	diameter of projectile
D_1, D_2, D_3, D_4, D_5	constants in the Poncelet Equation
g	gravitational constant
k	soil constant
k'	proportionality constant
K	soil constant
K'	equals $c/g^{1/2}$
K''	proportionality constant
K_1, K_2	constant coefficients in the Young Equation
K_3, K_4	constant coefficients in the Resal Equation
K_5, K_6, K_7	constant coefficients in the Poncelet Equation

ℓ	constant depending on projectile nose shape
L	length of projectile
m	mass of projectile
n	relative projectile nose shape constant
n'	projectile nose shape constant in the Resal Equation
n''	projectile nose shape constant in the Poncelet Equation
N	average standard blowcount over the depth of penetration
P	depth of penetration of projectile
P_A	actual depth of penetration
P_N	normalized depth of penetration
P_0	static depth of penetration
Q	weight-to-area ratio of projectile
S	soil constant
S'	soil constant in the Resal Equation
S''	soil constant in the Poncelet equation
V_0	vertical component of impact velocity of projectile
V_n	normal component of velocity
W	weight of penetrator

x_1, x_2	exponents in dimensional analysis
y_1, y_2	exponents in dimensional analysis
z_1, z_2	exponents in dimensional analysis
α	equals $(80 + N)\gamma_t C/(625{,}000\ LQ)$
β	constant depending on cross-sectional area of projectile
γ_t	unit weight of target soil
θ	boulder ejection angle
π_1, π_2	dimensionless parameters
ρ_p	mass density of projectile
ρ_t	mass density of soil

C H A P T E R 5

LUNAR STRATIGRAPHY AS REVEALED BY CRATER MORPHOLOGY

by

Francois E. Heuzé and Richard E. Goodman

CHAPTER 5

LUNAR STRATIGRAPHY AS REVEALED BY CRATER MORPHOLOGY

(Francois E. Heuzé and Richard E. Goodman)

I. INTRODUCTION

The stratigraphy of the moon's surface has been under investigation for a number of years and the consensus is that, over the maria, a fragmental layer of fine grained material overlays a hard base composed of one or several layers of possible volcanic origin. However, it is not until very recently (1966) that the first conclusive attempts were made to determine the extent and the thickness of this surficial layer. These efforts are important for lunar engineering because:

(1) The trafficability of planned traverses depends upon the depth of the "soft" surficial layer.

(2) The planning of borings for sampling or testing purposes can be optimized in terms of power requirements and adequate drilling tools only if the rock/soil profile is known.

(3) Analysis of foundation settlements for major structures (nuclear plants, observatories, etc.) requires a knowledge of the soil/rock profile.

(4) For construction of excavations and embankments, e.g., for foundations and thermal radiation shielding, one must determine what kind of material is available, and how much of it can actually be used.

Earlier studies (Baldwin, 1963; Engel, 1962; Baldwin, 1965) concerned themselves with the morphology of lunar craters in order to determine their origin. A scaling law (Baldwin, 1963) was proposed relating crater depth (d) and diameter (D) (meters):

$$D = 0.025\ d^2 + d + 0.630$$

This relationship was applicable to man made impact craters and to the small lunar craters (D less than a few kilometers).

Salisbury and Smalley (1963) then reviewed direct and indirect evidence for the nature, origin, and geometry (depth and extent) of the lunar surface materials.

They presented their conclusions as follows:

MEASUREMENT	CONCLUSION
Infrared Emission	Low thermal conductivity
Radio Emission	Low thermal conductivity
Radar Reflection	Low density. Surface gradient 1 in 11 on a meter and 10 cm scale
Polarization	Agglomerated powder composed of opaque grains
Photometry	High porous, complex and irregular surface. Relief many times the wavelength of light
Albedo and Color	Non-terrestrial reflectivity

The mechanisms cited for producing a fragmental layer were: meteoroid impact, micrometeoroid infall, radiation, internal seismic shock, volcanism, and thermal fracture. The pulverizing effect of meteoroid impacts was retained as being by far the most important of these mechanisms.

Besides considerations of entrapment of meteoridal debris and electrostatic transport, major conclusions were concerned with roughness and depth of the blanket. By analogy with the earth, the size of blocks ejected from craters,a trafficability constraint, was related to the volume of the craters they originated from. Typical block sizes would be 4.5 m around craters 100 m in diameter and 16 m around craters with D = 1 km if no secondary fragmentation occurs. Average depth estimates were obtained for maria and highlands based upon frequency and volume of primary craters. These and other conclusions are presented in Table 5-1.

However good these estimates proved to be in the light of later investigations, they could not be used as such for detailed planning of missions at specific sites. With the advent of spacecrafts and the availability of higher resolution photographs of the moon (Rangers), further studies (Jaffe, 1965, 1966a, 1966b; Walker, 1966) were made to estimate the depth of unconsolidated materials resting on a harder base on the lunar surface. They were followed as resolution still improved (Orbiters and Surveyors) by the development of new techniques based upon direct observations (Lunar Orbiter Photo Data Screening Group, 1967a, 1967b, 1968; Rennilson, 1966; Shoemaker, 1967a, 1967b; Jaffe, 1967) or modeling (Gault, 1966; Oberbeck and Quaide, 1967; Harbour, 1967; Quaide and Oberbeck, 1968; Ross, 1968).

II. DETERMINATION OF SURFICIAL LAYER THICKNESS

Four techniques can be recognized among the latest attempts to analyze surficial lunar stratigraphy.

A. Comparative Study of Ranger Photographs — Laboratory Simulation of Overlay Deposition

Observing Ranger VII photographs, Jaffe (1965) noted the "soft" appearence of some lunar craters and inferred that this was attributable to an overlay of dust or other granular material deposited after crater formation.

The erosion and depositional processes which affect the relatively small lunar craters are lunar "dusting" and downslope movement. Lunar dusting refers to the process by which fragments produced by primary and

secondary impacts rain down onto the lunar surface. If the assumption is made that meteoritic impact of the lunar surface takes place in a random manner, then it follows that a lunar dust blanket of uniform thickness would result if the fragments were deposited on an even surface. The term downslope movement can be used to include three different types of erosional processes. One type consists of the slumping of the walls of the crater. Another type of downslope movement occurs when the fragments produced by meteorite impacts elsewhere rain down onto the crater wall and bounce down the slope. A downslope movement associated with this latter type occurs when fragments which hit the crater wall induce the particles composing the wall to also move down the slope (Jaffe, 1965; Ross, 1968). If the assumption is made that the slumping process is not important in changing the morphology of small craters, then the lunar dusting process is seen to be the most influential.

To obtain an experimental relation from which to determine the depths of overlay on lunar craters, a number of dusting experiments were performed. They consisted of reproducing in the laboratory three types of craters. Two of them were made by impressing the surfaces of flattened spheres into dry silica sand, and the third was made to be somewhat flat-bottomed with conical sides produced by slumping. The criterion for choosing these particular shapes was that they showed similarity to those appearing on some Ranger VII photographs. Once a crater had been impressed into the sand, it was sprinkled with sand. Measurements of the depth of overlay at a number of places on its surface were made.

Pictures of the experiments were then matched with those taken of lunar craters by Ranger VII, and measurements in the laboratory were scaled up to what hopefully was the depth of the overlaying materials on the lunar surface. Jaffe concluded that at the sites of Ranger VII photographs, the depth of overlay was at least five meters, and possibly much more. The technique was refined and applied to Ranger VII (Jaffe, 1966a) and Ranger VIII and IX (Jaffe, 1966b) photographs giving results consistent with those of the first study.

Objections have been raised (Walker, 1966) against such a procedure; namely the insufficient considerations of crater age, of all possible erosional processes (including impacts), and the apparent

dependency of the results on crater diameter for small craters (D < 30 m). However, the main shortcoming of the technique remains the fact that only a lower bound of layer thickness is provided. It cannot be assumed that the layer existing prior to impact has significantly different properties than the one deposited after impact. "Upper bound" techniques had then to be developed.

B. Direct Study of Orbiters and Surveyors Photographs — Block Fields, Terraces, and Outcrops

Further improvement of photographic resolution was achieved by the Orbiter spacecrafts missions (Lunar Orbiter Photo Data Screening Group, 1967a, 1967b, 1968). Two direct techniques were then used by the Lunar Orbiter Photo Data Screening Group to analyze the lunar surface stratigraphy.

Wherever well developed annular terraces or prominent layers can be recognized on crater walls, direct measurements of the thickness of each layer can be achieved knowing the slope angle of the walls. This can usually be done for medium size craters (100 to several hundred meters), where the upper part of the walls is not covered by debris. In the presence of smaller craters one might thus look for the presence or absence of boulder fields inside and outside the crater. These boulders are assumed to originate from the hard substratum by fragmentation upon meteoritic impact. Accordingly, for a particular area of the lunar surface, the depth of the smallest crater or craters with blocky rim or floor is assumed to be the thickness of the surficial unconsolidated layer. Indeed, a scarcity of block fields, a subdued crater appearance, and/or the absence of outcrops are indicative of fairly deep fragmental layer. These techniques applied to a variety of sites (see Table 5-1) gave very consistent results.

Successful Surveyor and Luna missions (Rennilson, 1966; Shoemaker, 1967a, 1967b; Jaffe, 1967; Gault, Quaide, Oberbeck, and Moore, 1966) provided the highest resolution photographs. The stratigraphic interpretation of these photographs which was based on observations of block fields, yielded results agreeing with those of Orbiter photograph studies (see Table 5-1).

Besides thickness estimates, these studies resulted in some major conclusions which can be summarized as follows:

(1) Young or fresh craters (Lunar Orbiter Photo Data Screening Group, 1967b) will provide most of the needed information.

(2) The impact origin of small and medium size craters is hypothesized from the following observations: lunar crater size-frequency distribution (Showmaker, 1967a) is similar to the one of experimental impact craters, and block size distribution (Lunar Orbiter Photo Data Screening Group, 1967b) around lunar craters is similar to the one around explosion craters (i.e., Danny Boy).

(3) The fragmental lunar surface layer is very weakly cohesive since the impact craters observed have raised rims which would not exist in cohesive materials (Gault, Quaide, Oberbeck, and Moore, 1966). This obviously corroborates the Surveyors soil experiments and extends their results to greater depths. However, the cohesion is thought to increase somewhat with depth (Lunar Orbiter Photo Data Screening Group, 1967b).

It is to be mentioned that a drainage origin into subsurface fissures has also been proposed for a few small craters (Jaffe, 1967; Shoemaker, 1967b).

The technique presented here appears to be the most reliable for it does not involve any correlation or scaling. However, impact cratering experiments (Gault, Quaide, and Oberbeck, 1966, 1967) have suggested still another method of analysis whose application was attempted on a large scale.

C. Comparative Study of Orbiter Photographs — Impact Crater Morphology

1. The Technique. Quaide and Oberbeck (1968) presented the basis for their studies as follows:

> "In laboratory cratering studies inspired by the Ranger photographs, Gault, et al. (1966) observed that impacts against targets of fragmental materials overlaying a rock substrate could produce craters with a peculiar concentric or terraced structure. They found that craters with normal spherical segment or conical

> geometry developed when the fragmental materials were of such thickness that the rock substrate did not interfere with crater growth. Examination of Orbiter I photographs revealed that numerous craters with concentric geometry are present on the lunar surface, and that they might be used to estimate the thickness of the fragmental surface layer. Careful study of selected photographs revealed further that all fresh craters with diameters less than a few hundred meters can be structurally classified and that the crater structure is size dependent. This prompted an investigation of the conditions of formation of all crater structures arising through impact against a target consisting of fragmental materials resting on a cohesive substrate. These studies show that all the morphologic classes recognized can be produced by impact if the thickness of a fragmental surface layer resting on a cohesive substrate is varied."

The application of this procedure was restricted to craters with a diameter $D < 500$ m giving the stratigraphy to a depth of about 50 m. In view of the possible engineering applications mentioned above, this is a satisfactory depth limit. The study was also restricted to "fresh" craters defined as those with sharp appearance if $D < 70$ m or those surrounded by light rays or halos if $D > 70$ m for Orbiter I medium resolution photographs. This boundary will change if the photographic resolution changes.

Three (Oberbeck and Quaide, 1967) then four (Quaide and Oberbeck, 1968), morphologic classes were thus recognized to which an R value bracket was assugned for impact tests with R being defined as:

$$R = D_A/t \text{ or } D/t$$

where

D or D_A = apparent crater diameter (rim to rim)

t = surficial layer thickness

The four classes can be approximately presented here as*

normal craters	:	$R < 4$
flat bottom craters	:	$4 < R < 7.5$
central mound craters	:	$4 < R < 7.5$ (maximum mound height for $R \simeq 6$)
concentric craters	:	$R > 7.5$

Identifying the crater type and measuring D, one can thus compute.

Latest refinements in the correlation (Quaide and Oberbeck, 1968) include the effect of such variables as impact velocity, angle of impact, projectile properties, angle of repose of surficial debris, strength of substrate, and gravity. The substrate strength has a non neglible effect on R. A new parameter D_F/D_A (where D_F = diameter of the floor of the surficial crater in flat bottom and concentric craters) is also introduced and found to be subject to boundaries for each crater class. Application of this technique to selected Orbiter photographed sites gives results very similar to those obtained by the Orbiter Screening Group (see Table 5-1).

Other major conclusions of these studies can be summarized as follows:

a) A new weight of evidence has been produced in favor of the impact origin of small lunar craters.

b) The surficial layer is a slightly cohesive fine grained aggregated with in situ angle of repose from 33 to 35°.

c) Some past volcanic activity is exhibited under the form of terrace levels of flow layers.

d) Rock, not permafrost, is exposed on terraces in crater walls.

---

*See Ref. 18 and 20 for detailed presentation of R boundaries.

2. Objections to the validity of the technique. Whatever good agreement with other determinations was obtained by this method, it has been found inapplicable by some investigators. Moore (Lunar Orbiter Photo Data Screening Group, 1968)(Orbiter V-8 site) states, "Attempts to calculate the thickness of soil-like layer using the method and data of Oberbeck and Quaide (1967) indicate that the computed thickness is unfortunately a function of crater diameter and not any given thickness of a soil-like layer." Harbour (1967) (Orbiter III P-12 site) also comments, "Using moderate resolution photographs Quaide and Oberbeck (1967) estimate the thickness of the regolith in this area as 5 to 15 meters by noting the morphology of fresh craters less than 40 m in diameter. However craters much smaller than those they observed possess the same morphologic features.... The variety of morphology of fresh craters in this area and the variety in size of craters of similar morphology indicates the size and morphology relationships cannot be applied in any simple way to determine depth of the lunar regolith."

Five conclusions concerning the relationship between crater morphology and size are then possible according to Harbour.

a) Multiple layers may occur in the area and may affect the morphology of craters bottoming near their upper boundary.

b) Crater morphology may be governed more by velocity and density of the projectile than by layering of the target material.

c) The thickness of the regolith may vary within short distances.

d) Cohesion of mare material may vary within short lateral distances.

e) The regolith varies both in thickness and properties.

3. Discussion. Latest studies by Quaide and Oberbeck (1968) seem to exclude alternative *b*, the effects of projectile properties having been analyzed and found to be minimal. Alternative *a* would apply to the layers of consolidated igneous rocks deposited upon successive

volcanic floodings. The minimum depth of rubble/soil cover above them is an average 10 meters. Alternatives *c*, *d*, and *e* can apply to this layer. At a given site, the erosion-deposition processes due to impact will give it a complex structure (Salisbury and Smalley, 1963) owing to the wide variation in the size of craters formed through the ages and the intricate overlapping of the ejecta. Each crater, however small, might then reflect this non homogeneity and increase in bearing capacity which is known to start at the very surface of the blanket(Rennilson,1966; Shoemaker, 1967a; Jaffe, 1967).

D. Use of a Mathematical Model (Time-Dependent Lunar Crater Rim-Erosion and Floor-Deposition)

Meteoritic bombardment being taken as the primary source of erosion on the lunar surface, a simplified mathematical model for time dependent erosion of lunar craters was presented by Ross (1968). The model takes into consideration the angular distribution of impacting meteorites and ejecta and the topography and mechanical properties of the lunar surface. Calculations indicate that craters 1, 10 (D/d = 3) and 100 (D/d = 5) meters in diameter disappear almost completely after 10^7, 10^8, 10^9 years, respectively. Mass movement of eroded material is thought to accompany the meteoritic erosion process and probably result in an erosion rate 50 to 100 times greater than erosion due to ejection without downslope movement. This is believed to be a continuous process and no mention is made of large slope failures or slumps having been identified by the author.

Assuming that the maria are at least 2×10^9 years old, it is inferred that several generations of impact craters of the order of 10 m in diameter have been effectively removed as topographic features since formation of the maria. This process would have produced a depositional overlay at least 2 or 3 meters thick. The total depth of rubble and unconsolidated material is thought by Ross to be somewhat greater and and to vary considerably.

Discussion. Here, as in Jaffe's work, the question arises, from an engineering stand-point, of the usefulness of determining the thickness of an "overlay" when the total depth of unconsolidated material remains unknown. It is not clearly stated either what the significant differences might be in the engineering properties of these two constituents of the lunar surface or how sharply one could or should draw a boundary between them.

III. CONCLUSION — FURTHER RESEARCH

Altogether, studies based upon visual observation of lunar craters, comparison with experimental results, or analytical models have appreciably narrowed the range of conclusions regarding the lunar surface stratigraphy. Most of the maria's surface is believed to be overlain by a layer of fine grained, cohesionless to weakly cohesive fragmented rock whose thickness varies from a few meters to a few tens of meters, (see Table 5-1).* Compressibility decreases and average grain size increases from the surface down. Rubble is probably present. Still, this fragmental blanket can be excavated and handled without the use of explosives except in the vicinity of large craters where large size blocks, several cubic meters, would be buried. Further research is needed to determine if excavation and back-filling of this material of limited thickness would provide adequate meteorite and radiation shielding of structures. Drilling and construction planning based upon the above conclusions must condider the stability problem; uncased boreholes are unlikely to be stable and medium-height slopes might have to be rather flat to stand up (embankments, excavation walls, etc.). Additional research is therefore also suggested in the field of slope stability of the lunar surface blanket. Beneath it, non-fragmented rock layers are thought to exist as a result of successive lava floodings. As mentioned by Watkins and Whitcomb (1968), "Near surface lunar rocks may be shattered and broken as a result of stresses created during formation of large craters." This will have bearing upon underground storage projects or sealing off of underground cavities for dwelling purposes in the event the blanket is too thin to provide adequate shielding.

*For the reader's convenience, salient conclusions of each reviewed work are summarized in Table 5-1.

Previous discussion of techniques applied to lunar stratigraphy determination leads to the conclusion that for final mission planning, at a given site, extensive high resolution photographic coverage is mandatory, and the interpretation should rely upon visual observation, (Lunar Orbiter Photo Data Screening Group, 1967a, 1967b, 1968) with the other procedures still being too open to discussion. However, if the required resolution for using this technique is not achieved and if only the gross morphology of craters can be recognized, the method developed by Quaide and Oberbeck (1967, 1968) can then be used for a first estimate.

TABLE 5-1

STUDIES OF LUNAR CRATERS MORPHOLOGY AND LUNAR SURFACE STRATIGRAPHY.

REF.	TECHNIQUE	LOCATION ON MOON	CRATER D RANGE (m)	ORIGIN OF CRATER	DEPTH OF SURFICIAL LAYER (m)	REMARKS
1	COMPARE D/d FOR LUNAR AND MAN MADE CRATERS	--- (TELESCOPIC OBSERVATIONS)	UP TO 30 KM	METEORITIC IMPACT	---	SCALING LAW OBTAINED: $D = 0.025\, d^2 + d + 0.630$
4 AND COMMENT	STUDY OF D, d FOR LUNAR CRATERS	--- (TELESCOPIC OBSERVATIONS)	> 1 MILE (1.6 KM)	---	---	WHEN D ↗, d/D ↘ SHARPLY FOR EXPLOSION-IMPACT CRATERS. NOT TRUE FOR LARGE D'S. THUS THEY ARE NOT OF EXPLOSIVE IMPACT ORIGIN.
2	COMPARE D/d FOR MOON AND EARTH METEORITIC CRATERS	--- (RANGER VII PHOTOGRAPHS)	26 FEET (8 M) TO 26 MILES (40KM)	METEORITIC IMPACT	---	SCALING LAW OF REF. (1) CHECKED. APPLIED TO EARTH-METEORITIC AND MOON CRATERS. THUS THOSE MOON CRATERS STUDIED ARE OF IMPACT ORIGIN.
7	COMPARE MOON CRATERS WITH LABORATORY ONES WITH SAND OVERLAY	MARE COGNITUM (RANGER VII PHOTOGRAPHS)	3 M TO 13 KM	METEORITIC IMPACT	> 5 M (OVERLAY)	R = D/d VARIES FROM 20 TO 80 FOR D = 5 TO 600 M IN LUNAR CRATERS. THICKNESS OF COHESIONLESS OVERLAY IS ONLY A SMALL PART OF t OF SURFICIAL LAYER.
8	IBID	IBID	IBID	IBID	IBID	REFINED TECHNIQUE OF LABORATORY SIMULATION. AGAIN, t ESTIMATED FOR OVERLAY SPRINKLED OVER TERRAIN AFTER CRATER FORMATION.
9	IBID	MARE TRANQUIL, ALPHONSUS HIGHLANDS (RANGER VIII, IX PHOTOGRAPHS)	< 30 M > 75 M	METEORITIC IMPACT	4 M TO 40 M (AVERAGE 16 M) 20 TO SEVERAL TENS OF METERS	DEPTH OF OVERLAY FOR LOW COHESION SOILS 3 TO 10 TIMES GREATER THAN FOR COHESIONLESS OVERLAY. THREE GROUPS OF LABORATORY OVERLAY USED. GROUPS 2 AND 3 CORRESPOND TO COHESION OF SURVEYOR I LANDING SITE. ($\simeq 10^4$ DYNES/CM^2 OR 0.15 PSI)
22 (COMME... AND REPLY	COMPARE ACTIVE EROSION PROCESSES (IMPACT) WITH PASSIVE ONES (AFFEL'S EXPERIMENT)	---	---	IMPACT ?	---	NO AGES MENTIONED IN JAFFE'S STUDIES. EROSION PROCESSES MUST BE FURTHER STUDIED. OVERLAY THICKNESS SEEMS TO BE DIAMETER DEPENDENT FOR D < 30 TO 50 M.

TABLE 5-1 CONT.

REF.	TECHNIQUE	LOCATION ON MOON	CRATER D RANGE (m)	ORIGIN OF CRATER	DEPTH OF SURFICIAL LAYER (m)	REMARKS
11	PRESENCE OR ABSENCE OF BLOCKY FIELDS AROUND CRATERS OR ON CRATER FLOOR. ALSO OBSERVATION OF EXPOSED LAYER BASE ON CRATER WALLS.	ORBITER II SITES P-2 P-3,5 P-6 * P-7 P-9,11 MARIA	 100 M > 1000 M > 175 M > 100 M > 400 M 10 TO 500 M	---	 --- --- 10 M 15 TO 20 M 10 M ---	RATING OF SITES IN TERMS OF RELATIVE ROUGHNESS. LOOSELY COHESIVE SURFICIAL LAYER. CRATER SIZE-FREQUENCY IS NOT SOPHISTICATED ENOUGH A MEASURE OF TERRAIN ROUGHNESS.
12	STILL LOOK FOR: BLOCK FIELDS IN AND OUTSIDE CRATERS. WELL DEVELOPED ANNULAR TERRACES OR PROMINENT NARROW TERRACES ON CRATER WALLS.	ORBITER III SITES P-1 P-2 P-5 P-7 P-9 P-11 * P-12	 < 70 M > 200 M < 400 M > 800 M --- > 100 M --- --- ---	METEORITIC IMPACT	 > 10 M --- --- --- > 10 M 20 M 7 TO 10 M 8 TO 10 M 5 M	ALWAYS LOOK AT FRESHEST CRATERS. COHESION OF SURFICIAL LAYER INCREASES WITH DEPTH. BLOCK SIZE DISTRIBUTION AROUND CRATERS SIMILAR TO THE ONE OF DANNY BOY CRATER. THUS IMPACT ORIGIN HYPOTHESIZED.
13	PRESENCE OR ABSENCE OF BLOCK FIELDS. DEPTH OF ROCK OUTCROP ON CRATER WALLS. PRESENCE OF BOULDER TRACKS.	ORBITER V SITES V-5 V-10 V-13 V-16 V-24 V-28	 30 TO 300 M --- --- --- --- ---	METEORITIC IMPACT AND POST-IMPACT VOLCANISM	 > 1/2, 1 M VERY THICK > 10 M > 10 M FAIRLY DEEP 100 M	"COMPUTED THICKNESS BY QUAIDE AND OBERBECK METHOD (1967) IS UNFORTUNATELY A FUNCTION OF CRATER DIAMETER AND NOT ANY GIVEN THICKNESS OF A SOIL-LIKE LAYER" (QUOTE) MINIMUM DEPTH CAN BE DERIVED FROM BOULDER TRACKS. SCARCITY OF BLOCK FIELDS, SUBDUED CRATER APPEARANCE, AND ABSENCE OF OUTCROPS ARE INDICATIVE OF FAIRLY DEEP FRAGMENTAL LAYER.

TABLE 5-1 CONT.

REF.	TECHNIQUE	LOCATION ON MOON	CRATER D RANGE (m)	ORIGIN OF CRATER	DEPTH OF SURFICIAL LAYER (m)	REMARKS
3	ALBEDO OF MOON'S SURFACE. GROSS FEATURE ANALYSIS.	EARTH SIDE (TELESCOPIC OBSERVATIONS)	LARGE	IMPACT AND VOLCANISM	---	GROSS STRATIGRAPHY OF MOON'S EARTH SIDE INFERRED FROM TELESCOPIC OBSERVATIONS. CLASSIFICATION OF MATERIALS AND RELATIVE AGE DETERMINATION.
16	PRESENCE OR ABSENCE OF BLOCKS ON CRATER RIM.	SURVEYOR I LANDING SITE	0.7 TO 80 M	METEORITIC IMPACT	1 M	THE DEPTH OF THE SMALLEST CRATERS WITH BLOCKY RIMS IS ASSUMED TO BE THE THICKNESS OF THE SURFICIAL LAYER. NEED HIGH RESOLUTION PHOTOGRAPHS. HAVE TO ASSUME D/d RATIO (D ONLY MEASURED): I.E. D/d = 1/3 TO 1/4 FOR FRESH CRATERS.
19	IBID (BLOCKY RIMS)	SURVEYOR III LANDING SITE	SEVERAL METERS	METEORITIC IMPACT	> 1 M SEVERAL TENS OF METERS AT CENTER	IMPACT ORIGIN HYPOTHESIZED FROM CRATER SIZE-FREQUENCY DISTRIBUTION RESULTS. THE FLOOR SURFACE IN BROAD CRATERS LOOKS SIMILAR TO THE ONE IN BETWEEN CRATERS. (OVERLAY DEPOSITED AFTER CRATER FORMATION, EJECTA, AND FALL-BACK.)
9	IBID (BLOCKY RIMS)	SURVEYOR V LANDING SITE	---	IMPACT AND DRAINAGE	< 5 M	DRAINAGE ORIGIN OF SOME CRATERS INFERRED FROM THEIR ALIGNMENT AND ASSOCIATION.
20	IBID (BLOCKY RIMS)	IBID	---	IBID	A FEW METERS (TYPICALLY 3M)	RATIO D/d ASSUMED TO BE IN BETWEEN 1/3 AND 1/4.
5	COMPARE LABORATORY IMPACT CRATERS AND MOON CRATERS.	LUNA 9 LANDING SITE	10 TO 100 CM (LABORATORY - UP TO 50 CM)	METEORITIC IMPACT	> 20 CM (CRATER DEPTH) MUCH DEEPER IN FACT	IMPACT CRATERS HAVE DISTINCT, WELL DEFINED RAISED RIMS WHEN IN NON COHESIVE OR WEAKLY COHESIVE SOIL. COHESIVENESS PREVENTS RAISED RIMS IN SMALL CRATERS. AGE ALSO MATTERS: YOUNG CRATERS ONLY SHOULD BE STUDIED (HAVE WELL DEFINED RIMS).
21		LUNA 13 LANDING SITE	---	METEORITIC IMPACT		NO "DUST LAYER ON THE MOON(?). UPPERMOST 20 TO 30 CM HAVE EARTH - SOIL LIKE PROPERTIES.

TABLE 5-1 CONT.

REF.	TECHNIQUE	LOCATION ON MOON	CRATER D RANGE (m)	ORIGIN OF CRATER	DEPTH OF SURFICIAL	REMARKS
14	CRATER MORPHOLOGY EXPERIMENTALLY RELATED TO THICKNESS t OF LAYER OVER HARD BASE (IMPACT TESTS). RESULTS APPLIED TO LUNAR CRATERS IN TERMS OF R = D/t.	(ORBITER I PHOTOGRAPHS) OCEANUS PROCELLARUM SURVEYOR I LANDING SITE	40 TO 250 M (EMPHASIS ON 70 TO 250 M)	METEORITIC IMPACT OR VOLCANISM	5 TO 15 M (85% OF SITE) AVERAGE IS 8 TO 9 M	EMPHASIS AS MUCH ON ORIGIN AS ON MORPHOLOGY OF LUNAR CRATERS. CRATERS STUDIED ARE SMALL ONES AND FRESH ONES ONLY. FOUR MORPHOLOGIC TYPES RECOGNIZED: NORMAL, FLAT-BOTTOM WITH OR WITHOUT CENTRAL MOUND, AND CONCENTRIC. EACH TYPE HAS ITS RANGE OF R = D/t. CONCENTRIC ONES GIVE BEST ESTIMATE OF THICKNESS t OF SURFICIAL LAYER. ROCK NOT PERMAFROST IS EXPOSED ON TERRACES IN CRATER WALLS. HIGHLAND STUDIES ARE INCONCLUSIVE.
6	STUDY OF CRATER MORPHOLOGY BY QUAIDE AND OBERBECK TECHNIQUE.	ORBITER III AND IV PHOTOGRAPHS III 12*-1	FEW METERS TO SEVERAL 100'S M	IMPACT	2 TO 8 M	EVEN VERY SMALL CRATERS POSSESS MORPHOLOGIC FEATURES IDENTIFIED BY QUAIDE AND OBERBECK. THUS UNCERTAINTY ON VALIDITY OF THE TECHNIQUE. POSSIBILITY OF EXISTENCE OF MULTIPLE LAYERS OR THICKNESS AND PROPERTIES OF LAYER MAY VARY WITHIN SHORT DISTANCES (?).
15	IBID A NEW PARAMETER IS INTRODUCED D_F/D_A	ORBITER II AND III SITES II P-13 II P-7 III P-12	< FEW 100'S M < FEW 10'S M (NORMAL) 10'S TO 100'S M (CONCENTRIC)	METEORITIC IMPACT AND VOLCANIC CONTRIBUTION (INTERBEDS)	2.5 TO 5.5 M 6.0 TO 9.0 M 3.5 TO 5.5 M	D_F/D_A AS WELL AS D_A t USED FOR THICKNESS DETERMINATION. SURFICIAL LAYER IS A SLIGHTLY COHESIVE, FINE-GRAINED AGGREGATE. IN-SITU ANGLE OF REPOSE $\simeq 33 - 35^{\circ}$. (SIMILITUDE WITH 31° FINE QUARTZ SAND). REFINED TECHNIQUE - INVESTIGATE EFFECT OF VELOCITY, ANGLE OF IMPACT, PROJECTILE PROPERTIES, ANGLE OF REPOSE, STRENGTH OF SUBSTRATE AND GRAVITY. EVIDENCE OF VOLCANIC CONTRIBUTION UNDER THE FORM OF TERRACE LEVELS OF FLOW LAYERS.

TABLE 5-1 CONT.

REF.	TECHNIQUE	LOCATION ON MOON	CRATER D RANGE (m)	ORIGIN OF CRATER	DEPTH OF SURFICIAL LAYER (m)	REMARKS
17	MATHEMATICAL MODEL FOR LUNAR CRATERS *TIME-DEPENDENT* RIM-EROSION AND FLOOR-DEPOSITION.	MARIA (RANGERS, ORBITERS, SURVEYORS PHOTOGRAPHS)	1, 10. 50 M WITH D/d = 3 50, 100, 1000 M WITH D/d = 5 >1 KM	IMPACT IMPACT OR VOLCANISM IBID	2 TO 3 M FOR OVERLAY >10 M OVERLAY + RUBBLE >10 M	AGENTS OF EROSION SUGGESTED: FOR SMALL CRATERS - SMALL METEORITES; FOR LARGE *CRATERS (D >1 KM) - VOLCANISM, ISOSTRATIC* COMPENSATION, LARGE METEORITES. MARIA FORMED AND ERODED FOR 10^9 YEARS. DENSITY OF SURFACE MATERIALS TAKEN AS 1 OR 1.5 G/CM^3.
18	FREQUENCY AND VOLUME OF PRIMARY CRATERS	(TELESCOPIC OBSERVATIONS) MARIA MARIA (INTERCRATER) SOUTHERN HIGHLAND SOUTHERN HIGHLAND (INTERCRATER) APENNINE MOUNTAIN	 100 M --- 1.6 KM --- ---	METEORID IMPACT	AVERAGES FOR RUBBLE 15 M <1 M 83 M 14 M 1000 M	SURFACE LAYER COMPOSED PRIMARILY OF RUBBLE MANTLED WITH HIGHLY POROUS WEAKLY COHESIVE "DUST". DEPTH OF RUBBLE INCREASES ABRUPTLY AROUND CRATERS; IS MUCH SMALLER IN BETWEEN THEM. RUBBLE INCLUDES BLOCKS WHOSE HIGHLY VARIABLE SIZE IS RELATED TO THE VOLUME OF THE CRATERS THEY COME FROM. ABOVE RUBBLE, A STEADY-STATE THIN EQUILIBRIUM LAYER OF DUST IS ACHIEVED ON LEVEL GROUND. DEPTH OF RUBBLE MUCH GREATER IN HIGHLANDS "SHADOW AREAS" THAN IN MARIA DUE TO HIGHER CRATER FREQUENCY.

SYMBOLS

d	DEPTH OF CRATER
D OR D_A	APPARENT DIAMETER OF CRATER (RIM TO RIM)
D_F	FLOOR DIAMETER OF FLAT BOTTOM AND CONCENTRIC CRATER
t	SURFICIAL LAYER THICKNESS
R	D/d
*	INDICATES CANDIDATE APOLLO SITES

REFERENCES

1. Baldwin, R. B. (1963), The Measure of the Moon, University of Chicago Press.

2. Baldwin, R. B. (1965), "The crater diameter-depth relationship from Ranger VII photographs," The Astronomical Journal, v. 70, n. 8, Oct.

3. Department of the Interior, U. S. Geological Survey, Geologic Maps of the Moon, 1962 to date.

4. Engel, K., (1962), "Diameter-depth relations and origin of lunar craters" and comments by B. Warner and I. Halliday, J. Brit. Astron.

5. Gault, D. E., Quaide, W. L., Oberbeck, V. R., and Moore, H. J. (1966), "Luna 9 photographs: Evidence for a fragmental surface layer," Science, v. 153, n. 3739, Aug.

6. Harbour, J. (1967), "Preliminary geologic map of Ellipse III 12-1 and vicinity," U. S. Geological Survey.

7. Jaffee, L. D. (1965), Depth of the lunar dust," J. of Geophys. Res., v. 70, n. 24, Dec.

8. Jaffee, L. D. (1966a), "Lunar dust depth in Mare Cognitum, J. of Geophys. Res., v. 71, n. 20, Oct.

9. Jaffe, L. D. (1966b), "Lunar overlay depth in Mare Tranquilitatus, Alphonsus and nearby highlands," Icarus, v. 5, n. 5. Sept.

10. Jaffe, L. D., et al. (1967), "Principal science results from Surveyor V. Surveyor V mission report. Part II Science results," Jet. Prop. Lab., Calif., Tech. Rep. 32-1246, Nov.

11. Lunar Orbiter Photo Data Screening Group (1967a), "Preliminary geologic evaluation and Apollo landing analysis of areas photographed by Lunar Orbiter II," Langley Research Center, Hampton, Va., LWP-363, March.

12. Lunar Orbiter Photo Data Screening Group (1967b), Preliminary geologic evaluation and Apollo landing analysis of areas photographed by Lunar Orbiter III," Langley Research Center, Hampton, Va., LWP-407, June.

13. Lunar Orbiter Photo Data Screening Group (1968), "A preliminary geologic evaluation of areas photographed by Lunar Orbiter V including an Apollo landing analysis of one of the areas," Langley Research Center, Hampton, Va., LWP-506, Feb.

14. Oberbeck, V. R. and Quaide, W. L. (1967), "Estimated thickness of a fragmental layer of Oceanus Procellarum," J. of Geophys. Res., v. 72, n. 18, Sept.

15. Quaide, W. L. and Oberbeck, V. R. (1968), "Thickness determination of the lunar surface layer from lunar impact craters," J. of Geophys. Res., v. 73, n. 16.

16. Rennilson, J. J., et al. (1966), "Lunar surface topography Surveyor I mission report, Part II Scientific data and results," Jet Prop. Lab., Pasadena, Calif., Tech. Rep. 32-1023, Sept.

17. Ross, H. P. (1968), "A simplified mathematical model for lunar crater erosion," J. of Geophys. Res., v. 73, n. 4, Feb.

18. Salisbury, J. W. and Smalley, V. G. (1963), "The lunar surface layer," A. F. Cambridge Research Laboratories.

19. Shoemaker, E. M., et al. (1967a), "Television observations from Surveyor III. Surveyor III mission report. Part II Scientific results," Jet. Prop. Lab., Pasadena, Calif., Tech. Rep. 32-1177, June.

20. Shoemaker, E. M., et al. (1967b), "Television observations from Surveyor V. Surveyor V mission report. Part II Science results," Jet. Prop. Lab., Pasadena, Calif., Tech. Rep. 32-1246, Nov.

21. Tass Press Releases (1967), NASA Goddard S.F.C., Translation ST-PR-LPS-10545, Jan.

22. Walker, E. H. (1966), "Comments on a paper by L. D. Jaffee, 'Depth of the lunar dust'" and reply by L. D. Jaffee, J. of Geophys. Res., v. 71, n. 20, Oct.

23. Watkins, J. S. and Whitcomb, J. H. (1968), "Thumper final report. ALSEP active seismic experiment," U. S. Geological Survey, Interagency Report: Astrogeology 4, March.

C H A P T E R 6

GEOCHEMICAL STUDIES

by

I. S. E. Carmichael and J. Nicholls

CHAPTER 6

GEOCHEMICAL STUDIES

(I. S. E. Carmichael and J. Nicholls)

I. INTRODUCTION

Geochemical studies provide one source of information that can be used for development of an improved understanding of the composition, structure, and history of the moon. While geochemical studies have not formed a large part of the research under this contract, a limited amount of work has been done and is reported here.

In particular, study was made of the probable characteristics of lunar lava and the implications of these characteristics in the interpretation of lunar composition and history. An attempt was made to develop an answer to the following question: Assuming that lavas erupt on the lunar surface, in what way may the specific lunar environment stamp its influence on the lava and so perhaps modify it in a direction, or to an extent, unlike a terrestrial lava? The approach followed was to attempt isolation of the influence (if any) of the terrestrial atmosphere from that of the "atmosphere" carried by the lava itself. Then, since the lunar environment is essentially free of atmosphere, tentative conclusions should be possible concerning possible differences between terrestrial and lunar lavas.

II. SUMMARY OF RESULTS

The one component of the terrestrial atmosphere that is most likely to affect the crystallization of lavas is oxygen. In sufficient amount oxygen has the capacity to change the Fe^{2+}/Fe^{3+} ratios in the basaltic liquid. This will in turn change the nature or the order of precipitating solid phases, as well as the viscosity of the liquid lava and its ability to flow long distances. This hypothesis implies that the volatile phase impresses its oxygen requirements on the molten basalt. Since the

availability of oxygen in the terrestrial and lunar atmospheres is markedly different, it is possible that the properties of lunar and terrestrial basalts may differ.

These considerations form the background for the study reported by Carmichael and Nicholls (1967). From the results of this work it was concluded that there appears to be no reason for the pristine mineralogy of terrestrial and lunar lavas to differ. On the other hand, because of the influence of atmosphere on the cooling crystalline basalt, lunar basalt may have different properties than terrestrial basalt, especially with respect to the magnetic minerals.

Although terrestrial lavas never precipitate metallic iron, there seems to be no reason a priori why a lunar lava might not contain iron as a phase. If metallic iron is absent, then the iron-titanium oxide phases, which are unlikely to be involved in the common terrestrial superimposed oxidation, will have less intense magnetization than terrestrial lavas, regardless of the very weak or absent lunar magnetic field.

An interesting possibility that emerges from this is that the carriers of magnetization, the Fe-Ti oxides, could have Curie temperatures intermediate between the diurnal lunar temperature limits, i.e., "daily fluctuating magnetization". This could provide a constraint on the interpretation and collection of the remanent magnetization in returned lunar samples.

Following this an attempt was made to estimate activity coefficients of iron and titanium in natural liquids. Unfortunately all attempts to do so were unsuccessful.

The next line of inquiry concerned if and how lack of oxygen could totally suppress the precipitation of Fe-Ti oxides (magnetic materials). Apparently oxygen is not the only inhibitor of their precipitation, and variation of gross composition of a silicate liquid could have the same effect. This aspect of Fe-Ti oxide suppression in a small group of Fe-Ti free terrestrial lavas has been described by Nicholls and Carmichael (1969). These lavas are so rare in the Earth's igneous budget that it would be unwise to assume that lunar lavas generally do not carry magnetic minerals.

REFERENCES

1. Carmichael, I. S. E. and Nicholls, J. (1967), Iron-Titanium Oxydes and Oxygen Fugacities in Volcanic Rocks. Journal of Geophysical Research, V. 72, N. 18, September.

2. Nicholls, J. and Carmichael, I. S. E. (1969), Peralkaline Acid Liquids — A Petrological Study. Beitrage Mineralog. Petrologie, V. 20, pp. 268-294.

A P P E N D I X

LIBRARY OF LUNAR SURFACE EXPLORATION REFERENCES

by

Francois E. Heuzé

APPENDIX

LIBRARY OF LUNAR SURFACE EXPLORATION REFERENCES

(Francois E. Heuzé)

During the course of this research effort, a library of lunar exploration reports and papers was built up as a supporting facility. In addition to readily available material in each department, over 500 references were thus indexed. Each one is characterized by a few KEY WORDS (average: five) among those presented in the following pages.*

The retrieval system is a Jonker-Termatrex (plastic cards and light table) enabling easy and fast cross-indexing of up to 10,000 references.

A card file by author is also available.

---

*Apparent duplications exist. They are intentional, allowing more specific report characterization. Present set-up allows also for introduction of new key words (missing numbers).

LUNAR EXPLORATION BIBLIOGRAPHY

KEY WORDS LISTING

GENERAL

1 Abstract
2 Conferences, Symposia
3 Data
4 Maps and Mapping — Surveying

6 Periodicals
7 Photos
8 Final Reports
9 Review — Bibliography

YEARS

1960	Report Numbers	0 — 29
1961	Report Numbers	30 — 59
1962	Report Numbers	60 — 99
1963	Report Numbers	100 — 199
1964	Report Numbers	200 — 299
1965	Report Numbers	300 — 399
1966	Report Numbers	400 — 499
1967	Report Numbers	500 — 699
1968	Report Numbers	700 —

RESEARCH ORGANIZATIONS

11 Bendix
12 Douglas
13 Grumman
14 IITRI (Illinois)
15 Jet Propulsion Laboratory
16 Langley Research Center
17 Lockheed — Mimosa
18 Marshall S.F.C.
19 NASA (general)
20 North American
21 SSL & LRL (Berkeley)
22 Schlumberger
23 UCB
24 U. S. Bureau of Mines
25 U. S. Geological Survey
26 General Electric
27 Philco
28 Westinghouse
29 Martin Marietta
30 Texaco Experiment
31 A. D. Little, Inc.
32 A. F. Cambridge
33 Northrop
34 U. S. Army
35 Bellcomm Inc.
36 AIAA
37 G.M.C.
38 W.G.E.R.
39 Hughes Aircraft
40 Ames Research Center
41 Boeing

SPACECRAFT MISSIONS

51 Ranger 7
52 Ranger 8
53 Ranger 9
54 Luna 9
55 Luna 10
56 Luna 13
57 Orbiter 1
58 Orbiter 2
59 Orbiter 3
60 Orbiter 4
61 Orbiter 5
62 Surveyor 1
63 Surveyor 3
64 Surveyor 4
65 Surveyor 5
66 Surveyor 6
67 Surveyor 7
68 Apollo
69 Zond

EXPLORATION PROGRAM

72 Missions

73	Phase I	1970-1973 Apollo
74	Phase II	1974-1976 Semi-Permanent
75	Phase III	1977-1980 Bases

76 Landing Sites

MOON

78	Origin — History	79	Mascons		
81	Geology	82	Erosion — Comminution — Transportation		
		83	Glaciation — Ice		
		84	Meteorites — Impact — Explosion		
		85	Moonquakes — Tectonics		
		86	Volcanism		
87	Morphology	88	Craters	89	Primary
				90	Secondary
				91	Depth
				92	Diameter
				93	Profiles — Slopes
				94	Boulders and Tracks
				95	Ejecta
		96	Maria	97	Lava Flows and Tunnels
				98	Profiles — Slopes
		99	Highlands	100	Profiles — Slopes
		101	Rilles		
		102	Calderas		
103	Stratigraphy	104	Formations		
		105	Depth		
106	Environment	107	Pressure		
		108	Magnetic Field		
		109	Micrometeorites		
		110	Gravity		
		111	Radiation — Sputtering — Sintering		
		112	Temperature and Heat Flow		
		113	Gases		
		114	Water		
115	Stress Fields				

LUNAR OR SIMULATED MATERIALS

116	Rocks	117	Basalt	118	Flow
				119	Vesicular
		120	Obsidian		
		121	Welded Tuff		
		122	Serpentinite		
		123	Granodiorite		
		124	Ryolite		
		125	Dacite		
		126	Pumice		
		127	Gabro		
		128	Dunite		
		129	Scoria		
		130	Quartz		
		131	Tektites		
135	Soils and Powders	136	Quartz Sand		
		137	Olivine (Powder)		
		138	Obsidian (Powder)		
		139	Enstatite Sand		
		140	Pumice (Powder)		
		141	Clay		
		142	Basalt (Powder)		

LUNAR SURFACE PROPERTIES

146	Nature — Structure	147	Crystalline Structure		
		148	Density		
		149	Grain Size		
		150	Grain Shape		
		151	Porosity		
		152	Model	153	Granular
				154	Solid
155	Mechanical Properties (Soils)	156	Bearing Capacity	157	Static
				158	Dynamic
		159	Penetration Resistance	160	Static
				161	Dynamic
		162	Shear Strength		
		163	Cohesion		
		164	Angle of Friction		
		165	Behavior	166	Angle of Repose
				167	Dilatancy
				168	Mode of Failure
		169	Compressibility		
		170	Pore Pressure		
		171	Permeability		
172	Mechanical Properties (Rocks)	173	Elastic Constants	174	Static
				175	Dynamic
		176	Unconfined Strength		
		177	Confined Strength		
		178	Tensile Strength		
		179	Angle of Friction		
		180	Porosity		
		181	Permeability		
182	Thermal	183	Thermal Inertia		
		184	Conductivity		
		185	Specific Heat		

LUNAR SURFACE PROPERTIES (cont'd)

186	Chemical	187	Composition		
		188	Interparticle Bonds		
		189	Spectrography		
		190	Contamination	191	Adsorption
				192	Desorption
193	Electrical				
194	Electromagnetic				
195	Magnetic				
197	Radioactivity				
198	Photometric	199	Polarization		
		200	Radar		
		201	Albedo		
		202	Infrared		

GAS

209	Thermal Conductivity
210	Dynamics
211	Viscosity
212	Diffusion
213	Gas Mixtures

ENGINEERING

216	Locomotion (Trafficability)	217	Soil-Vehicle Mechanics and Models		
		218	Roving and Flying Vehicles		
		219	Shelters		
224	Bases — Observatories	225	Sites		
226	Soils and Rocks Engineering	227	Excavations and Stability	228	Surface
				229	Subsurface
		230	Blasting and Wave Propagation		
		231	Soil Compaction		
		232	Soil Stabilization		
		233	Rock Drilling		
		234	Rock Drills	235	3m
				236	30m
				237	300m
		238	Soil Sampling		
239	Adhesion Friction in UHV	240	Metal-Mineral		
		241	Metal-Metal		
		242	Mineral-Mineral		
		243	Lubrication		
247	Surface Probes	248	Mechanical		
		249	Thermal		
		250	Seismic		
		251	Electrical		
		252	Nuclear		

ENGINEERING (con't)

254	Subsurface Probes	255	Mechanical (Other than Drills)
		256	Thermal
		257	Seismic
		258	Electrical
		259	Nuclear

261 Insulation (Temperature)

262 Mining and Lunar Resources

263 Returned Samples

264 Shielding (Radiations — Meteorites)